MONITORING LAND COVER CHANGES BY REMOTE SENSING IN NORTH WEST EGYPT

Submitted by

Timothy Steven Richards

for the degree of MPhil at

The School of Oriental and African Studies

London University

1986

ProQuest LLC.
789 East Eisenhower Parkway
P.O. Box 1346
Ann Arbor, MI 48106 – 1346

ABSTRACT

The Mediterranean coastal strip of Egypt is a semi-arid environment which supports a variety of agricultural practices ranging from irrigated sedentary agriculture to semi-nomadic pastoralism. The sedentarisation of the nomadic Bedouin coupled with an increase in population of both people and livestock and a decrease in the extent of the rangelands, has resulted in severe pressure being exerted upon the environment. Satellite remote sensing of vegetation offers the potential to aid regional management by complementing conventional techniques of vegetation mapping and monitoring. This thesis examines the different techniques available for vegetation mapping using visible and near infra red spectral wave bands.

The different techniques available for vegetation mapping using remotely sensed data are reviewed and discussed with reference to semi-arid environments. The underlying similarity of many of the techniques is emphasised and their individual merits discussed. The spectral feature-space of Landsat data of two representative study areas in northern Egypt is explored and examined using graphical techniques and principal components analysis.

Hand held radiometric field data are also presented for individual soil types within the region. It is proposed that by using reference data for individual soil types, improved estimates of vegetation cover can be ascertained.

A number of radiometric corrections are applied to the digital Landsat data in order to convert the arbitrary digital values of the different spectral bands into physical values of reflectance. The effect of this standardization on the principal components is examined. The stratified approach to vegetation mapping which was explored using the field data is applied in turn to the digital Landsat images. Whilst the stratified approach was not found to offer significant advantages over the non-stratified approach in this case, the analysis does serve to provide an accurate datum against which to measure vegetation.

In conclusion a satellite based system for operational vegetation monitoring is proposed.

ACKNOWLEGEMENTS

Principally I would like to thank Dr Tony Allan of SOAS for his support, encouragement, and most of all for his patience during the course of this degree. I would also like to thank Professor Ayyad and all of the members of his staff in the Botany Department of Alexandria University, for the help, friendship and hospitality which they extended to me during my stay in Egypt. Thanks are also due to the Central Research Fund of London University which financed the fieldwork, and also Bristol University which provided time and image processing facilities for the completion of the work. And lastly I would like to thank Joy my wife for all of her support and sacrifice over the past five years.

CONTENTS

7 CONCLUSIONS AND RECOMMENDATIONS

LIST OF FIGURES AND ILLUSTRATIONS

1 INTRODUCTION

2 THE STUDY AREA

3 REMOTE SENSING OF VEGETATION A LITERATURE REVIEW

4 INITIAL DIGITAL PROCESSING

CHAPTER 1

INTRODUCTION

1.1 INTRODUCTION

The role that remote sensing can play in surveys of semi-arid agriculture and rangeland is potentially an immense one. The ability to detect and map vegetation and terrain over large and often inaccessible areas, such as Egypt's coastal strip, makes remote sensing an obvious choice as a mapping tool. Whilst this observation may be true in a general sense it is necessary to consider at what level a remote sensing input would be most appropriate. The term 'level', here, has a variety of meanings. It can be taken to mean level as in scale, ie the scale of imagery whether photographic or MSS data, it can also be taken to mean the level of sophistication at which remotely sensed data are integrated into a survey. The potential of remotely sensed data is great indeed, but practicalities in terms of the availability of data, processing facilities, climate, cost, politics, sociology, timeliness and a host of other factors serve to limit that potential. Remote sensing must, in order to make an effective contribution, be appropriate.

The remote sensing input to the SAMDENE and REMDENE studies, which commenced in 1974, has for the most part been in the form of aerial photography. This has proved a valuable source of information, at a level at which it can contribute to diverse studies ranging from soils mapping and erosion estimation to vegetation mapping. Aerial photography at a scale of 1:20 000 is undoubtedly an appropriate input. It is, however, expensive, particularly when repeated coverage is required and it is not generally in the public domain. At what level though, can satellite remote sensing contribute to wide ranging ecological

studies such as SAMDENE and REMDENE? Had a conscious decision been made to use satellte data at the outset of these studies then only a relatively small number of laboratories, principally in the United States, could have made a rigorous multi-temporal digital study of the environment. The historical fact that Landsats one to three (1972 - 1982) were principally research satellites and that commercially available computer technology, in particular software, is only just becoming generally available on a national basis (in the UK at least), has meant that remote sensing has not been able to play an important role in these two ecological surveys. In addition because of the political interactions between the Egyptian Remote Sensing Centre in Cairo and other bodies, such as Alexandria University, an indigenous Egyptian remote sensing input to the studies has not been forthcoming.

A significant input to the studies from satellite remote sensing has, due to the constraints mentioned above and the fact that the REMDENE study officially finished in 1984, not been possible. However, it may be that the most important contribution that satellite remote sensing can offer to the region will be in the future, by monitoring the changes which are occurring within the coastal tract due to the increasing ecological pressure being exerted by man.

Probably the most important monitoring role which remote sensing may be able to perform is in monitoring the spatial extent and quality of the rangeland vegetation. The possibility of remote sensing being able to contribute to this specific end is marginal. The potential benefits ,however, more than justify the costs of investigation.

The activities of the REMDENE (Regional Environmental Management of Mediterranean Desert Ecosystems of Northern Egypt) project have been fourfold:

First, 'representative sectors' of the coastal strip have been mapped to provide information on topography, soils, hydrology, vegetation, and ancient and modern land use systems.

Secondly, a procedure for land resources assessment has been devised involving the identification and description of land units on the basis of the criteria mentioned above. These units are then evaluated in terms of the degree to which they have been affected by man, ie to what extent they are affected by urbanization, grazing, agriculture, erosion, shrub cutting, water use etc.

Thirdly, the various different forms of landuse which have been prevalent throughout the region during the past few decades have been studied and their effects upon the region's ecosystems established.

Fourthly, the ecosystems themselves have been modelled in order to try and assess and describe the effect of exogenous factors upon them. (Source REMDENE 1983).

The purpose of this thesis has been to examine the different techniques available for vegetation mapping using visible and infrared remotely sensed data in the context of northern Egypt. Since the Landsat data used in this study were acquired, many things have changed in the remote sensing world. New sensors

have been introduced and large scale vegetation monitoring has become possible on an operational basis with the introduction of the NOAA Global Vegetation Index (GVI) product. In addition the concept of Geographic Information Systems (GIS) has become vogue in relation to remotely sensed data. All of these developments have implications with respect to vegetation mapping in Egypt. It has become my opinion that only with the introduction of powerful small scale computer systems which take full advantage of the resolution of NOAA AVHRR data and which allow comparisons to be made with data from other sources in the framework of a regional geographic information system, will truely useful operational systems become available. Such information systems, in which remotely sensed data would be only a component, can clearly act as aids to regional resource management and planning. The utility and merits of such information systems specifically designed for use in Somalia have been discussed by Watson and Nimmo (1985).

The physical, conceptual and technological elements of new resource management tools now exist. It remains to be seen, however, to what extent these new tools will be developed in the context of the developing world and to what extent they will impact upon real problems within the social and economic restraints in which they will be constrained.

This thesis addresses the techniques for vegetation mapping in arid regions. It should be born in mind, however, that these techniques form only an element within the larger task of providing meaningful data in a useable and useful form.

CHAPTER 2

THE STUDY AREA

2.1 LOCATION AND PHYSIOGRAPHY

The study area of this thesis was originally defined as being the whole of the coastal tract of northern Egypt between Alexandria, in the east, and Salum in the west, near Egypt's border with Libya. Due to the problems of physically handling such large quantaties of data (four full Landsat scenes) and of the need to focus activity, two small sub-areas were chosen. These sub-areas were chosen so that they covered the REMDENE study's Transects 1 and 3. These two areas were picked because they are representative of much of the coastal tract and characterise the climate and physiography of large regions within it. In addition, the staff of the REMDENE poject have studied these two transects in detail and there is therefore much important data recorded for the two sites. The transects are also within easy striking distance from Alexandria for the purposes of fieldwork.

Figure 4.1.1 shows the coastal tract and the location of the nine REMDENE transects, numbers one and three being the study areas for this thesis. The two transects are centred on the towns of Burg el Arab and El Omayed respectively.

Three major physiographic systems (1) exist along the extent of the coastal tract. The system which we are predominantly concerned with here is that between Alexandria and El Daba. This system is characterised by the physiographic units found

---

(1) A physiographic system is a physically homogeneous unit or group of units which characterize the landscape.

at El Omayed. Figure 2.1.1 shows an elevation cross- section taken through Transect 3 from the coast to some ten kilometres inland. Three physiographic systems have been identified within this major physiographic system (REMDENE 1981). The three systems are: first, the 'coastal system' which consists of the beach and the coastal sand dunes, this system is very distinctive. Second, the 'ridge and depression system' which consists of a series of ridges and depressions which run parallel with the coast and are the remnants of former coastal dune systems. Third, the 'inland system' which consists of an inland plateau which slopes gently upwards and generally to the south-east.

The coastal system can be found along the entire extent of the coast and is quite apparent on the satellite images, it appears as a bright white strip following the coast line. The ridge and depression system can be found at various places along the coast but is very variable in terms of the width and deepness of the depressions. It is particularly prominent between Alexandria and El Alemein. It can be seen from the Figure 2.1.1 that at El Omayed the depressions are broad and shallow with the land rising towards the south. At this position along the coast, the inland plateau rises steeply from about fifteen to twenty metres above sea level at it's base, to about eighty metres above sea level at it's highest point. Plate 2.1.1 shows a view looking southwards just outside the town of El Omayed. In the distance the ridge of Khashm El Eish is visible, this being the edge of the inland plateau; whilst in the foreground scatterd shrubs of Thymelia Husuta, an important shrub in the make up of the range, are visible. The

REMDENE poject has identified fifteen physiographic units which make up the three basic systems.

These units are annotated on Figure 2.1.1 and are tabulated in Table 2.1.1. Unit 7a, 'waterlogged depression', is generally localised to relatively small areas in Transect 3 but in Transect 1 forms the basis for Lake Mariut. At Burg El Arab (Transect 1) the physiographic systems are essentially the same but differ in the detail of the units. In Transect 1, physiographic unit 7 is completely inundated with saline water and is considerably wider. The second and third rocky ridges are still present but the inland plateau is reached by gently rising ground over the ridges rather than via a steep escarpment as in unit 13 of Transect 3. To the west of El Omayed the inland plateau and the system of ridges and depressions progressively diverge from the coast.

The other two major landscape types which occur along the coast are first, the major system which occurs in the Dabaa/Fuka area and which is characterised by hills and ridges and broad level valleys; and second, the system which is found further west and which consists of upland plains incised by deep broad wadis which drain into the sea. This last system generally occurs to the west of Mersa Matruh and is characterised by Wadi Garawla. A description of physiographic features which are visible on the Landsat imagery appears in chapter four.

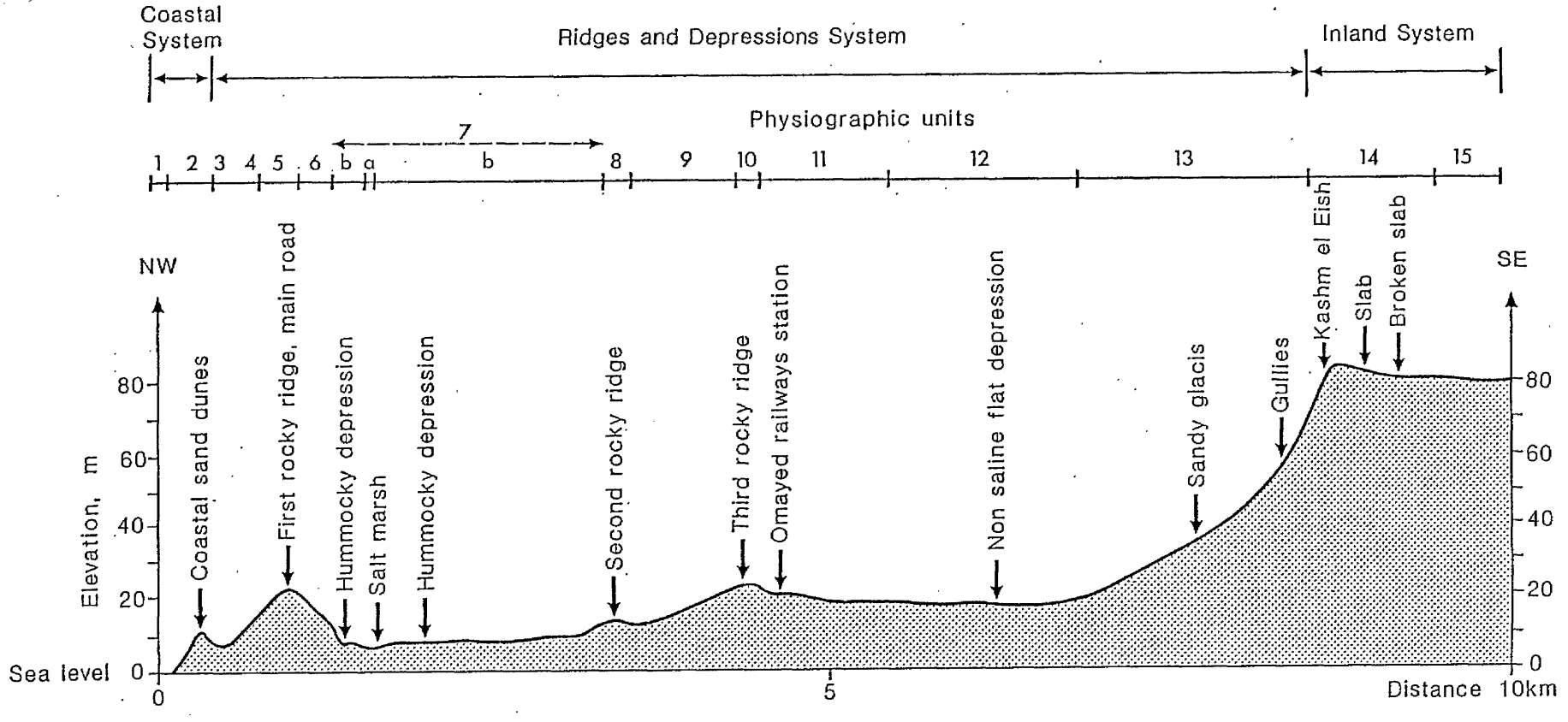

Figure 2.1.1
The physiographic units occuring at El Omayed. (Source REMDENE 1983)

TABLE 2.1.1

UNIT No	DESIGNATION	DISTANCE FROM COAST	GEOLOGICAL AND GEOMORPHOLOGICAL FEATURES
1	beach	Ø - 200m	
2	coastal dunes	200-500m	present active dunes on consolidated material.
3	first depression	500-900m	flat and stretched depression (sand deposits).
4	northern slope of 1st rocky ridge	600-900m	hillside (sandy colluvions).
5	first rocky ridge	900-1100m	summit of stretched hill (oolitic limestone & ancient consolidated dune).
6	southern slope of 1st rocky ridge	1-1.3km	hillside (sandy colluvions).
7	saline depression:		
a	. salt marsh	1.1-2.5km	waterlogged depression (loamy and clayey sand).
b	. hummocky depression	1.1-3km	flat area (locally waterlogged with numerous sandy hummocks).
c	. sandy meso-deposit	1.1-3km	gently and irregularly sloping sandy hill.
d	. sandy indurated con-convexity	2km	low and stretched convexity (indurated sand).
8	second rocky ridge	3-3.3km	summit of stretched hill (oolitic limestone -ancient consolidated deposits).
9	interidges sandy slope	3-3.3km	gently sloping surface overlain by drifted sand.
10	third rocky ridge	4.3-4.6km	summit of stretched hill (ooliti limestone-ancient consolidated deposits).
11	southern sandy slope of 3rd rocky ridge	4.6-6km	gently sloping surface overlain by drifted sand.
12	non-saline flat depression	5.5-7km	plain more or less drifted.
13	sandy glasis with gullies	6.5-8.5km	sandy glacis dissected with gullies in the upper part.
14	cliff and outcrop of inland plateau	7.5-8.5km	cliff with outcrop of calcareous sandstone and stretched and gently sloping inland plateau.
15	undulating sandy surface	8-10km	slightly undulating surface with drifted sand.

2.2 CLIMATE

2.2.1 Factors Determining Climate

FAO (1970) identifies four pincipal factors which determine the climate along the northern coastal tract:

(1) The situation of the region with regard to the general circulation of the atmosphere.
(2) The proximity of the Mediterranean sea.
(3) The orientation of the coast.
(4) The orography.

Factor one is controlled by the subtropical high pressure belt in summer and by the cyclones moving eastwards with westerlies in winter. The summer months are characterised by clear skies no rain, high solar radiation and light winds. During the winter months, November to April, Atlantic and Mediterranean cyclones extend sufficiently far eastwards to account for virtually all of the winter rainfall which is associated with cold front cumulus clouds. Factors (2) and (3) affect the air temperature and humidity and the variation in rainfall along the coast.

2.2.2 Average Distribution of Rainfall

FAO (1970) quotes the values shown in Figure 2.2.1 as being the mean annual rainfall figures in mm, for the thirty year period 1925-1939, 1951-1965. Factor (3) above is cited as being the main contributor to the variations in mean annual rainfall

Plate 2.1.1

A southerly view at El Omayed towards the inland plateau and the ridge of Khashm el Eish.

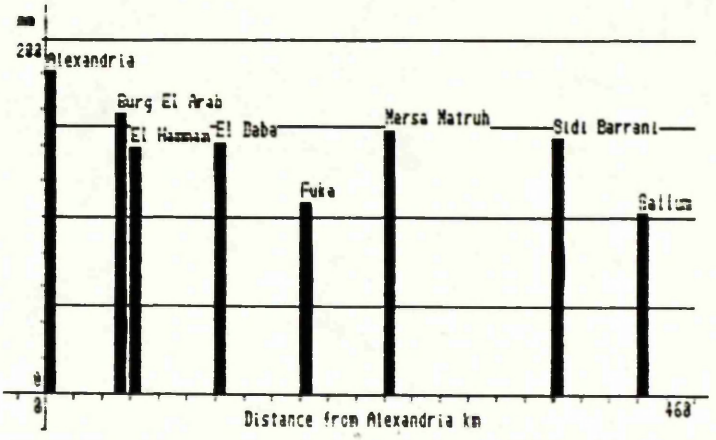

Figure 2.2.1

Mean annual rainfall in mm at selected locations along the coast.

Source FAO (1970)

along the coastal tract. The extreme variability, both spatially and temporally, in the rainfall and the sparcity of reliable data both contribute to the difficulty in defining isohytes. The rainy season commences during the second part of October and lasts until mid March. Figure 2.2.2 shows the seasonal distribution of rainfall at El Daba, with seventy five percent of the annual total falling between November and February. Figure 2.2.3 shows the relationship between rainfall and the distance from the coast, the relationship being most striking.

The very low mean annual values, all of which are below 200mm in Figure 2.2.1, impose very severe constraints upon dryland farming in the region. The nature of the curve in Figure 2.2.3 means that any dryland farming which does exist in the region is confined to areas very close to the coast. FAO (1970) state that dryland farming is 'practically impossible with a rainfall which is so scarce and erratic', while Kay et al (1985) regard 500mm as being the minimum rainfall for 'normal' rainfed farming. Arnon (1972) states that a figure of 500mm is for areas with summer rainfall and Brichambaut and Wallen (1963) quote a minimum mean annual rainfall of 240mm with a variability of 37 per cent as being the minimum amount for viable rainfed production. Although the mean annual values in Figure 2.2.1 are all below 200mm dryland farming is, nevertheless, practised in the region, as it has been for thousands of years. Not only is the rainfall highly variable spatially and temporally within individual years, it is also very variable on an interannual basis. FAO (1970) calculate that the relative interannual variability at El Daba is in the order of forty per cent.

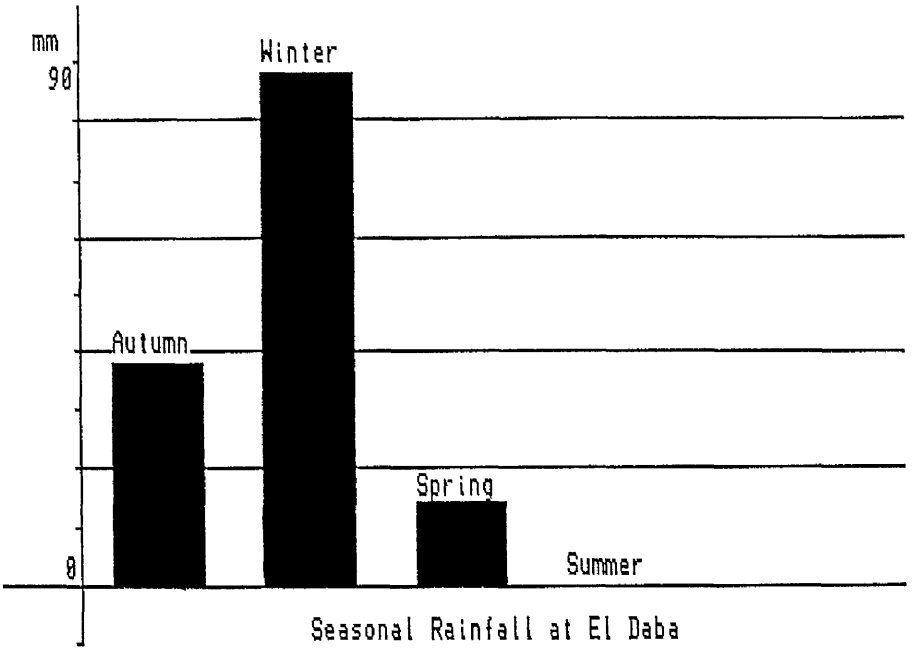

Figure 2.2.2

Seasonal rainfall at El Daba.

Source FAO (1970)

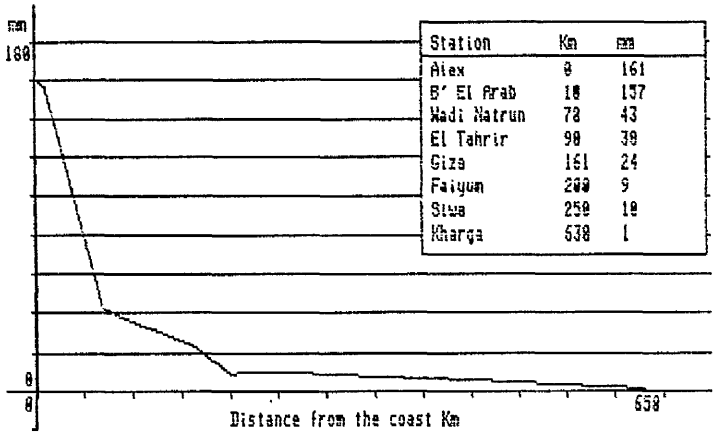

Figure 2.2.3

The relationship between rainfall and distance from the coast.

Source FAO (1970)

In such conditions the importance of moisture derived from dew is considerable to both flora and fauna. Migahid and Ayyad (1959) estimated that during 1955 the total annual depth of dewfall as being 115mm. This value being half as much again as the mean annual rainfall.The proportion of this figure which would have been available to plants is however open to debate. In addition, FAO (1970 pp26) question the effects of the physical properties of the Dudvedani dew gauge (used by Migahid and Ayyad) on the volume of dew collected.

Figure 2.2.4 shows the relationship between precipitation and potential and actual evapotranspiration throughout the year at Burg el Arab. It is clear from the figure that only from mid November to the end of February does a surplus of moisture exist within the rooting zone.

In conclusion, FAO (1970) describes the climate of the northern coast of Egypt as being 'one of the mildest of the Mediterranean' with high winter temperatures and reasonable summer ones, with relatively high air humidities. The limiting factor to agriculture, however, being the high variability of the rainfall in all of it's aspects.

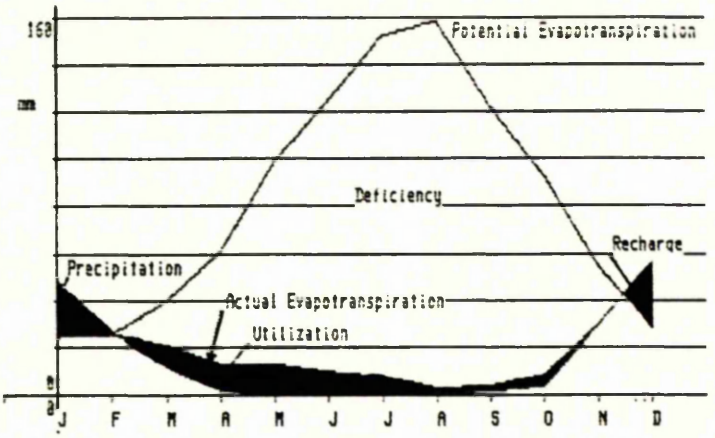

Figure 2.2.4

Seasonal water balance.

Source REMDENE 1983

Plate 2.3.2

Barley mounds used for the storage of surplus grain grown during good years of dryland production.

2.3 AGRICULTURE

2.3.1 IRRIGATED AGRICULTURE

The nineteen sixties saw the implementation of governmental rural management policy in the Burg el Arab area, and with it great changes in the region's agricultural practice and sociological structure, and specifically in the mobilization of the labour force. Soliman (1981) indentifies three major aspects of the resulting changes. These being:

(1) A great increase in the available cultivated land, which was reclaimed by both the state and by individuals.
(2) A shortage of water as a result of the vast increase in land reclamation. This limited the possibilities of cultivation of all the reclaimed land.
(3) A decrease in the area available for grazing.

The land 'reclaimed' by individuals, in addition to that expropriated by the state, led to an increase in water demand above and beyond the design supply of the new irrigation systems. This, coupled with high water losses through the unlined canal walls and the diversion of irrigation water to orchards, led directly to water shortages and salinization in low lying areas and those areas adjacent to the canals. I have myself seen salinized olive orchards adjacent to the irrigation canals in Burg el Arab. Ironically potentially productive land has been lost both through a lack of irrigation water on the one hand and by salinization through excessive water seepage and irrigation on the other.

The crops which are successfully cultivated in the Burg el Arab area are listed below:

Winter crops and orchards 1979/80	Crop	Area (feddans)
	Barley	156
	Trifolium (clover)	365
	Beans	229
	Almond	208
	Olive	359
	Guava	58
	Peaches	17
	Citrus	50
Summer crops 1979/80		
	Maize	262
	Water Melon	187
	Tomatoes	85
	Cucumbers	39
	Marrow	17
	Beans	31
	Cabbage	12
	Egg-plant	17
	Peppers	5

(Source REMDENE 1981 pp4-19)

2.3.2 DRYLAND AGRICULTURE

The expansion of irrigated agriculture around Burg el Arab during the nineteen sixties was accomplished at the expense of dryland agriculture and rangeland resources. The principal crop cultivated by rainfed farming alone is barley. Tree crops, which mainly consist of olives and figs, are also grown without the aid of irrigation. Both the cereal and tree crops are cultivated by the Bedouin who have been encouraged to settle permanently along the northern coastal tract.

Evidence from Landsat imagery indicates that rainfed cultivation in the Burg el Arab region is exclusively associated with features known as 'karms'. These karms are of ancient origin and were certainly in use during the Roman period when the three thousand or so drinking water cisterns, to be found in the region were built. References to karms in the literature are very scant and no definitive explanation of their function seems to exist. They are, however, due to their exclusive association with dryland farming, of no small importance. In addition to the karms FAO (1970) identifies 'man-made' soils which are associated with small ancient field systems which also occur in large numbers. These smaller field systems are not identifiable on Landsat MSS imagery and were not known to local farmers when inquiries were made during the field visit, consequently they are not pursued further here. The karms, however, which consist of substantial earth works are still prepared and cultivated each year; rains permitting. With reference to the karms and the ancient cultivation methods FAO (1970 pp 45) suggests that 'If it could be discovered what

these methods were and why they were used, possibly they could be adopted again, and agriculture in the region be improved at low costs'.

The karms consist of fields of deep clay loam soils which are surrounded by banks of soil sometimes five metres or so high (see Plate 2.3.1). FAO (1970) Table 18 indicates that the karm walls are more compacted than the central fields with higher proportions of sand and much higher salinity levels. It is suggested by the same author that the banks were formed by the removal of saline soil from the central field which was then deposited at the field's edge. Other suggestions to the formation of the banks include theories as to the creation of a micro-climate and of the banks forming donor areas for runoff farming. Dregne (1981) favours the latter explanation. An appreciation of the size of the karms can be gained from Plate 2.3.1 which shows a panoramic view of one of the larger ones some twelve kilometres due south of Burg el Arab. It is clear from the Plate that the surrounding banks are now severly eroded. Evanari et al (1971) state that ancient earth works in the Negev associated with dryland farming have by now totally disappeared. This is obviously not the case in northern Egypt although the karms may not be as old as the features described by Evanari. The Landsat MSS images presented in a later chapter show that cultivation at the karm sites is not restricted to the inner field but that substantial areas are also cultivated surrounding the karms. The sheer size of the surrounding banks, especially when one considers that at one time they may have been considerably larger, leads me to think that the notion of them having been formed by the removal of saline soil is

Plate 2.3.1

The perimeter banks of one of the larger karms to the south of Burg el Arab.

erroneous. The fact that cultivation occurs both inside and outside of the karms would be indicative of the banks acting as donor areas for runoff farming. The true nature of the karm banks however, remains a mystery.

In good years when yields are sufficient to produce a surplus of grain, the surplus is stored under mounds of earth as depicted in Plate 2.3.2. Conversely in dry years when the rains are not sufficient to produce a crop, animals are allowed to graze on the shoots that do emerge. Traditionally the Bedouins would cultivate barley fields at the beginning ot the wet season, only to return when the crops had matured. In more recent times the Bedouin who live locally to Burg el Arab cultivate the fields with tractors and can return easily to the fields for further cultivation or to allow grazing on poorly developed crops.

2.3.3 PASTORAL AGRICULTURE

The Bedouin inhabitants of the coastal strip are famous for their pastoral way of life. Although many are now settled and are sedentary, the traditional values and forms of wealth remain. The principal commodity and form of status and wealth has traditionally been the Bedouin's herds of livestock, which are comprised of sheep, goats and camels, although the latter are far less prevalent in modern times. Even though many Bedouin gave up their nomadic way of life during the settlement periods of the fifties and sixties, many still retain their flocks of goats and sheep. The result has been an increase in the numbers of livestock coupled with a decrease in the quality and area of

the range. The quality of the range has declined through the pressures of overgrazing whilst the areal extent of the range has declined as a result of the increased area of irrigated and reclaimed land. It has also been the case that the rangeland which has been put to irrigation has been that which was favoured by good quality soils. This general decline in the natural forage has meant that increasing amounts of feed materials from the delta have had to be used in order to maintain the levels of stocking which now exist. Not only has the Bedouin become sedentary but he has also become dependent upon the Nile Delta for a reliable supply of supplementary feed stuffs. Soliman and Ahmad (1982) also regard the increase in animal numbers in response to an external demand as representing a dependence in that the market is driven by external rather than internal needs and demands. The same authors also highlight the problems that arise through supplementary feeding in the Nile Delta during the dry months through the infection of animals by parasites.

FAO (1970) estimates that in the coastal area some 70 per cent of the population is involved in pastoral activity. These people are therefore very dependent upon the economic and ecological well-being of the region. The ecological pressures being exerted on the ecosystem are illustrated by the following figures quoted by Soliman and Ahmad (1982). The current carrying capacity of the range in 1971 can be expressed by dividing the total surface area of the region by the total number of animals:

$$\frac{3\ 500\ 000}{1\ 331\ 000} = 2.6 \text{ Feddans / animal}$$

(Source Soliman and Ahmad (1982))

Thus 2.6 feddans are available for each animal for grazing. FAO (1971), however, estimate that a suitable carrying capacity for the region would be 25 feddans per animal, while the Egyptian Agricultural Department estimates that 50 feddans per animal would be more appropriate. This example amply illustrates the severe pressure being exerted on the region's natural resources.

2.4 SOILS

FAO (1970) reports that virtually all of the soils of the northern coastal tract are of alluvial origin. Those soils not formed by alluvial processes are the result ofæolian transportation and deposition. All of the region's soils are derived from the limestone bedrock and therefore contain high proportions of calcium carbonate, between 10 and 15 per cent in the top soils and in some cases much higher. Accumulations of calcium carbonate and sodium chloride occur in the alluvial fans and saline depressions respectively.

FAO (1970) identifies six major soil classification units, these being:

Soils of the coastal dunes

Soils of the inland dunes

Soils of the former beach plains and dune depressions

Soils of the elongated depressions in the plateau

Soils of the alluvial fans and out wash plains

Soils of the wadis

The majority of the soils are poorly developed and contain little organic material.

In Transects 1 and 3 the most productive soils are those of the former beach plains and dune depressions. These soils, where not saline, are generally sandy or clay loams of variable thickness. All of the karms (see above) are located on the deepest of this series, soil B1 of the FAO reconnaissance soil maps. In addition to the karms the majority of the modern irrigated agriculture occurs on this soil type although it is, for the most part, limited to the areas to the north of the irrigation canal. The B1 soils which occur in the dune depressions near the coast are predominantly very saline, and are vegetated by hummocks of saline tolerant plant species. The rangeland used for grazing covers various soil types. In and around El Omayed the rangeland occurs on soils of the D series which are windblown soils of quartz sand over rock or caliche. FAO 1970 reports that these soils are deep and support natural vegetation and trees well. In the Burg el Arab area, however, the range occurs mainly on the B1 soils which are to the south of the third rocky ridge, where no irrigated agriculture is found. Plate 2.4.1 shows goats and camels grazing in this area. Another prominent soil type of the region are the Rd soils which are formed on the former coastal dunes and dune ridges. These soils are generally very stoney.

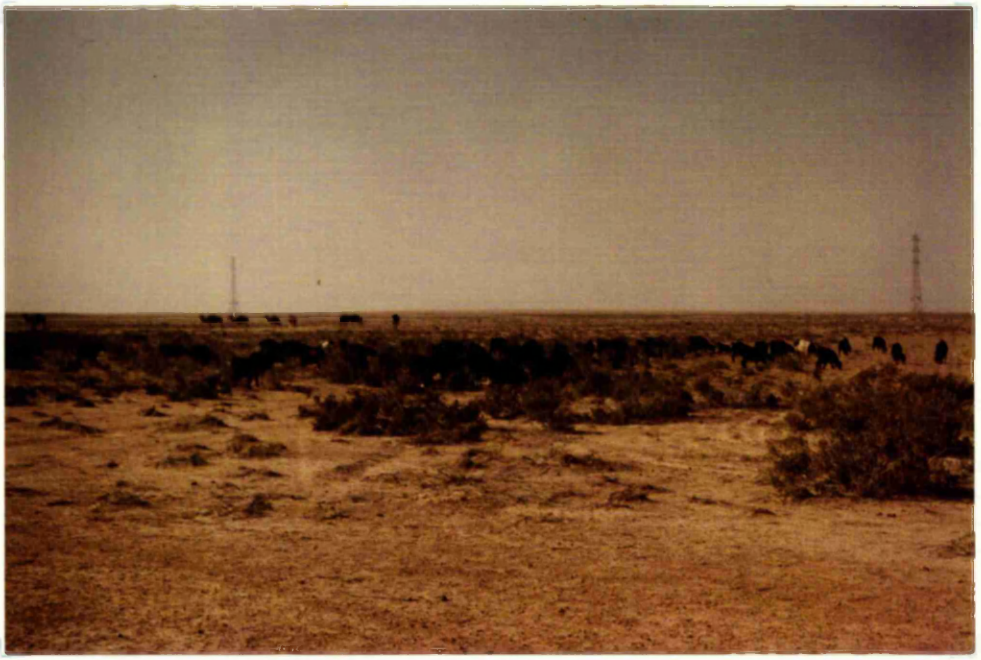

Plate 2.4.1

Goats and camels grazing to the south of Burg el Arab.

CONCLUSIONS

Environmental conditions along the northern coastal tract have a profound influence upon and ultimately determine the land use and agricultural practices of the region. Both rainfall and soil type serve as limiting factors in the cultivation of rainfed crops. Soil type serves as the primary spatial limiting constraint, with much of the area being unsuitable for cereal production. The extreme variability of rainfall serves as the secondary limiting constraint, by virtue of both its depth and its areal extent.

In the past these adverse environmental conditions have led to novel management systems which make the marginal production of cereal crops a viable activity. The problems of limited soils has been resolved by the production of 'man made soils' (FAO 1970) and by cultivation being restricted to suitable soils in areas of sufficient rainfall. This sometimes involves cultivation occuring in very localized areas. The second constraint of limited and variable rainfall, has been resolved by cultivating extensive areas in the hope that if rainfall is not sufficient in one area then it shall be in another.

The karm system may indeed be an attempt to tackle both of these problems. First, although the karms are all located on the more favourable soils for crop production, the high levels of salt in their banks may indicate that the soil of the central area has been improved by the removal of saline soil. Secondly, the structure of the perimeter banks may act as a donor surface for runoff farming. The fact that today cultivation occurs not

only on the inside of the karms but also on their outer flanks may support this supposition.

The introduction of irrigation to the region has in the irrigated areas removed the constraint of soil moisture deficit, although water shortages can still occur. The expansion of the irrigated area has been at the expense of rainfed cultivation and of the rangelands, and in some cases salinization by canal seepage and poor drainage has actually led to a decrease in cultivated area.

CHAPTER 3

REMOTE SENSING OF VEGETATION
A LITERATURE REVIEW

3.1 REMOTE SENSING OF VEGETATION - A LITERATURE REVIEW

Although statistical classification algorithms can identify clusters of data in 'n' dimensional space, they rarely give any qualitative descriptive information which can easily be understood and which is of great value to the earth scientist engaged in the classifcation of satellite data. An appreciation of the distribution of the data throughout the four-dimensional Landsat feature-space, and an understanding of the reasons for that distribution, are vital for the effective utilization of such data for vegetation mapping. In order to conceptualise the four-dimensional structure of Landsat Multi-Spectral-Scanner data, some authors have used qualitative descriptions of the data to aid their understanding and to further algorithm design and development (Kauth and Thomas (1979)). Conventional cartographic and display techniques do not allow the representation of four-dimensional data, as we are generally confined to projections of the data onto two, or two and a half (3-D projections) dimensions. Not only can graphical descriptions of the data aid our understanding of the distribution of data within space, they can also be used to relate the data structure to physical conditions such as crop development, soil moisture status and soil type. Probably the best known graphical metaphor for the Landsat data set is 'The Tasselled Cap' of Kauth and Thomas (1976).

Kauth and Thomas (1976) use two dimensional scatter plots of Landsat data to build up a conceptual picture of the 4-D data space. Plots of #6 vs #5 and of #5 vs #4 show that the data are distributed in the bands 4, 5 and 6 feature-space in the

form of a flattened triangle. A plot of #7 vs #6 confirms that the data set is of this 'flattened triangle' form within the 4-D space. It is this 'flattened triangle' which forms the basis of the Tasselled Cap.

By reference to the crop canopy model developed by Suits (1972) the authors are able to relate the triangular shape of the data to the physical development of a crop. Results calculated by the model, for the development of a crop on two different soil types, trace out the triangular shape of the Landsat data indicating that the spectral reflectance from a crop develops throughout the season from a point on the 'soil line', or 'soil plane', at the start of the season, towards the apex of the triangle at maturity, when chlorophyll absorption and near infrared reflectance are maximal. On senescence reflectance from the crop canopy returns once again towards the soil line, forming the tassel of the cap. In this case, however, the progression is in a different plane to that of the body of the cap.

The soil line (in two dimensions) or the soil plane (in three dimensions) is a phenomenon caused by the high correlation in all bands of the reflectance from soils. A two dimensional plot, for instance #7 vs #5, of soil pixels will result in a soil cluster which can be approximated to a straight line. The position of a particular pixel on the soil line is determined by the organic matter content, soil moisture, soil colour, surface structure, slope and aspect. Principal components analysis of Kauth and Thomas' soil data revealed that the soil cluster was a 'flattened cigar shape, about seven times as long

as it is wide, about twice as wide as it is thick, and twice as thick as it is thin' (Kauth and Thomas 1976 p 4b-42). The term 'twice as thick as it is thin' refers to the fourth dimension.

The role played by shadow within the crop helps explain the shape and structure of the tasselled cap. As the crop emerges and develops, band 7 reflectance from the green crop will increase, at the same time, however, the crop will cast shadows onto the soil. Thus the reflectance from a crop, planted on a bright reflective soil will at first decrease due to the shadow cast by the emerging crop. For a crop planted on a dark soil overall reflectance will not be so influenced by shadow as the difference in reflectance between shaded and unshaded soil is not so great as that for a light soil. As leaf area index increases the effects of shadowed soil on the overall reflectance will be reduced and reflectance will be dominated by the canopy. The path traced from the soil line to the apex of the tasselled cap is determined then, initially by the nature of the soil and later by the crop canopy. Cropping practice, such as the direction of planting of row crops in relation to the sun azimuth angle, will also have a significant influence upon the plant, soil, shadow relationships and hence spectral reflectance.

The authors also note that the path traced through feature-space by a senescing canopy is different to that of an emerging one. After maturity the tassel of the cap folds over and the path back towards the soil line is in a different plane to that of the main body of the cap. The authors call these features the 'fold of green stuff' and the 'point of yellow stuff'.

Whilst Kauth and Thomas recognize the importance of shadow in the initial development stages of a crop they neglect to address the question of how shadow can influence the overall reflectance from different plant species.

When data are distributed in a space in more than two dimensions it is difficult for us to perceive the important axes of variance, unless perhaps we have a three dimensional model of the data around which we can walk, such as a plastic model of an organic molecule. Attempts to project the data onto a two dimensional graph may or may not be informative depending upon the distribution of the data and the location of the axes of variance. A way around this problem is to rotate the data so that the axes of maximum variance are aligned with the axes of the data set. Thus the major axes of variance can be easily projected onto a two dimensional space, for example a sheet of paper. This forms the basis of Principal Components Analysis (PCA), which will be discussed in detail later.

Kauth and Thomas present a linear transformation which is designed to aid viewing of the 4-D data. The transformation, although not a Principal Components transformation, performs a very similar function to PCA. The transformation is supervised in that the first axis is aligned with the soil line. The advantages of such a transformation are threefold; first, the data distribution is more easily perceived; secondly, the transformation can lead to a data compression and thirdly, the transformation can act as a diagnostic feature extractor.

In Kauth et al (1979) the qualitative description of Landsat

data in terms of the Tasselled Cap is expanded and extended to form the basis for digital screening and correction. In addition to the tasselled cap the authors identify associated clusters of cloud, thin cloud, cloud shadow and water, and describe the systematic effects of haze and varying angles of solar illumination on the Tasselled Cap. Figure 3.1.1 is redrawn from Kauth et al(1979 pp 709) and shows the association of the tasselled cap to the other feature clusters. The presence of haze on a Landsat scene reduces contrast and increases pixels associated with the cloud cluster. This is exhibited as a translation and scaling of the tasselled cap within feature-space.

Kauth et al (1979) have used their knowlege of the data structure to outline a number of preprocessing techniques based upon the Tasselled Cap. They propose that a knowlege of the data structure can be used to screen out bad pixels, or scanner errors, which fall outside the known data structure and that secondly, the effects of haze can be minimised by first rotating the data using the 'Kauth Thomas' transformation and then adjusting the data to a reference position.

The graphical description of Landsat data by Kauth and Thomas provides a particularly useful paradigm for the study of vegetation detection using remote sensing techniques. It also allows for a visualization of the data structure. The quantitative measurement of leaf-area-index (LAI) using remote sensing techniques, however, requires that further refinements be made to the tasselled cap analysis. The tasselled cap description does however represent an analysis in all four

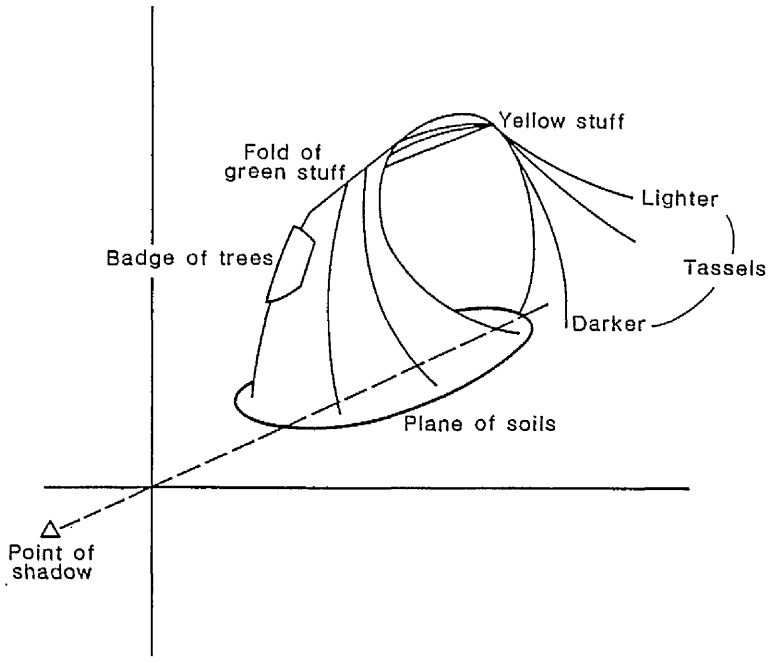

Figure 3.1.1

The 'Tasselled Cap'.
Source Kauth and Thomas (1976)

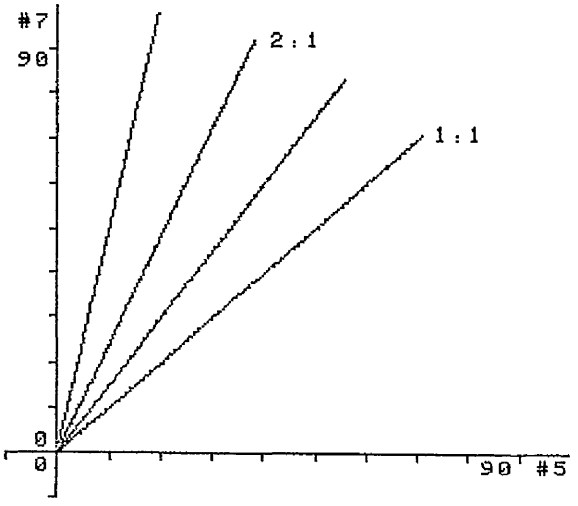

Figure 3.2.1

Landsat band 7 vs band 5 feature-space
showing the structure of a #7/#5 ratio.

dimensions of the data whereas subsequent developments along similar lines, for instance the Perpendicular Vegetation Index (PVI) (Richardson and Wiegand, 1977) have tended to reduce the analysis to a two dimensional problem, thereby disregarding potentially useful information. For a rigorous analysis of Landsat MSS data all four bands, or dimensions, of the data should be used. The problems, however, of visualising and hence implementing a supervised three or four dimensional rotation of the data, such as the Kauth Thomas transformation, have led researchers to simplify the problem by reducing the number of dimensions they work with, by either discarding one or more bands or, more significantly, by using principal components analysis.

Richardson and Wiegand (1977) developed further the notion of the soil line, or plane of soils, to try and explain and separate the effect of soil background reflectance on the spectral response of a mixed soil / vegetation pixel. Their analysis, based principally upon #5 vs #7 feature-space, revealed that a linear regression of reflectance values of dark soil, light soil, cloud and cloud shadow produced a best fit line with a slope of 1.2 and an intercept near the origin. This best fit, or soil, line was found to be constant from one satellite overpass to another and was therefore considered to be a suitable datum against which to measure leaf area index (LAI). Landsat data, collected at an earlier date, of sorghum fields of known LAI were plotted on the same graph as the previously established soil line. The authors noted that the LAI values deviated perpendicularly away from the soil line and tended to be distributed with the low LAI values near to the

soil line and the high LAI values furthest away from the soil line. This pattern forms the basis for the Perpendicular Vegetation Index, the index being the measure of the perpendicular distance from a vegetation point to the soil line.

Examination of the author's experimental results does indeed reveal a broad relationship between LAI and perpendicular distance form the soil line. The relationship, however, is not as marked as one might be led to believe, although this may be due to the fact that their soil line and LAI values were recorded on different dates, and also that LAI is difficult to measure in the field. The authors even suggest that the LAI estimates from the Landsat data may characterise the LAI estimates of the fields better than the field measurements themselves.

The soil line then, is regarded by Richardson and Wiegand as being an invariant datum of constant slope. In practice, however, this assumption is not necessarily valid unless the soil line is re-evaluated for each separate date and soil type.

3.2 THE VEGETATION INDEX

All of the, so called, vegetation indices, which are commonly described in the literature on remote sensing vegetation analysis, rely upon the absorption and reflectance characteristics of red and near infrared radiation by green vegetation. Figure 3.2.1 shows band 7 vs band 5 feature-space subdivided into simple 7/5 ratios. Hence, if the soil line has a slope of one and an intercept on the y axis of zero

then the 'vegetation triangle' will be sliced by the different ratios, thus crudely classifying the data. Similar subdivisions of the space can be accomplished by using difference indices, such as #7 - #5. A commonly used vegetation index, though one which is rarely fully described, is the Normalized Difference (NDVI).

$$ND = \frac{\#7 - \#5}{\#7 + \#5}$$

The difference between the reflectance in band 7 and band 5 is normalized by the total intensity of the two bands, ie their sum. The normalization, by division by intensity, helps eliminate effects caused by shadow, sun elevation and system characteristics. Other variations on the ND are also used, such as the Transformed Vegetation Index (TVI), where a constant of Ø.5 is added to the ND and the squareroot taken in order to prevent negative values occurring.

An alternative to difference and ratio indices is the Perpendicular Vegetation Index (PVI) of Richardson and Wiegand (1977). The PVI characterizes a pixel in terms of the perpendicular distance from that pixel, in feature-space, to the soil line. Figure 3.2.2 diagramatically shows the principle of the PVI. Whereas the subdivision of the vegetation triangle by a ratio is dependent upon the slope and intercept of the soil line the PVI measures the distance to the soil line wherever it may be, assuming that the correct position of the soil line, or soil lines, has been determined. Theoretically

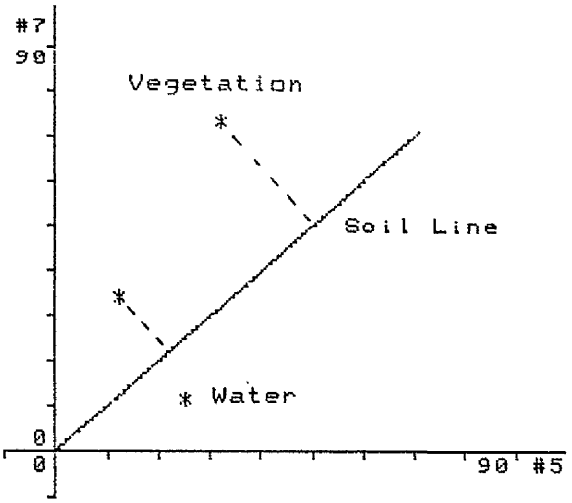

Figure 3.2.2

The Perpendicular Vegetation Index
after Richardson and Wiegand (1977).

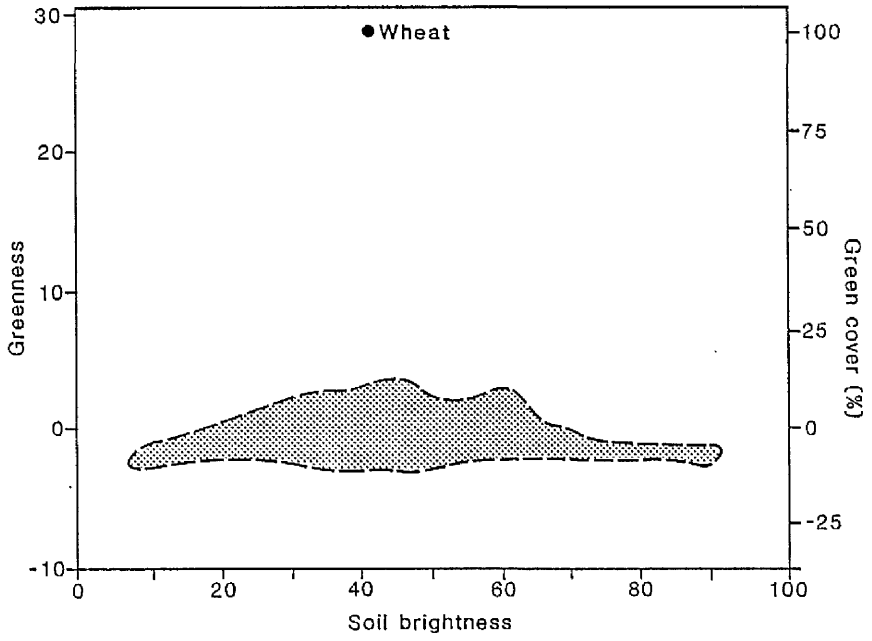

Figure 3.2.3

Soil spectra in the main soil brightness-
greenness plane.
Source Huete et al (1983).

the PVI is independent, through time, of the variations in the slope and position of the soil line through atmospheric and system conditions.

Hielkema (1981) used a simple #7/#5 ratio to map vegetation in northern Africa for a series of different dates. Variations in the slope of the soil line, between the different dates of data collection, meant that some form of data normalization was required. Hielkema approaches this problem by rotating and translating the data so that the soil line has a slope of one and an intercept at zero. By performing this transformation, the data from the different dates can be directly compared. However, had Hielkema used the PVI then this rotation and translation of the data would not have been necessary.

The notion of the soil line, the PVI and Hielkema's rotation, whilst providing meaningful information regarding green vegetation cover these methods all reduce the problem of vegetation detection to a two dimensional one, disregarding bands 4 and 6 and the potentially meaningful information in them. In this way the PVI reduces the three or four dimensional tasselled cap to a two dimensional vegetation triangle, thereby losing the discrimination between green vegetation and yellowing vegetation on either side of the 'fold of green stuff'. In addition the PVI, and simple ratios, only slice the data in one dimension, ie parallel or at an angle to the soil line. Much information about vegetation is present within the vegetation data along the axis of the soil line, thus a two dimensional slice may be more informative. The Kauth and Thomas transformation allows the Green Vegetation Index (GVI)

to be calculated. In essence it is a four dimensional PVI which considers all of the data. It can be seen that Richardson and Wiegand's assumption; that the same rotations which Kauth and Thomas applied to their data, to align the data axes to the soil line, could be transported to their study area, is not valid when one considers the variability of Landsat data between different dates. It is therefore not surprising that in their evaluation of different vegetation indices Richardson and Wiegand found the PVI to be a better indicator of leaf area index than the GVI.

The notion of a single unique soil line has been prevalent for some years but has been challenged by Huete et al (1983) who examined the spectral properties of some twenty different soil types with differing physical and chemical properties. The authors argue that if the slope of the soil line varies between soil type, and hence spatial location, then the assumption that the soil line is a single entity will lead to inaccuracies in estimating vegetative cover. This will be particularly true with low levels of vegetation cover. Principal components analysis of their data revealed a plane of soils similar to that described by Kauth and Thomas (1976), a cluster with percentage variances of 98%, 1.6%, Ø.2% and Ø.1% along the four principal components respectively. The variance of 1.6% in the second component, which is normally associated with greenness, although relatively small, meant that vegetation cover below 26% cover could not be distinguished from bare soil.

Figure 3.2.3 taken fron Huete et al (1983 pp3) shows their results and highlights the uncorrelated nature of the soil

cluster made up from a large number of soil types.

An average Landsat scene would probably not contain such a wide variety of soil types as Huete's data and would therefore have a narrower soil cluster, or second principal component. Huete's analysis of the data in terms of the individual soil lines, revealed a wide deviation in the lengths and slopes of individual soil lines from the mean. The majority of lines, which were not coincident with the mean soil line, had a positive slope compared with the zero slope of the rotated mean soil line. For those soil lines with a positive slope, estimates of PVI will, for vegetation on that soil type, be erroneous when the mean soil line is used as the PVI datum. The authors found that in some cases a vegetation cover of ten percent would be interpreted as bare soil. An analysis of the individual soil lines revealed more highly correlated clusters with widths in the greenness component equivalent to only seven percent cover. The mean soil line, on the other hand, had a width in the greenness component of some twenty six percent. The width of the soil line, whether an individual or mean line, effectively determines a vegetation density limit, below which remote sensing cannot hope to detect vegetation.

The work of Heute et al reveals the need to stratify vegetation mapping in terms of soil types. This is particularly the case in areas where vegetation cover is low and areas with diverse soils. The procedure for stratified digital processing, along these lines, obviously demands more computer processing time and more diverse digital inputs. The benefits, however, of such an approach should lead to increased estimates of

vegetation cover, particularly in the arid regions. The 'vegetation density limit' is an important concept and the implication of Heute et al's results is that remote sensing of vegetation cover down to ten percent may be possible. The 'vegetation density limit' specifies a theoretical minimum detectable cover on the basis of the degree of correlation of the soil line.

3.3 MULTITEMPORAL CLASSIFICATION

Some authors have noted the hysterysis curves obtained when multi-temporal spectral measurements are made throughout it's growing cycle (Curran (1981)). The reason for the shape of these curves can be explained by the development of the canopy / shadow relationship as the crop emerges, as discussed above. The form of the curves essentially determines the shape of Kauth and Thomas' Tasselled Cap. The scattergram of #7 vs #5 for a Landsat scene will contain data from many different crops at different stages of development and consequently the scattergram is very general. However, measurements of individual crops can reveal the spectral path through feature-space throughout the growing season.

Misra and Wheeler (1978, 1979), in their analysis of wheat fields in Kansas USA, noted that the high correlation between the two visible bands and also that between the two infrared bands leading them to suggest that Landsat data is essentially two dimensional and that only the two principal dimensions need be analysed. Kauth and Thomas also noted this attribute of the

data but considered the information contained in the other two bands to be significant.

Misra and Wheeler (1978) base their analysis upon the observation that the variability of spectral response from different wheat fields, at all stages of crop development, is so great as to invalidate the assumption that a given ground cover type can be identified by its spectral signature. Not only do the authors consider that the response of wheat fields are not sufficiently similar to form the basis of classification, but also, that the response of wheat and bare soil are not sufficiently dissimilar to distinguish between these two basic cover types. Such observations, if true, invalidate the majority of research into the detection and classification of crops using remote sensing. Whether one accepts these observations or not their subsequent analysis represents a very interesting and significantly different approach to the main stream of research.

The schematic plots shown in Figure 3.3.1 form the basis of Misra and Wheeler's classification. Analysis of their multitemporal data revealed that wheat invariably exhibited an 'e' shaped trajectory in it's progression through feature-space, the trajectories of non-wheat classes being significantly different. Thus the problem of crop classification is reduced to a problem of pattern recognition not dissimilar to handwriting analysis. More recently other authors have used the multitemporal nature of radiometric data to classify crops. Tucker et al (1985) have used NOAA AVHRR data to perform mulitemporal principal components classifications while

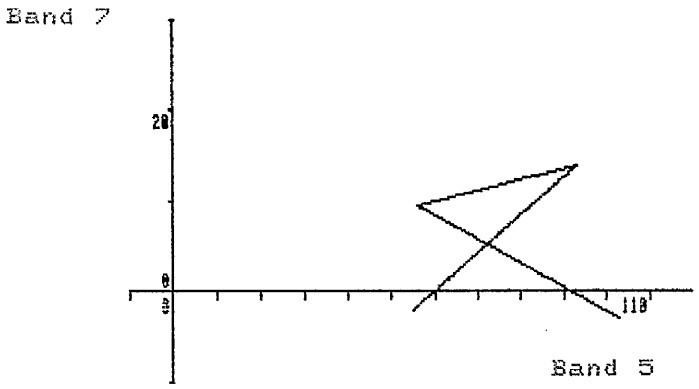

Figure 3.3.1

The temporal changes in the spectral response of wheat fields.
Source Misra and Wheeler (1978).

Ajai et al (1985) have used multitemporal handheld radiometer data to make non-destructive classifications of crops in the field.

3.4 PRINCIPAL COMPONENTS ANALYSIS

To relate in human terms to Landsat data we must first 'escape' from the four dimensional nature of the data to a lower, more manageable, number of dimensions. Being restricted in life to only three physical dimensions it is impossible for us to be able to perceive the way in which data can be distributed in four, or more, dimensions. The escape from four dimensional space can be accomplished in a number of different ways. An escape can be made by simply disregarding one or more of the dimensions. This leaves us with a data set which we can understand and manage; it does not, however, necessarily leave us with a data set which contains the important information. Of the papers discussed so far Richardson and Wiegand (1977), Hielkema (1981) and Misra and Wheeler (1978, 1980) have all adopted this particular form of escape by recognising that Landsat data are essentially two dimensional and consequently concentrating on only bands 5 and 7. Mulder (1975) in his paper 'How to escape from 4-dimensional space, or statistics versus knowlege' outlines a method of not only escaping from 4-D space, but of escaping with the most significant information. The escape is accomplished by a Principal Components Analysis (PCA) of the data. Although used by some of the authors quoted above in their papers Mulder (1975) emphasises the importance of PCA in itself, rather than using the transformation to demonstrate the basic two dimensionality of the data and using

this as an excuse for disregarding two of the bands. Principal Components Analysis can be defined as a linear transformation by which the data are rotated in 'n' dimensional space to define a new set of axes which are aligned with the axes of major variance within the data. Each new axis, or principal component, accounts successively for as much of the remaining variance within the data as possible. Each of the new axes are at right angles to each other and 'n' is the dimensionality of the data. Principal Components Analysis of Landsat data, Mulder argues, will result in two new axes which will typically contain 98 per cent of the variance within the data. Assuming that variance is correlated with 'meaning' then these first two principal components can be substituted for the original bands thus resulting in a data compression, in that two bands can be disregarded, and a concentration of that data which is meaningful.

This paper represents a divergence from the more conventional statistical classification of MSS data and is one which, in the field of vegetation mapping, has gone largely unnoticed. Mulder argues that the statistical description of multi-dimensional data, based upon the assumption of Gaussian distributions, is not necessarily a valid basis for classification. He further argues that a trained interpreter can analyse two dimensional PC feature-space without the aid of either the assumption of Gaussian distribution or statistics, and that he or she can define decision boundaries on the basis of real distributions of the data and not the 'assumed distribution functions'. In addition, mixed or overlapping clusters should be displayed as such and not assigned to one class or the other on the basis of

maximum likelihood. In conclusion Mulder states:

> "Statistics are the crutches of the mind in high dimensional space."
> Mulder (1975) p 359

A further development of Mulder's PCA approach is presented in Donker and Mulder (1977). In this paper the procedures outlined in Mulder (1975) are applied to a test site in the Netherlands. Principal Components Analysis of the data revealed that the first two components accounted for some 98 per cent of the total variance within the data. From their analysis Donker and Mulder conclude that the first principal component 'represents a general picture of overall radiance intensities' (Donker and Mulder 1977 p 454). The second component, on the other hand, they name the ' green or non-green factor'. We can see that this analysis is similar to that of both Kauth and Thomas (1976) and Richardson and Wiegand (1977) in that the soil line (plane) in analagous to PC1 and that the Perpendicular Vegetation Index is analagous to PC2.

Donker and Mulder colour code their image by projecting PC1 in red and PC2 in green. In this way an overlay of the PC2 vs PC1 feature-space can be placed over an image of the red-green colour space to form a key for visual interpretation. In addition the authors suggest a rotation of the PC feature-space to maximise the colour contrast between classes of particular interest. Whilst being a novel and effective technique it does not lend itself to any form of standardization between multi-temporal data as does the Kauth and Thomas transformation

which, in effect, is a supervised PCA standardized to the soil line as a datum.

3.5 INTENSITY, HUE, SATURATION COLOUR CODING

The recognition of two significant components in Landsat data, an intensity component and a greenness component, has led Mulder to develop the IHS transformation in it's application to scalar and particularly MSS data.

Mulder emphasises the need to select the 'significant' transformations for mapping 'n' dimensional data into a three dimensional colour cube, and states:

> "We are looking for interpretations which show (in the most simple way) a homomorphism between structures / effects in data space and structures / effects in colour space"
>
> Mulder (1982) pp2

Mulder next defines four requirements which a transformation should adhere to, these being:

(1) Maximum homomorphism between Nn and N3 structures with the simplest (linear) transformations.

(2) If useful models exist for the multispectral interactions of light and matter (classes) then the structure of the model must be reflected in the mapping transformation of these classes.

(3) Useful separation between classes will remain or be increased by significant mapping.

(4) Choice of colour axes (hue) must be such that a simple and constant relation exists between colour and class (mnemonic legend).

These four requirements are adhered to by the IHS transformation but are all too frequently not considered when other transformations of multispectral data are made. Examples of transformations which frequently do not adhere to these requirements are the principal components transformation and the false colour composite. Principal components are frequently displayed as multispectral images, ie mapping PC1 to red, PC2 to green and PC3 to blue. This mapping does not adhere to points (3) and (4) above as principal components displayed in this way do not relate visually to meaningful attributes of the data, for example the intensity of such an image does not relate to the intensity of radiation received at that point. Similarly false colour composites fail to meet requirement (4) as their colour mapping is not done in a mnemonic way, ie they are 'false colour'.

Mulder uses three distinct colour co-ordinate systems both to describe and to manipulate the data. Only one, however, is of interest here, this is the Intensity Hue Saturation co-ordinate system.

Figure 3.5.1 shows the colour triangle and the colour cube. The colour cube is defined by RGB colour space, while the colour

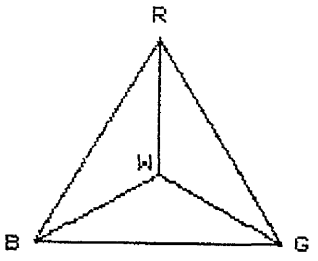

Figure 3.5.1a

The colour triangle.

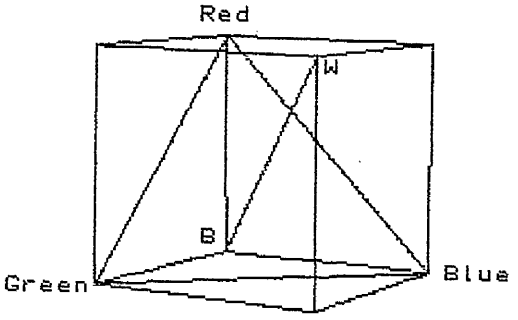

Figure 3.5.1b

The colour cube.

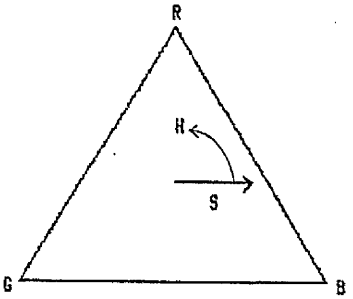

Figure 3.5.1c

The relationship between hue and saturation.

triangle is a subset of this colour space and is a plane of equal intensities. The position of the colour triangle within the RGB colour space is shown in Figure 3.5.1b, in this case it is a plane of intensity equal to one third. Also annotated in this figure is the intensity line, lying between points B(lack) and W(hite). It is along this axis that intensity increases; black being at point (Ø,Ø,Ø) and white being at the point (255,255,255). It is about this axis that the IHS system is based. The relationship between hue and saturation is defined in polar co-ordinates; hue being the angular rotation from the datum (red) and saturation being the radial distance from the origin (white) to a point. The relationship between hue and saturation and the colour triangle is shown diagramatically in Figure 3.5.1c.

By using the IHS methodology of colour coding the Landsat data can be isomorphically mapped into RGB colour space. In other words; the intensity of reflectance (B4+B5+B6+B7) in the Landsat bands is displayed as intensity in the colour image. There is therefore a relationship between the data space and the colour space, and a meaningful interpretation of the image may be made. IHS colour coding, in a similar way to principal components analysis, separates the intensity and greenness components within feature-space. IHS not only separates the components but it does it in a physiologically meaningful way which is not achieved by using false colour principal components images. False colour principal component images are not used in chapters four and six and it was therefore not felt necessary to pursue the alternative of IHS.

3.6 ARID ENVIRONMENTS - A SPECIAL CASE

The applications of multispectral digital data to vegetation mapping discussed above, are all concerned with temperate environments. The arid environment, however, is a special case in that although many of the techniques described above can be used for the detection of green vegetation , the Landsat feature-space distribution is somewhat different. The reflectance from the earth's surface in arid regions, due to the sparcity of vegetation cover, is dominated by the spectral properties of the soil. The influence of vegetation on overall reflectance is consequently of a secondary nature.

The familiar graph showing the spectral properties of vegetation, soil and water in the Landsat bands, shows the reflectance of vegetation in the band 7 region as being much higher than that for soils. In many arid regions, however, and particularly in northern Egypt, the reflectance from the soil can be greater than that of even a dense green vegetation canopy. Consequently the position of vegetation pixels within Landsat feature-space in an arid region is somewhat different from data recorded in a temperate region. Curran (1981) has shown that as leaf area index increases over a highly reflective substrate, near infrared reflectance can actually decrease.

Another factor characteristic of arid regions is the fact that vegetation is only green for part of the year. For the remainder of the year, during the hot dry summer, annual species die off and perennials yellow and enter a dormant

period. As the yellowing process happens band 5 reflectance increases as chlorophyll absorption declines, and band seven reflectance may remain more or less the same and possibly increase. Whilst the plants are dormant, although they are leafless and brown they will still have an effect upon the surface reflectance in that they will cast shadows on the surface, thereby reducing overall reflectance. The only author to have addressed this problem directly has been Otterman (1981, 1984,1985), Otterman and Robinove (1982) and Otterman et al (1983). Otterman has developed a model to describe the reflectance of a bright Lambertian surface randomly covered with a sparce dark canopy. The canopy consists of randomly located vertical protrusions with horizontal facets. The model is designed to mimic the perennial vegetation cover of the Sinai and Negev deserts. It is derived from the plant canopy model developed by Suits (1972). Otterman argues that a plant canopy is a complex surface which does not act as a Lambertian reflector. The bright soils found in many arid regions can, he argues, be regarded as being Lambertian and are one of the few natural surfaces which can indeed be regarded as such. Otterman quantifies the canopy by using two dimensionless parameters; 's' and 'u'. 's' is the area of the projections of the vertical cylinders onto a horizontal surface per unit surface area and 'u' is the area of the horizontal facets projected onto the horizontal plane. Using this model Otterman defines a procedure for evaluating spectral albedo measurements which are independent of sun/sensor viewing geometries and which can subsequently be used to monitor environmental change. The work of Otterman et al probably represents the most significant research into arid land

vegetation remote sensing to date. The approach represents a significant divergence away from the analysis of temperate region vegetation by remote sensing and much work remains to be done in the field.

3.7 SUMMARY

We have seen how Landsat MSS feature-space can be sub-divided in a variety of different ways so as to isolate the data pertaining to vegetation. This process can be done in two, three or four dimensions. Some of the methods are more meaningful than others in describing vegetation, in that the way they divide the feature-space can be related to the physical properties of the crops. Not only can we meaningfully sub-divide static feature-space, but we can also classify vegetation in terms of multitemporal feature-space which is determined by the phenological cycle of the crop. The problem of separating the spectral response of soils and that of vegetation can also be accomplished in more than one way. Richadson and Wiegand (1977) have dealt with this problem by using the PVI whilst Donker and Mulder (1977) have used PCA and Mulder (1982) has used IHS colour coding to separate surface reflectance from surface intensity. It should be appreciated, however, that all of the methods examined (with only the exceptions of Otterman (1981, 1984,1985), Otterman and Robinove (1982) and Otterman et al (1983) and Misra and Wheeler (1978)) are different expressions of the same phenomena, that is the spectral properties of the green leaf in the visible and near infrared. The PVI, NVI, TVI, GVI, PCA and IHS are all doing basically the same thing, although some have more favourable

and meaningful effects than others. The thrust of work in this thesis is to try and improve the results obtained using these techniques in the arid northern coastal tract of Egypt. Further comments on the multitemporal aspects of monitoring are made in the final chapter.

CHAPTER 4

INITIAL DIGITAL PROCESSING

4.1 AVAILABILITY OF LANDSAT IMAGERY

Landsat MSS imagery of the coastal tract was available for two periods; February 1973 and February 1978. The five year separation between the two dates meant that change monitoring over this period would be possible, given certain image processing facilities, (ie the ability to match (warp) the images spatially , either to a map reference or to each other), and the [illegible] software to correct the data for sensor calibrations and the effects of sun angle. These facilities were not available until the latter part of the study.

Unfortunately cloud obscured, or partially obscured, the two principal study areas on the 1973 imagery, thereby limiting the usefulness of the data. The 1978 imagery, however, were for the most part cloud free, although some of the images showed signs of dust close to the ground in streaks aligned with the direction of the prevailing winds. One image also exhibited what is presumed to be an aircraft vapour trail, although this did not obscure any areas of particular interest.

The very large volumes of disc space taken up by even a single Landsat scene and the need initially to understand the distribution of the data meant that two relatively small study areas were chosen for investigation, with a view to extending the scope of the study after this initial learning phase. The two study areas chosen were Transects one and three of the REMDENE study. These transects were chosen as they have been particularly thoroughly mapped by the REMDENE staff. The transects are located around the settlements of Burg el Arab

and Omayed respectively. Figure 4.1.1 shows the location of and scenes available for this study.

4.2 AVAILABILITY OF IMAGE PROCESSING FACILITIES

The image processing for the first phase of the study was conducted on the GEMS image processor at the Royal Aircraft Establishment, Farnborough. Although the GEMS was an operational system at the time, the software package GEMSTONE was still in the course of development and to a degree the availability of specific functions dictated the course followed in the initial phase of the study. In particular a maximum likelihood classifier was not available at the time although this has now been implemented. The image processing presented in this chapter was, on the whole, conducted at RAE Farnborough, whilst that presented in later chapters was done at University College, London; and Bristol University on I2S image processors.

4.3 TRANSECT 1 - THE FALSE COLOUR COMPOSITE

Transect 1 is located in and around the town of Burg el Arab and stretches from the coast to 50 km inland, it's location is indicated in Figure 4.1.1. A wide variety of agricultural crops and practices occur within the transect, ranging from irrigated vegetables, cereal and fodder crops, through dryland cereal production to semi-natural rangeland vegetation. This wide range of agricultural practices provides a most useful and diverse study area. The physiography, climate and geology of

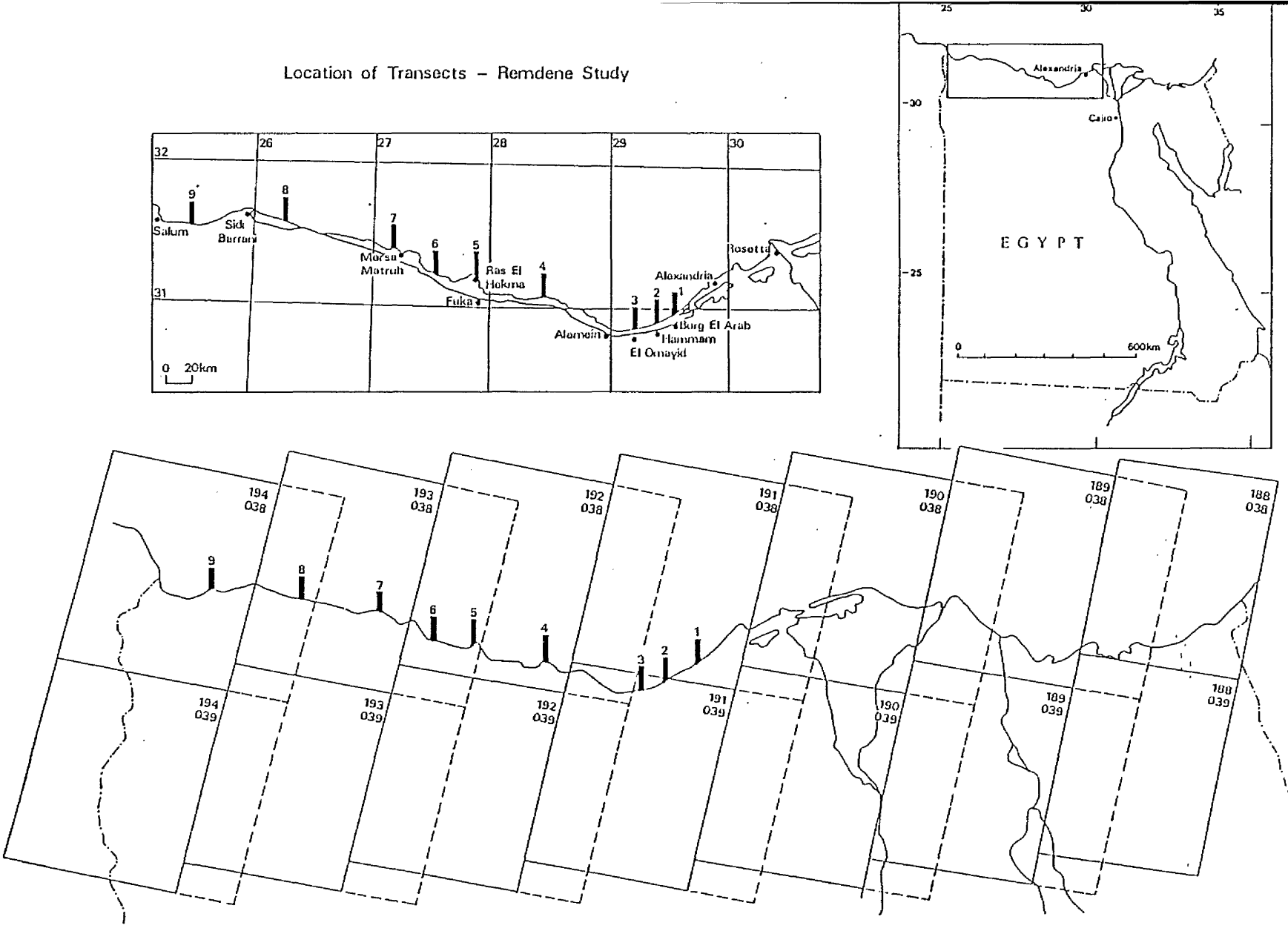

Figure 4.1.1 Location map showing the association of the REMDENE transects with the path and row numbers of the Landsat scenes.

the transect are described in chapter two.

The town of Burg el Arab has a population of some ten thousand people and is situated on the railway line which makes it's way along the coast from Alexandria to Mersa Matruh. The fresh water pipeline, built by the British during The Second World War between Alexandria and El Alemein, also passes through the town. In addition to the pipeline, Nile water is brought to the area by canal for the irrigation of crops. Irrigation occurs as far west as Hammam, which is located mid-way between Burg el Arab and Omayed (Transect 3). The irrigated area consists of a narrow band following both the cultivable soils and the irrigation canal, the fields often being protected by windbreaks of well established trees.

The coastal tract is characterised by a system of ridges and depressions which run parallel with the coast and which form the most prominent feature of the landscape. Plate 4.3.1 is a false colour composite image of Transect 1 which has been enhanced by a linear contrast stretch. The image in fact covers a wider area than the REMDENE transect and does not extend to 5Ø km inland, it does, however, contain all of the major featues, both agricultural and physiographic, of the transect.

Working from the coast inland the first prominent feature on the image is the system of coastal sand dunes, the bright white strip running along the shore line. To the immediate south of the coastal dunes lies the first inland depression. This depression is narrow and relatively shallow and in places supports thecultivation of figs and occasionally palm dates,

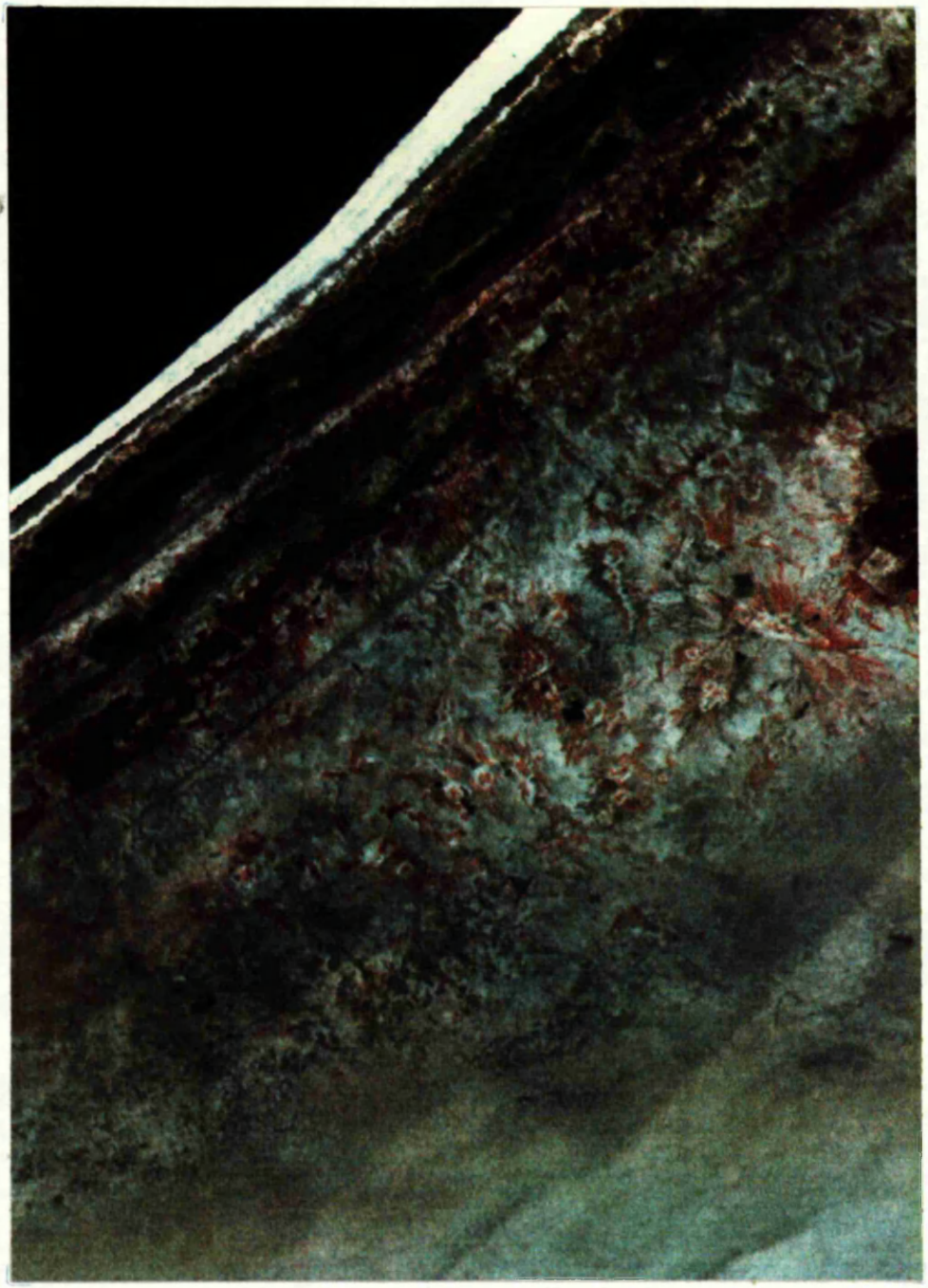

Plate 4.3.1

Transect 1 false colour composite. An extract from Landsat 2 scene 191/039, imaged on 11.2.78.
Linear contrast stretch.
Scale 1 : 220 000

although in some parts it is permanently inundated with water. The cultivation of tree crops within the depresson is more often on the slopes rather than in the valleys thus providing better drainage. Natural vegetation which occurs within the depression is of the leafless succulent type which forms hummocks by the accumulation of windblown sand around the base of the plants. This depression is often so narrow that it only consists of one or two pixels on the false colour image.

To the south of the first depression is the first ridge of the system. This ridge is hard and stoney and supports no crops on it's apex. On it's southerly side, however, tree crops are cultivated and red areas, indicating vegetation, are evident on Plate 4.3.1. To the south of this ridge is a wide depression which is an extension of the depression which forms Lake Marjut to the north-east. Large areas of this depression are permanently underwater or waterlogged, the water and soils being very saline with, in places, a thin salt crust. The areas of standing water and salt marsh are evident on the false colour image. No cultivation occurs anywhere within the depression other than on the northern and southern banks where salinity is low.

To the south of this broad depression is another ridge and to the south of that another much smaller depression. It is clear from the Plate that the irrigated agriculture is confined between the Mariut marsh and the inland ridge. To the south of the inland ridge is the majority of the dryland barley cultivation, although some does also occur just to the north of the ridge and in scattered places among the irrigated

cultivation. The irrigated agriculture is evident from the deep red areas on the false colour image, while dryland barley exhibits a pinkish colour. The darker reds associated with the irrigated vegetation are the product of two factors. First, in this environment the irrigated crops will be more vigorous and will have more complete canopies, both due to the types of crop and the availability of water, than the dryland crops; this will be the case in all but the wettest of years. Secondly, the wetness of the soil in the irrigated fields will tend to reduce the proportion of irradiance reflected by the soil where the canopies do not completely cover the ground.

The cultivation of dryland barley at Burg el Arab is of particular interest. It can be seen from Plate 4.3.1 that the barley cultivation to the south of the inland ridge is, for the most part, located in and around circular structures. These structures, called Karms, date from the Roman period and are still in use for barley cultivation today. The structures consist of banks of earth, often five or more metres high, which form a square or horseshoe shaped enclosure. For a description and discussion of the karms see section 2.3.2.

4.4 DISTRIBUTION OF THE DATA WITHIN LANDSAT FEATURE-SPACE

Transect 1 contains a wide variety of cover types including a number of different soil types, different depths and qualities of water and a whole spectrum of vegetation types and levels of cover. The Landsat feature-space would be expected to reflect this diversity by a well distributed data set. Looking

at and perceiving the distribution of the data is, however, problematic. If the data are not aligned with the axes of the data set, then it is not always possible to appreciate the distribution of the data. Principal Components Analysis can help to this end and is discussed in the next section. Here we are concerned with only the two dimensional band combinations possible with the raw data.

Figure 4.4.1 shows the band 7 vs band 5 scatterplot for Transect 1. The scatterplots for the other band combinations are highly correlated and are not reproduced here. The scatterplot of band 7 vs band 5 is the least correlated of the combinations, as we might expect, and the combinations of the two visible and the two infrared bands being the most correlated. This pattern within the data is typical of Landsat scenes of agricultural areas. The somewhat unexpected lack of variation in the band 7 vs band 5 combination is partially a feature of the highly reflective soils of the region. The difference in reflectance between the bright dry soils and the dark wet soils is far greater than that between the response of bare soil and one hundred percent vegetation cover. However, the scatterplots for Transect 1 do exhibit a far greater variation than those for Transect 3, this difference being a direct result of the respective range of vegetation cover types in the two transects.

The distribution of Transect 1's data within the Landsat feature-space can be regarded as being typical of data recorded in an arid region with a wide variation in vegetative cover. The dominant feature of the distributions is the wide variation

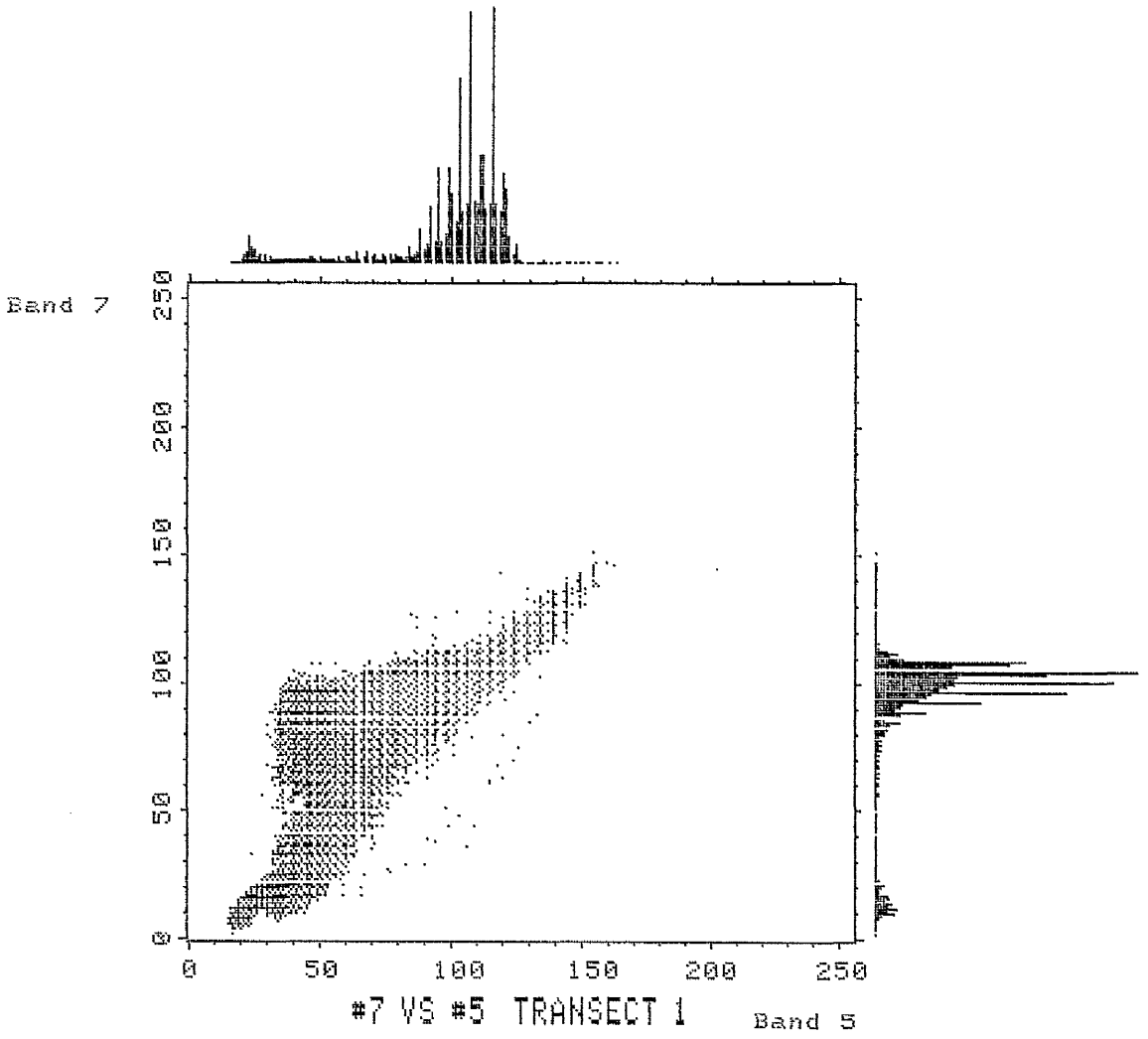

Figure 4.4.1

Scatterplot of band 7 vs band 5 for the Transect 1 area.

in the reflectance from wet and dry soils; this feature being far more evident than the difference in bare and vegetated soil. In addition, the infrared reflectance from vegetation, which in temperate regions is considered to be high, is very much less than that from dry soil, thereby resulting in a decline in infrared reflectance with increasing vegetative cover. This causal relationship between increasing vegetative cover and decreasing overall infrared reflectance is documented by Curran (1981).

4.5 TRANSECT 1 PRINCIPAL COMPONENTS ANALYSIS

As mentioned above, it is not usually possible to perceive the true distribution of data within a space by simply looking at two dimensional scatterplots. This is especially true if the major axes of the data are not aligned with those of the data set. Principal Components Analysis, if used carefully, can help to overcome this problem by rotating the data so the the major axes of the data are aligned to the axes of the data set. In this section two different PCA studies are presented, the difference between them being in the method of sampling used for the transformation.

Table 4.5.1 shows the statistics obtained by conducting a principal components analysis on bands 4,5 and 7 of Transect 1.

TABLE 4.5.1

Means	:	78	62	52
Standard Deviations	:	37.23	25.74	14.44
Percentage Eigen Values	:	96.84	2.58	Ø.58
Eigen Vector Matrix	:	-Ø.788	-Ø.541	-Ø.292
		-Ø.585	Ø.512	Ø.627
		Ø.189	-Ø.666	Ø.721

The eigen values, expressed as percentages, clearly show that the data are highly correlated, with the first principal component accounting for nearly 97% of the total variance in the three bands. The eigen vector matrix defines the relationship between the original data and the principal components. It is this matrix which is used to transform the data to produce the new PC images. The product of the raw data vector, multiplied by the eigen vector matrix comprises the new PC vector.

Thus:

B4 B5 B7		EV Matrix		PC1 PC2 PC3
* * *	x	* * *	=	* * *
		* * *		
		* * *		

With the knowlege of the general distribution of the data within feature-space, gained from the scatterplots in Figure 4.4.1, we can assume that the first principal component lies close to the soil line. This is a valid assumption in that the soil line is obviously the dominant feature of the data. If this is truly the case then we can use the transformation as a way of performing the PVI of Richardson and Wiegand (1977); as the first PC will be aligned with the soil line and the second PC will be aligned with the greenness axis. In this way it should be possible to slice PC2 into different levels of leaf area index.

Figure 4.5.1 shows the scatterplot obtained by plotting PC2 vs PC1. It is quite apparent that the scatterplot is far less correlated than that of band 7 vs band 5 in Figure 4.4.1. This is due both to the PCA finding the least correlated axes within the data and also to the scaling which has been applied to the data to ensure that it still fits into the feature-space.

A number of important and interesting features can be seen in this figure. First, although distinct clusters occur the data forms a continuum, each cluster merging with the next or being joined by a series of points. This continuum is a reflection of the real world where discrete land cover classes rarely exist, for instance the boundary between greater than and less than thirty percent vegetation cover, where the distinction is merely a contour rather than a strict division. The continuum indicates that a whole spectrum of soil, water and vegetation states exist in Transect 1.

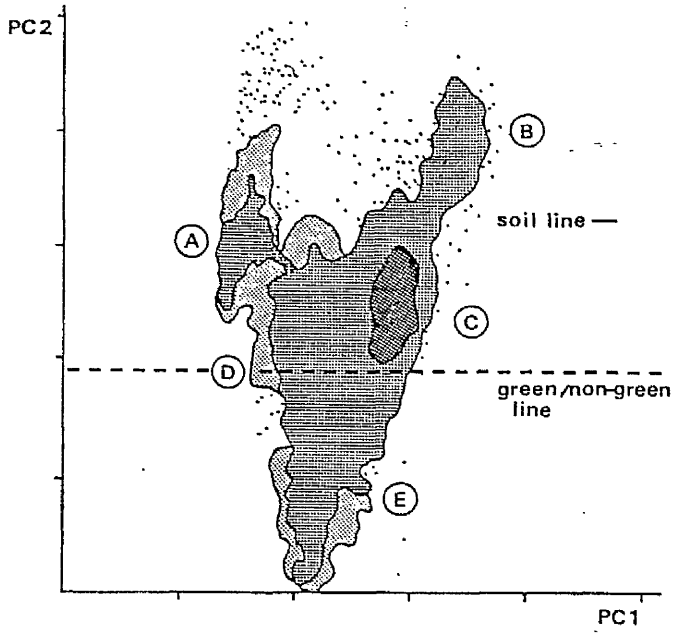

Figure 4.5.1 a

Transect 1 PC1 vs PC2 feature-space.

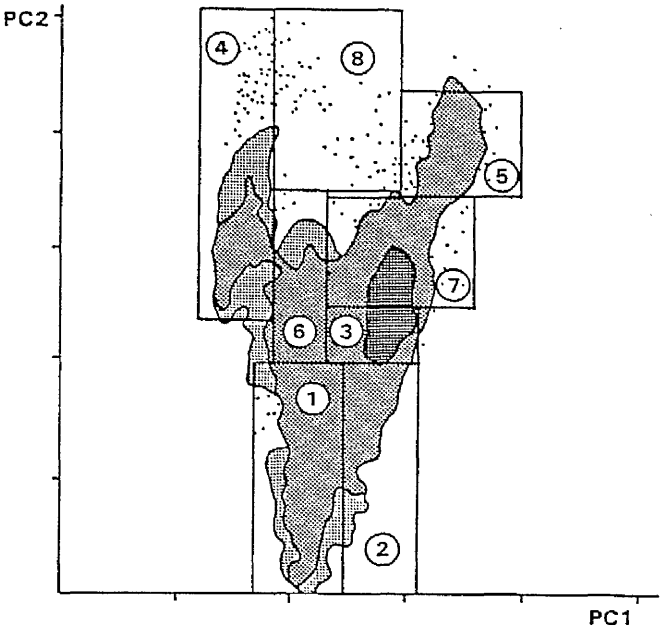

Figure 4.5.1 b

Transect 1 classification decision boundaries within PC1 vs PC2 feature-space.

Secondly, the data have been rotated so that the soil line is horizontal and the vegetation axis is vertical, although inverted. This is as we might expect and will allow the second PC to be sliced thereby performing a PVI. Figure 4.5.1 is annotated with the five major classes which may be inferred to exist and a green/non-green line which defines the effective boundary between vegetation and soil. The five classes represent:

A	Water
B	Coastal sand dunes
C	Soil
E	Vegetation
D	Salt marsh

Thirdly, by a process of parallelpiped classification and interpretation of the PC images associated with the scatterplot, it is possible to subdivide the feature-space into further classes. In this way the feature-space was subdivided in two dimensions into eight of the major classes occurrng in Transect 1. Figure 4.5.1b shows this subdivision and Table 4.5.2 shows the associated land cover classes.

TABLE 4.5.2

Cluster	Class	Colour	Percentage Area
1	Irrigated vegetation	Dark green	5.20
2	Dry-land farming	Green	3.88
3	Range vegetation	Orange	22.74
4	Water	Blue	13.66
5	Coastal dunes	Cyan	1.17
6	Salt marsh	Brown	3.83
7	Bare soil	Grey	48.95
8	Beach	Red	0.18

The colours in the above table refer to the classified image of Plate 4.5.1.

The differences in soil moisture between the irrigated and the non-irrigated fields suggests that if a crop canopy does not obscure all of the soil surface then the soil's spectral properties will influence the overall radiometric value of that field. Thus, an irrigated field with eighty percent plant cover will yield a lower radiometric reading than a non-irrigated field with eighty percent plant cover, because of the difference in soil moisture status between the two fields, the irrigated field being wetter and hence darker. Therefore, we may reasonably expect irrigated and non-irrigated vegetation to occupy different places in feature-space. This hypothesis was borne out by the decision boundary selected between classes one and two. The vertical division on PC1 successfully separated these two cover types in the classification.

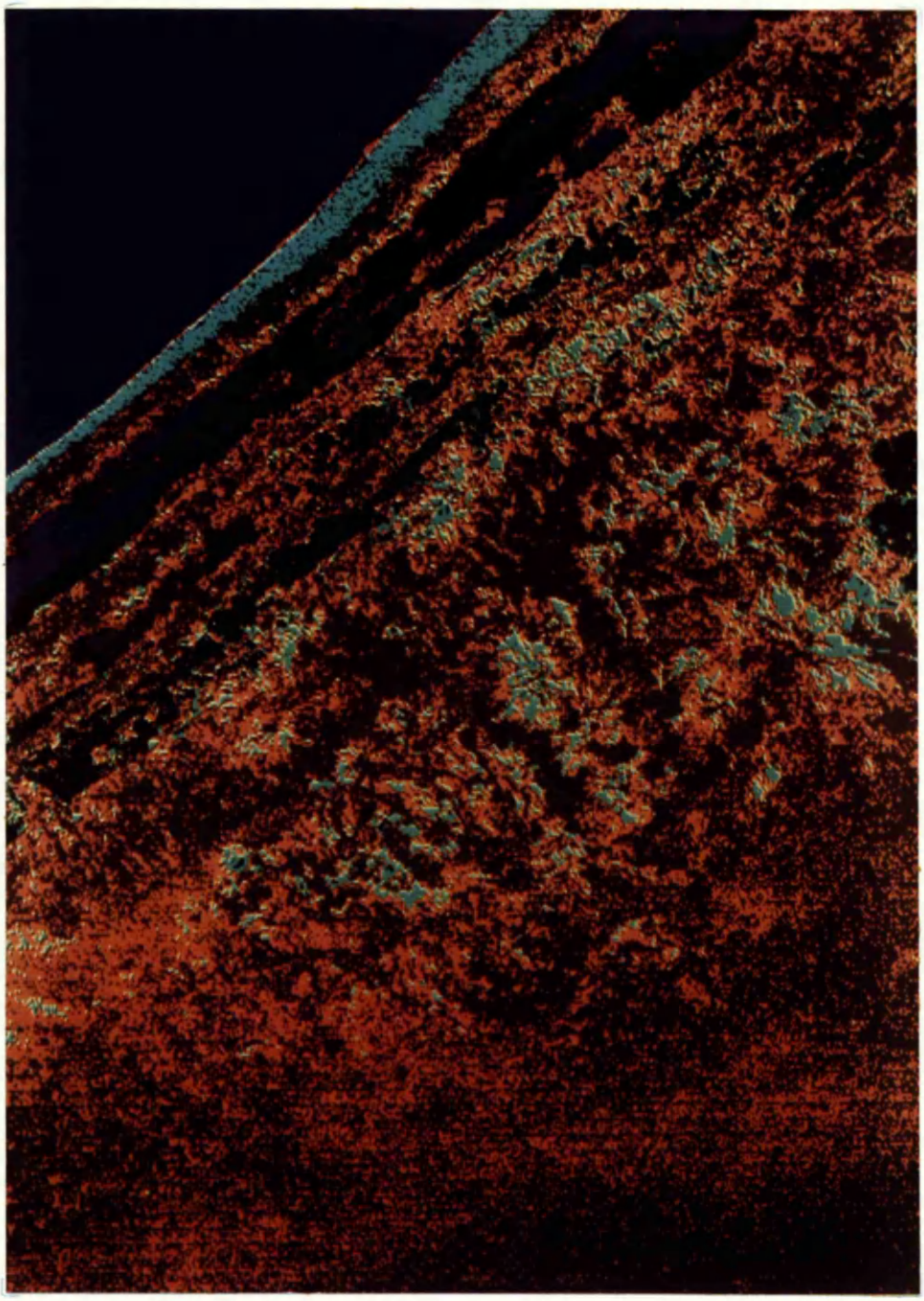

Plate 4.5.1

Transect 1 principal components classification of PC1 vs PC2 feature-space. Refer to Table 4.5.2 for the colour key.
Scale 1 : 220 000

Moving up in the feature-space the wet irrigated fields merge into the salt marsh, as the spectral response of these two cover types is very similar. Likewise the salt marsh merges into the water cluster. Thus, we can see a continuum from wet soil through inundated soil to shallow water and then to deep water as we move up the left hand side of the scatterplot, Figure 4.5.1. A similar continuum can be followed clockwise around the scatterplot from the water cluster. Joining clusters four and five, water and coastal dunes, is a thin scatter of points making up cluster eight. This class can be regarded as either being pixels of wet sand near the waters edge, or of mixed pixels of water and sand along the sea/dune boundary. The continuum can then be followed from cluster five into cluster seven as pure pixels of dune are mixed with pixels of soil. Cluster three can be regarded as a confusion boundary between bare soil and stands of dense vegetation, or in other words an area of sparce vegetation. This cluster can exclusively be regarded as containing pixels of semi-natural rangeland vegetation. Finally, cluster six (salt marsh) is bounded by clusters of water, soil, natural vegetation and irrigated crops.

The classification in plate 4.5.1 is not supposed to represent a definitive classification of the area. What it does do, however, is provide feedback to the interpretation of the feature-space and to a degree an indication of the accuracy of that classification. It is not possible to assess comprehensively the accuracy of the classification because the image has not been resampled to square pixels and is therefore difficult to compare with areal photographs and field data.

It is possible to tell by eye, however, that the classification has indeed separated the classes with some success, a subjective estimate of the classification accuracy would be in the region of sixty percent.

This method of classification has limitations for a number of reasons. First, on the GEMS image processor it is only possible to define square or oblong decision boundaries within the feature-space. The data are not of course arranged in boxes and the classification is therefore limited by this restriction. Secondly, this methodology of Principal Components Analysis assumes that the soil line will always be aligned with PC1. This will not always be the case and indeed from Figure 4.4.1 it can be seen that PC1 in fact lies between the water cluster and the sand dunes rather than the base of the soil line to the sand dunes.

The value of sampling in Principal Components Analysis is stressed by Mulder (1977) and in Transect 1 it is possible to make use of sampling to align PC1 with the soil line. This processing was done on the I2S at University College on which it is not possible to perform the type of classification described above. Using the following methodology, however, it is possible to perform the Green Vegetation Index (GVI) of Kauth and Thomas (1976).

As discussed above, PC1 is not necessarily coincident with the soil line, and in the case of Transect 1 is aligned with the water and dune clusters. By calculating the covariance matrix, used to find the principal components, on a subset or sampled

area of the image, it is possible to align PC1 with the soil line. It should be noted that this is possible because of the different soil moisture conditions which prevail in this transect. If no significant variation in soil moisture existed in this area then Principal Components Analysis would offer no meaningful enhancement to the data. By selecting one or more specific areas of bare soil which exhibit a wide variation in soil moisture, it is possible to sample a subset of data which characterises the soil line. Once the covariance matrix has been calculated using this sampled data set, the whole image data set can be rotated so that the soil line is truly horizontal. Principal component two can then be sliced with the knowlege that it is as representative as possible of the greenness axis. Further implications of this type of analysis, with reference to discrete soil lines, are discussed later.

4.6 TRANSECT 3 - THE FALSE COLOUR IMAGE

Transect 3 is centered on the town of El Omayed and is some ninety kilometres to the west of Alexandria. This transect differs considerably from Transect 1 in it's agriculture. It's climate is very variable and differs from that at Burg el Arab, particularly the rainfall. There is no irrigated land at Omayed and agriculture is dependent solely upon dry land cereals, fig and barley cultivation and pastoralism. Like Transect 1, Transect 3 is characterised by the system of ridges and depressions which run parallel with the coast. This system diverges towards the west and at Omayed the depressions are rather wider, though more shallow, and the escarpment of the

inland plateau more pronounced, the ridge of Khashm el Eish being a particularly striking feature of the landscape. Plate 4.6.2 shows the view inland from the second saline depression with the ridge of Khashm el Eish on the horizon. The first saline depression to the south of the coastal dunes is relatively narrow and is cultivated with figs and in some places palm dates. Parts of this depression are permanantly inundated with water. The second depression is higher and broader and is characterised by hummocks of succulent, saline tolerant, vegetation. Barley fields do occur in this depression and some can be seen on the false colour composite image shown in Plate 4.6.1 This image was recorded on the 11.2.78. These fields presumably occur on slightly higher ground where the drainage is better than the surrounding area. Although the fields can be seen on the image, (they also occur on the REMDENE land use maps), they do not seem to contain crops on this date. The dry land barley fields in Transect 1 show the typical pinkish colour associated with vegetation in false colour images. The difference between the two areas is probably an effect of the highly variable rainfall, manifest, in this case, spatially rather than temporally. The false colour images of the region dating from 1973, a much drier year than 1978, also exhibit barley fields which have been prepared but which lack any vegetation cover. Also evident in this depression are wet areas which match very closely the particularly saline fields mapped by the REMDENE staff. The third depression exhibits a number of interesting features on the enhanced false colour image. Firstly the town of Omayed can be seen, this is surprising as the town is small and, like all Bedouin settlements, the buildings are well spaced. It's

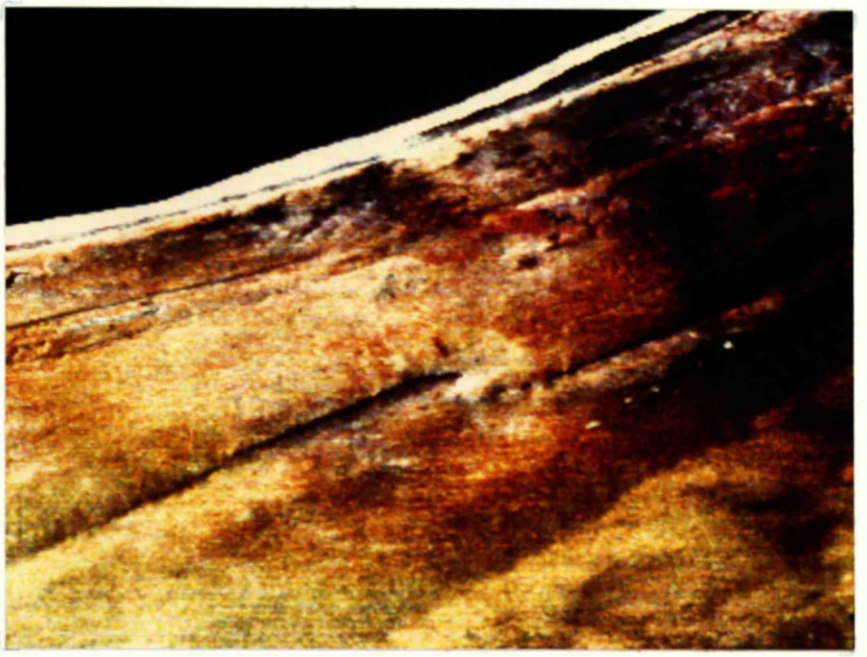

Plate 4.6.1

Transect 3 false colour composite. An extract from Landsat 2 scene 191/039, imaged on 11.2.78. Histogram equalized contrast stretch. Scale 1 : 350 000

appearance is probably due to the shadow cast by the building in the early morning sun. It is also apparent that the town is surrounded by a belt of totally bare soil, stripped clean by animals for food and by humans for fuel. This feature was confirmed in the field. Just to the north of Khashm el Eish a dark rectangular area is visible. This feature is the REMDENE project's exclosure in which controlled grazing occurs. The exclosure is a UNESCO Biosphere Reserve. Figure 4.6.1 shows a plan view of the exclosure, the four internal plots and the area outside the exclosure providing five different levels of grazing pressure; these being:

A: freely practised grazing,

B: fenced in July 1974 and kept without grazing,

C: fenced in July 1974 and subject to 66% of the freely practised grazing pressure since May 1977,

D: fenced and subject to 66% of the freely practised grazing pressure since May 1977,

E: fenced and subjected to 25% of the freely practised grazing pressure since May 1977.

(Ayyad and El-Kady 1980)

It is unfortunate that plot B, the area kept without grazing, is only seventy metres wide as this means that it is sub-pixel size in width and pure pixels of it will not occur on the Landsat imagery. The absolute cover of perennial species in plot B is about 37%, whilst that in plots C and D are 9% and 11% respectively (Kamal 1984). Plate 4.6.2 shows a southerly view from the eastern end of the exclosure. In the background

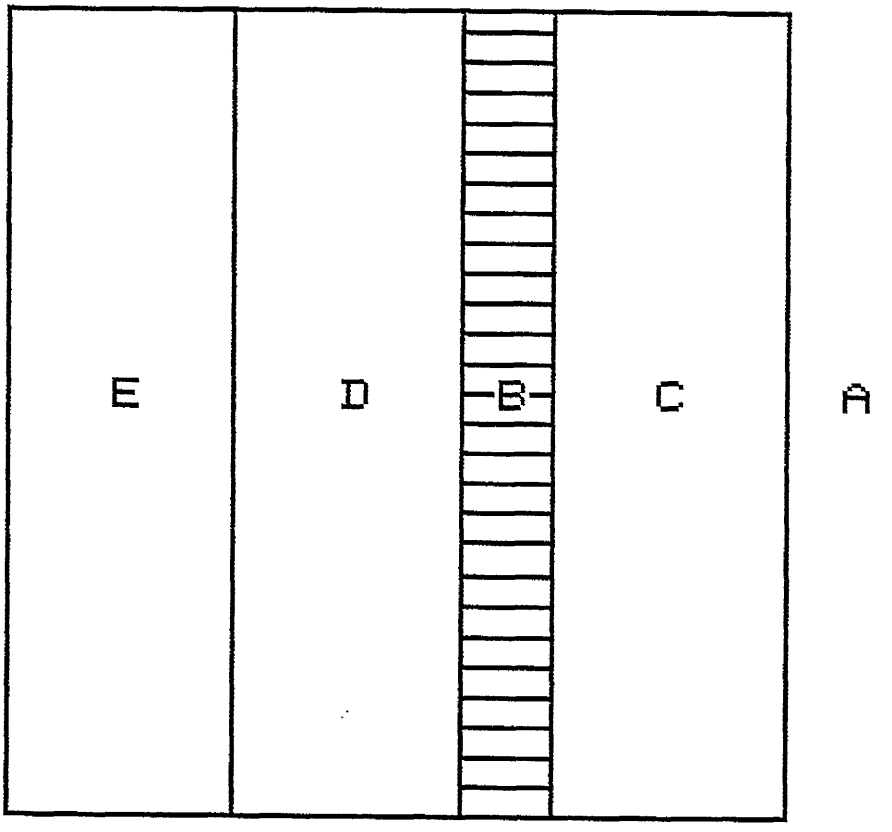

Figure 4.6.1

Plan view of the UNESCO Biosphere Reserve at El Omayed.

Plate 4.6.2

A southerly view at the Omayed exclosure showing freely practised grazing on the left and sixty six per cent of the freely practised grazing on the right. In the distance is the ridge of Khashm el Eish which forms the edge of the inland plateau.

is the ridge of Khashm el Eish, while in the foreground is the excluding fence between grazing levels A and C; that is between freely practised grazing and 66 percent of the freely practised grazing.To the west of the exclosure there are two red fans indicating a higher level of vegetation than the surroundings, although not as high as that in the exclosure. These fans of vegetation correspond with a number of outwash gullies on the south side of the ridge and are probably associated with higher soil moisture than the surroundings. The gullies can be seen on Plate 4.6.1. The very marked shadow along the ridge line is evidently a result not of actual shadow, but of the reduced reflectance due to the angle of incidence on the north facing side of the ridge. On a visit to the field during February it was noted that at 9.30 am the northern face of the slope was illuminated and not in shadow. Conversely, the very bright white patch where the ridge curves around to face the south is particularly bright, not only because of the high calcium content of the soil, but also because of orientation of the surface reflecting light towards the sensor.

4.7 DISTRIBUTION OF THE DATA WITHIN LANDSAT FEATURE-SPACE

The unenhanced false colour image of Transect 3 is extremely bland and featureless. Although a one or two step linear stretch does enhance the image it does not bring out all of the features mentioned above. It was found that only a stretch which equalises the distribution of the data throughout the data space resulted in an informative image. It is not normally necessary to use such a severe stretch to enhance an image but

in this case it was deemed to be so. This particular stretch was used to produce the image presented in Plate 4.6.1. It is obvious from Plate 4.6.1 that Transect 3 contains little, or no, dense green vegetation, from the absence of any bright red areas. The area within the exclosure certainly contains the most dense vegetation in and around the area of Omayed, although similar levels occur in the eastern part of the image on a broad scale.

We would expect that the lack of contrast between different features of the image would be reflected in the distribution of the data within the Landsat feature-space. Indeed, this is the case and Figure 4.7.1 shows the highly correlated nature of the data in bands 7 and 5. In this Figure the soil line and the water cluster are the only two identifiable features with just a handful of pixels in the area of the 'tasselled cap' where we would expect vegetation readings to occur. Those pixels which do contain some degree of vegetation will be located very near to the soil line and may in fact merge with it. The problem then, is to define a decision boundary parallel with the soil line which defines the effective boundary between soil and a soil/vegetation mixture. Bands 5 and 7 are the most uncorrelated bands of the Landsat MSS and other scatterplots, with different band combinations, exhibit even higher correlations. Once again Pricipal Components Analysis of the scene should reveal the most uncorrelated axes within the data, thus providing a measure of the greenness component.

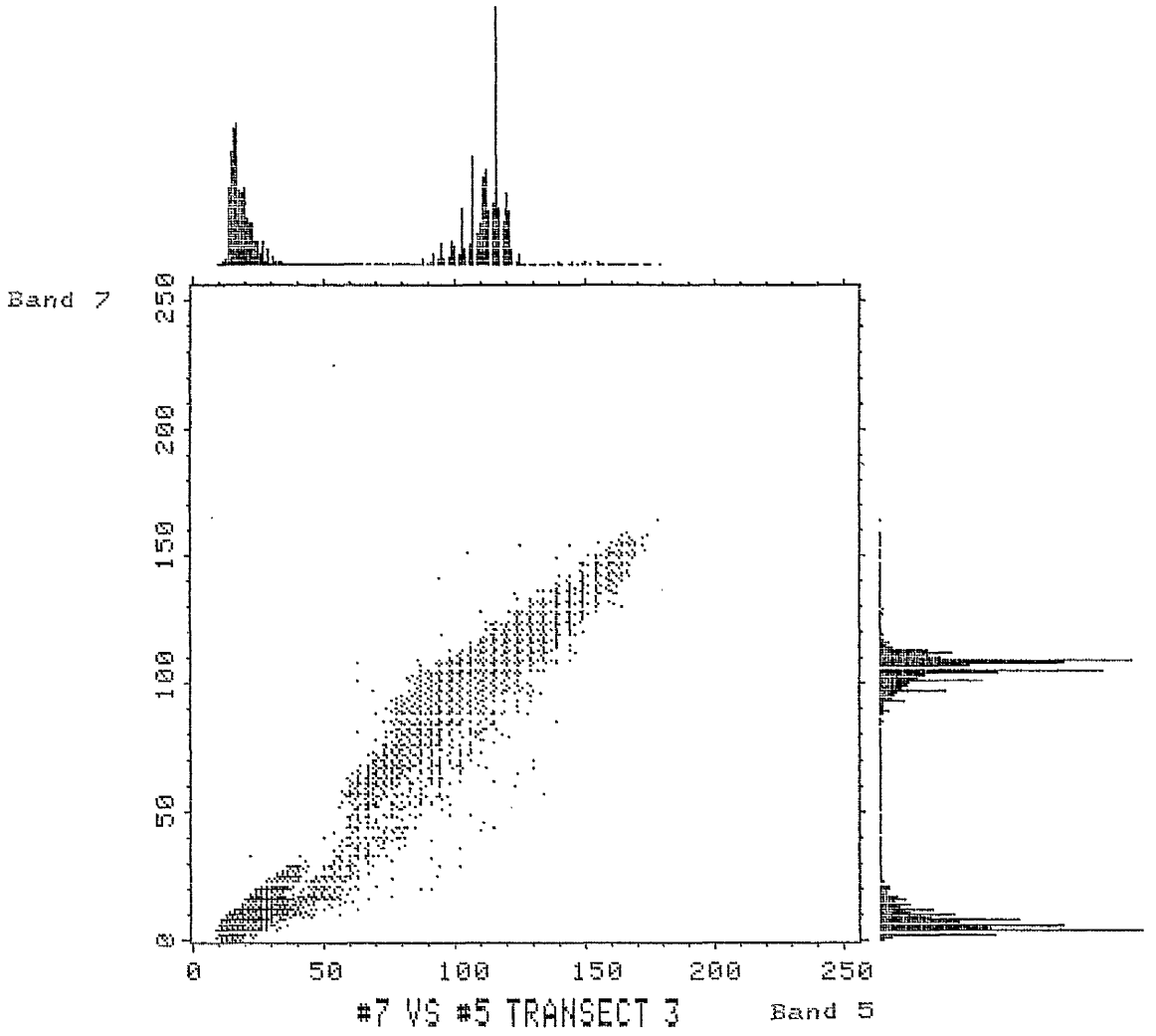

Figure 4.7.1

Scatterplot of band 7 vs band 5 for the Transect 3 area.

4.8 TRANSECT 3 PRINCIPAL COMPONENTS ANALYSIS

Table 4.8.1 shows the statistics obtained by conducting a principal components analysis on bands 4, 5 and 7 of Transect 3.

TABLE 4.8.1

Means	56.1	96.1	88.1
Standard Deviations	54.9	4.6	2.7
Percentage Eigen Values	99.07	0.684	0.240
Eigen Vector Matrix	0.267	0.672	0.691
	0.834	0.198	-0.515
	0.483	-0.714	0.508

The eigen values expressed as percentages clearly show the highly correlated nature of the data. The first value of 99.07% indicates that the first principal component accounts for nearly all of the variance within the data. This is also apparent from the standard deviations, variance being the square root of standard deviation. The eigen vector matrix defines the relationship between the original data and the principal components, as described in section 4.5. We might expect then, that the plot of PC1 vs Pc2 will exhibit little or no data in the greenness region. Figure 4.8.1 shows this plot and, as might be expected, the shape is very similar to the plot of PC1 vs PC2 for Transect 1, with the exception that there is little data below the greenness line. Once again the transformation separates water from the two or three soil clusters, of wet soil, dry soil and coastal dunes. The

transformation also allows us to apply a crude perpendicular Vegetation Index to the data by slicing the second principal component. As with Transect 1 a two dimensional slice will further allow us to classify the data into the basic cover types of soil, water and vegetation. By interpretation of the feature-space and by parallelpiped classification a two dimensional subdivision of the feature-space was arrived at which classified the image into eight classes. Figure 4.8.1 shows this subdivision and Plate 4.8.1 shows the associated classified image.

The annotation used in Figure 4.8.1 is the same as that used for Transect 1 in figure 4.5.1. Please also note that Plate 4.8.1 does not have the same aspect ratio as that used for Transect 1 in Figure 4.5.1.

TABLE 4.8.2

Cluster	Class	Colour	Percentage Area
1	Shallow water	Magenta	Ø.21
2	Vegetation 1	Orange	5.78
3	Vegetation 2	Green	4.6Ø
4	Water	Blue	17.98
5	Coastal Dunes	White	1.63
6	Salt Marsh	Cyan	Ø.73
7	Bare Soil	Grey	67.9Ø
8	Beach	Red	1.Ø4

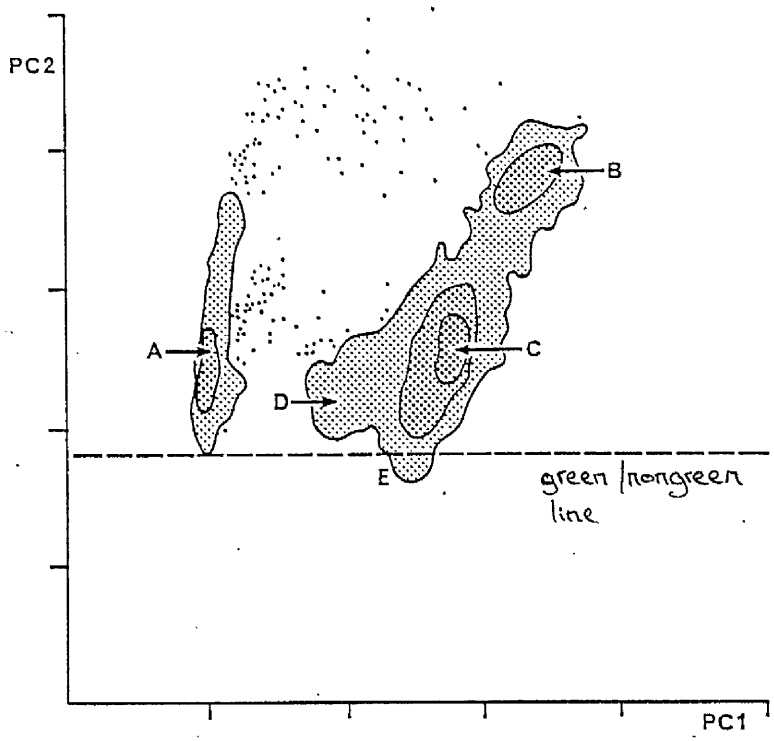

Figure 4.8.1a

Transect 3 PC1 vs PC3 feature-space

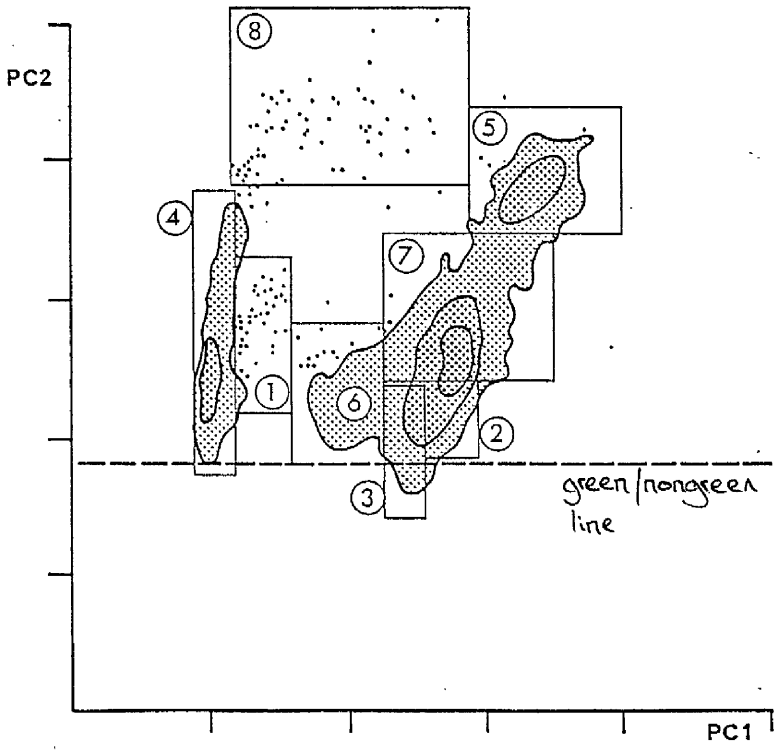

Figure 4.8.1b

Transect 3 classification decision boundaries within PC1 vs PC2 feature-space.

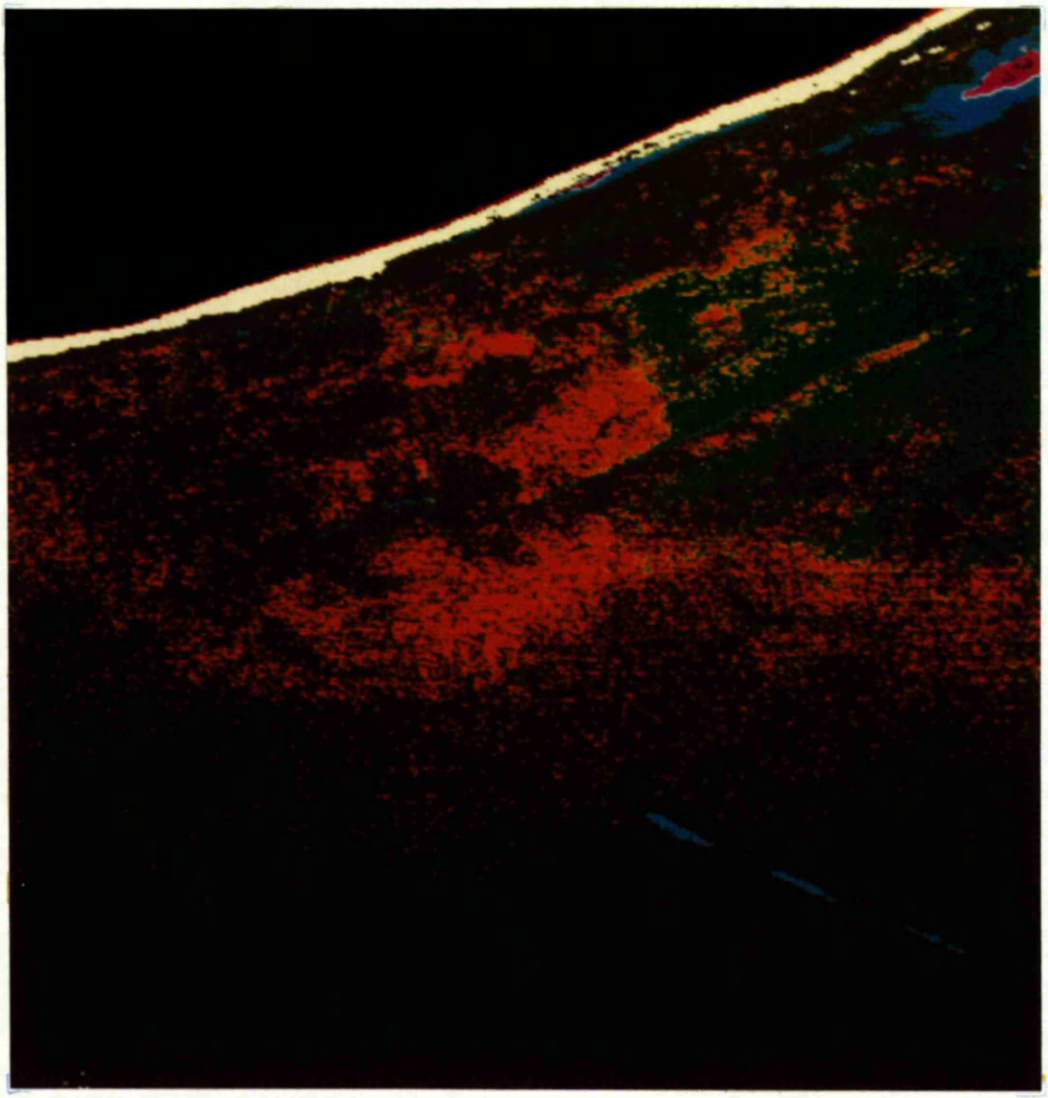

Plate 4.8.1

Transect 3 principal components classification of PC1 vs PC2 feature-space. Refer to Table 4.8.1 for the colour key.
Scale 1 : 220 000

CHAPTER 5

FIELDWORK

5.1 INTRODUCTION

Whilst remote sensing can provide a synoptic view of a region from the other side of the globe, it can only provide one which is biased. It is biased because it is an abstraction of reality in terms of the spectral bandwidths, spatial and temporal resolutions and because it only provides a view of the surface terrain. It does not show subsurface features nor does it directly reveal any of man's socio-economic and political activities, although indirect attributes of these activities are visible. A visit to the field was a way of redressing some of these biases in the perception of the author, although other biases may have been acquired. It also provided an opportunity to investigate the spectral properties of some of the more important cover types found in the region and to establish relationships between reflectance features of the imagery and the physical features on the ground. The author visited Egypt for the period Febuary 20 to March 20 1984, during which time fifteen field sites along the northern coast were visited. In addition to the field visit the author had the opportunity to spend about two weeks at the University of Alexandria where he was able to examine aerial photography of selected representative sites along the coast. This period proved invaluable in terms of the information derived from the photography and discussions with the REMDENE staff.

5.2 FIELD RADIOMETRY

The collection of multi-spectral data in the field may be conducted in a variety of different ways and using a range of different equipment. The method which is finally selected may be governed more by the availability of equipment and practicalities rather than by any academic or theoretical considerations. The aim of any field study must be to collect data, of a chosen nature, which is as accurate as possible under the given conditions. In addition, the inherent biases and inaccuracies which exist within the data must be appreciated and accounted for. With these considerations in mind an experimental procedure was established.

In this study the choice of radiometer type was predetermined in that a radiometer with fixed band passes would be required. A fixed band pass radiometer with filter characteristics similar to the MSS sensor was available in the form of a four band Milton radiometer. The filter characteristics of both the Landsat MSS and the Milton radiometer are shown in Figure 5.2.1.

Two methods of data acquisition using a broad band radiometer are possible. First, by using a meter with a single sensor head readings may be taken sequentially of a standard reference reflector and of the target. Hemispherical reflectance, a dimensionless ratio, may be calculated using the formula:

$$Rr = \frac{\text{Target Radiance}}{\text{Standard Radiance}} * Kr$$

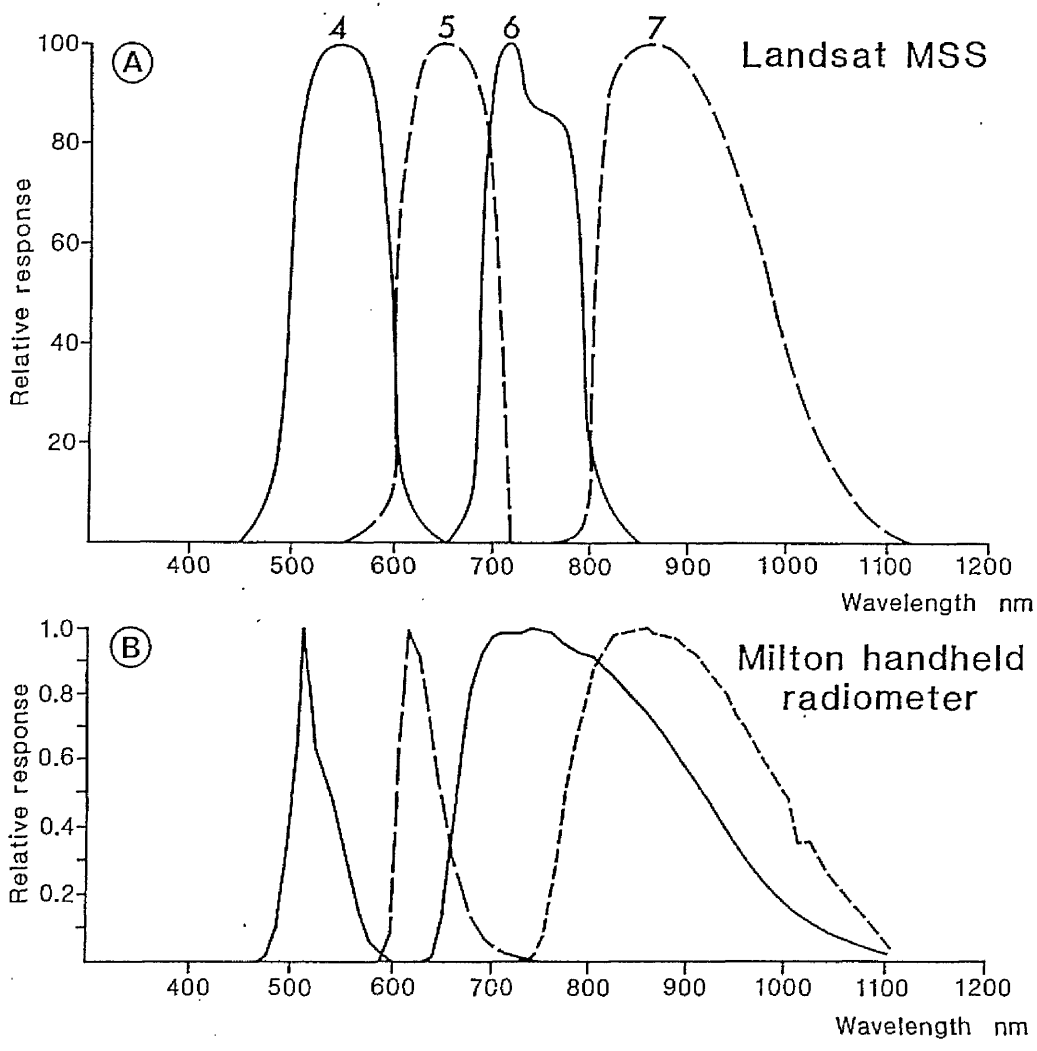

Figure 5.2.1
Filter characteristics of the Landsat MSS and the Milton four band radiometer.

Where: Rr = Reflectance in band pass 'r'

Kr = Reflectance of standard reflector in band pass 'r'

The hemispherical reflectance is expressed as the percentage of incoming radiation in bandpass 'r' being reflected by the target. Although this method can, under certain conditions, yield reasonable results, it suffers from the drawback that the target radiance and the standard radiance are both measured at two different times; 't1' and 't2'. During the elapsed time 't2 - t1' the solar illumination may have changed. Duggin (1974) reports that random variations in solar illumination, caused by the atmosphere, may be in the order of five to ten percent, even on apparently clear days. Such variations will obviously lead to random inaccuracies in 'Rr' reflectance values.

In addition to random variations caused by clouds and water vapour in the atmosphere, systematic variations in the intensity and composition of solar illumination occur throughout the day with variations in solar zenith angle. A familiar effect of this is the red cast of light during the early morning and dusk.

Duggin and Philipson (1981) propose an alternative method of data collection by measuring both the target and reference reflectance simultaneously, thereby eliminating random errors caused by the atmosphere. This method is considered to be far superior to making sequential measurements. Unfortunately the Milton four band radiometer used in this study only allowed sequential measurements of the standard and the target to be

e. A two head Milton radiometer does exist although one was available for the field trip. Using this method random ctuations in solar irradiance could only be minimised by ing measurements on clear days. Restraints on time and nsport limited the extent to which this could be achieved, fortunately during this field study good weather and clear s prevailed during the majority of visits to the field. tematic variations, on the other hand, could only be imised by taking measurements around solar noon, thereby ucing the effects of sunangle upon the reflectance of ffering cover types. Again however a compromise had to be reached, as if measurements had been limited to plus and minus one hour around solar noon, the study would have been severely limited in terms of the number of sites visited. Consequently measurements were made only between 10.00 hrs and 14.00 hrs.

A Kodak grey card was used as the standard reflector. These cards have a standard reflectance of eighteen percent on their grey side and ninety percent on their white side. In this study the grey side of the cards was used as the standard reflector. The equation for hemispherical reflectance therefore becomes:

$$Rr = \frac{\text{Target Radiance}}{\text{Standard Radiance}} * 18.0$$

5.3 APPROACH AND METHODOLOGY

A total of eighteen field sites were visited and spectral measurements made at fifteen. Figure 5.3.1 shows the location of the first fifteen sites, site sixteen was at Wadi Garawla, to the east of Mersa Matruh, and sites seventeen and eighteen were near Rashid in the Nile Delta. The sites were chosen so as to cover the major soil types of the Burg el Arab and El Omayed areas. Section 2.4 should be referenced for a description of the region's soils. Table 5.3.1 outlines the soil types at each of the field sites, the soil types are those as described in the FAO Preinvestment Survey (1970).

TABLE 5.3.1

Field Site No	Description
Site 1	C2:deep sandy loam to loam
Site 2	C2/B1 : clay loam
Site 3	B1 : deep sandy loam
Site 4	Karm centre : clay loam
Site 5	Rd : former coastal dune
Site 6	B1 : loam
Site 7	B1 : loam
Site 8	B1 : loam
Site 9	Bp:poorly drained / saline
Site 10	Rd : former coastal dune
Site 11	D02 : cemented oolitic dunes
Site 12	Ds1:low dunes of quartz sand
Site 13	Rd : former coastal dunes
Site 14	Ds7 : sheets of quartz sand
Site 15	Bp : poorly drained/saline

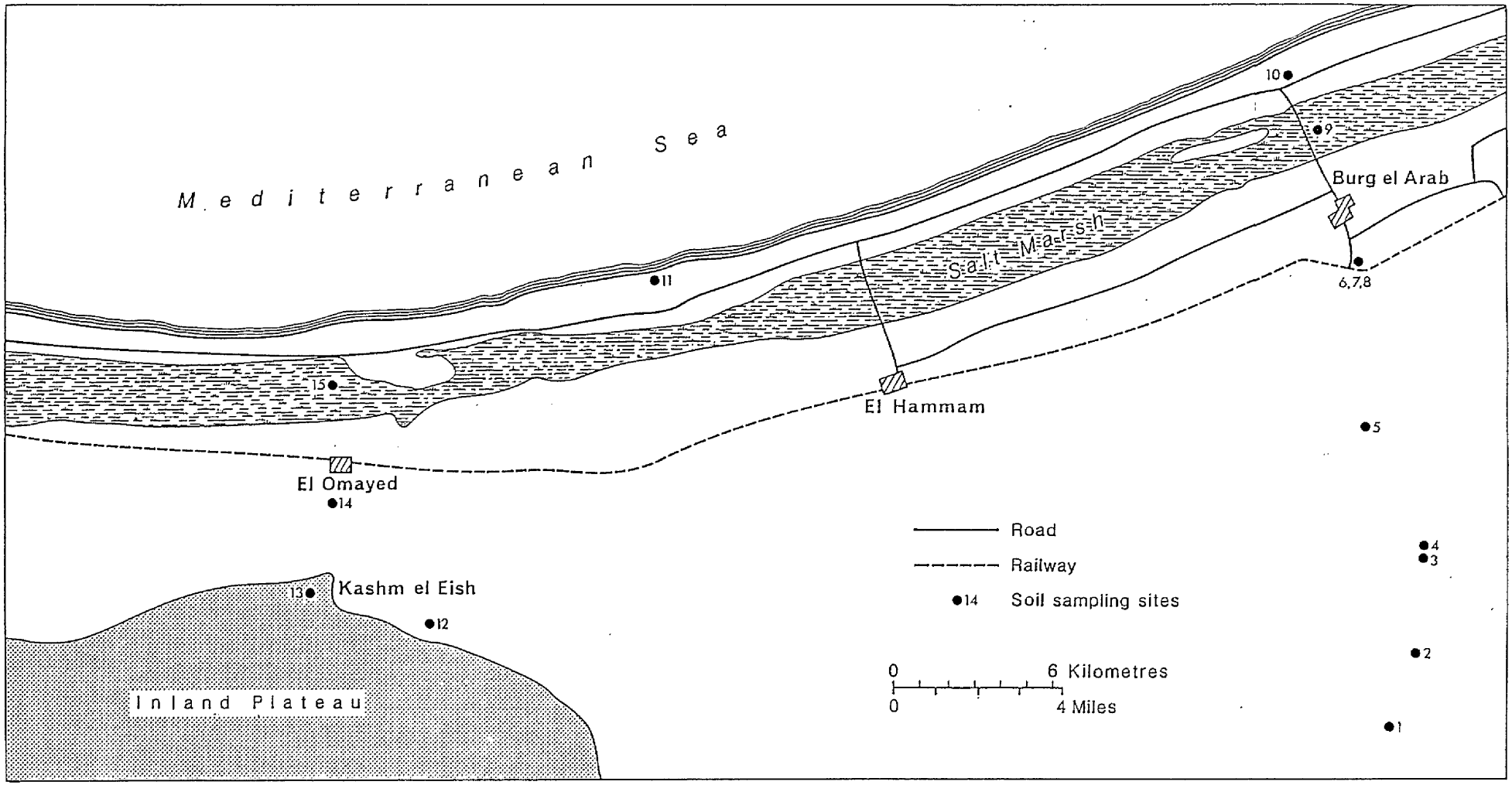

Figure 5.3.1 Field site location map.

As discussed in chapter four, vegetation indices are very dependent upon the location of the soil line, or soils plane, within the 4D Landsat feature-space. This is particularly the case in arid regions and areas with very sparse vegetation cover. If vegetation indices are to be used for vegetation mapping in these conditions then an understanding of the interaction between soil and vegetation reflectances is most important in making classifications and maps which are meaningful. In these terms only the Perpendicular Vegetation Index of Richardson and Wiegand (1977) and, perhaps more significantly, the Green Vegetation Index of Kauth and Thomas (1976) provide a rigorous analysis of the feature-space. Huete et al (1983) have shown the importance of dealing with individual soil lines rather than the single unique soil line of Richardson and Wiegand, and it was the aim of this field study to attempt to distinguish those soils of the Burg el Arab and el Omayed areas which are the significant ones in terms of differing soil lines. It follows that those soils with obviously different soil lines should be separated and dealt with individually, thus effectively stratifying the area in terms of soil type in order to estimate and map vegetation more accurately. This methodology has implications not only in arid regions but also in areas with healthy green vegetation which does not entirely cover the ground.

In order to construct a soil line for each soil type it was necessary to take measurements when the soils were both wet and dry. This was achieved by taking measurements of the soils in their soil moisture state as found in the field, this was, with the exception of the saline soils, invariably very dry, and

then by wetting the soils and repeating the measurements. Ideally the soils should have been wetted and allowed to dry, measurements being taken during the drying process, so as to provide points along the whole length of the soil line. The restrictions of time on the number of sites to be visited, however, prevented this procedure being followed. The majority of the soils were very dry and actually dried to a degree after wetting whilst measurements were being taken. The saline soils exhibited a range of moisture contents and more individual measurements were taken on these soils. No attempt was made to measure the moisture content of the soils as the position of the soil line as a whole was of interest rather than that of individual points. At each site at least three readings were taken of the soils both wet and dry. Once again the number of readings taken were limited by the pressure of time and sites to be covered.

Radiometric field data collected in Egypt by Allan and Richards (1983) is shown in Figure 5.3.2. The scatter plots show the spectral response of various cover types of the Egyptian coastal tract. The similarity of the band 7 vs band 5 plot with Figure 4.4.1 (the equivalent Landsat scatter plot) is quite apparent. Higher levels of LAI occur above the lower left-hand portion of the soil line, whilst lower levels of LAI occur just above the central portion of the soil line, and actually merge with it. The soil lines shown in this figure were calculated from regressions of the bare soil readings only. These bare soil readings represent a range of soil types at different locations within the region. It is important to note the non-linear nature of those soil lines constructed

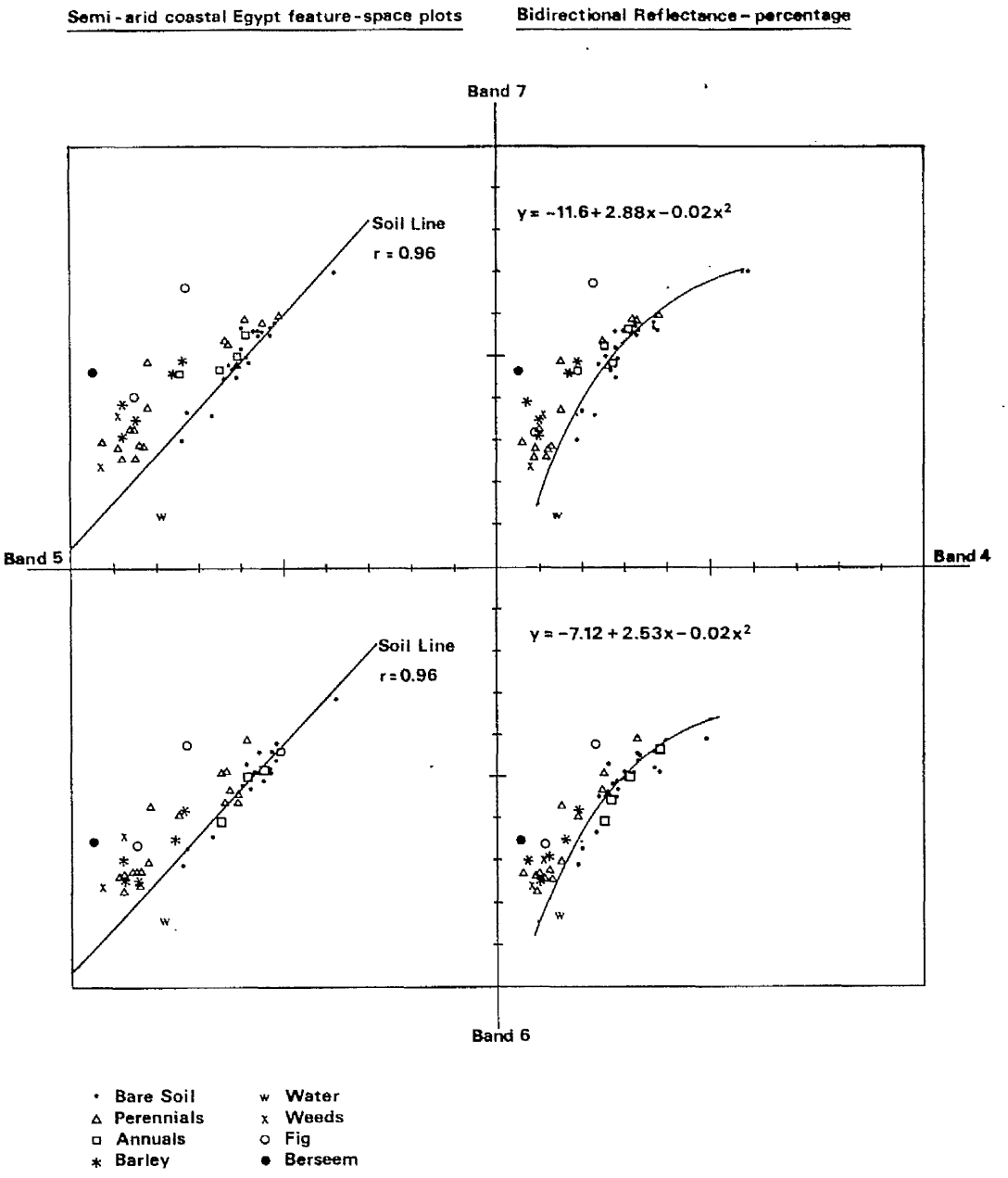

Figure 5.3.2

Scatter plots of the significant band combinations for field data collected in April 1983. Source Allan (1983).

using combinations with band 4. A linear regression of these points subdivide the feature-space in a non-meaningful way, with the soil line cutting through the lower left-hand vegetation cluster. However, if a polynomial equation is fitted to the points the resulting curves ('soil curves') once again subdivide the space into soil and vegetation. The equations fitted to the curves are shown in the figure. It is suggested therefore, that these 'soil curves' are a manifestation of a number of different soil lines fused into one. By estimating the position and relationship between the individual lines in feature-space, it may be possible to establish a minimum detectable cover for each individual soil, and to separate soil from vegetation in the area of confusion which exists where the soil and vegetation clusters merge.

5.4 GRAPHICAL AND STATISTICAL ANALYSIS OF THE FIELD DATA

Figure 5.4.1 shows the six most significant scatter plots of the field data collected during Feburary and March 1984. The plots contain all of the data for twelve soil sites and three vegetation sites. Once again the band 7 vs band 5 plot is similar to the plots described above. It is of interest to note the relationship between the general soil and water clusters and the vegetation cluster. The vegetation cluster forms only the peak of the tasseled cap, with a gap between this and the soil line. This is because only dense green irrigated crops were sampled, all with high LAI and therefore high values in terms of PVI, or distance from the soil line. As with Allan and Richards data (1983), those scatter plots with band 4 as an

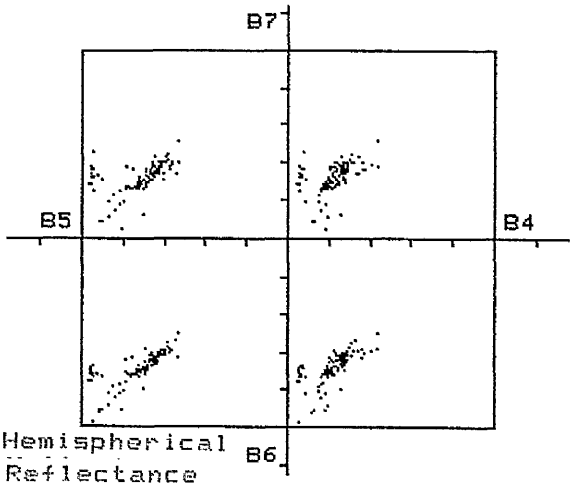

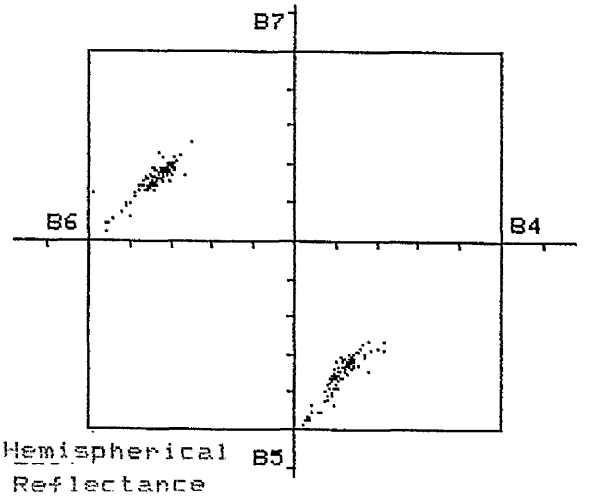

Figure 5.4.1

Scatter plots of the significant band combinations for field data collected in February and March 1984.

axis exhibit a curvi-linear nature, once again indicating a band 7 vs band 4 combination may provide superior separation between individual soil lines than a band 7 vs band 5 plot. To provide an appreciation of the distribution of data from different sites Figure 5.4.2 shows plots of band 7 vs band 5 with annotated points and key.

Table 5.4.1 shows the statistics derived from linear regressions of the spectral data collected in bands 5 and 7 for each individual soil types. It is clear from the values of Pearson's correlation coefficient, in Table 5.4.1, that at a number of the sites the correlation of the points is unacceptably low, such that the values of slope and intercept for sites ten, thirteen and fourteen are meaningless. These sites are therefore excluded from further analysis. The scatter plots shown in Figure 5.4.2 do, however, include these points.

The two scatter plots shown in Figure 5.4.3 illustrate the differing slopes of the soil lines, both between the individual soil lines and between the two band combinations. It is apparent from these two plots that the band 7 vs band 4 combination provides a wider scatter between the lines, showing a greater variation in the slopes of the lines than in the plot of band 7 vs band 5. This point is also illustrated by the standard deviations and variances of the slopes between the two combinations (Ø.2Ø5 & Ø.ØØ42 for #7 vs #5 and Ø.417 & Ø.174 for #7 vs #4). Given that the the definition of the PVI is the distance between a vegetation point and the soil line, we should be able to measure how significant the difference is between the two band combinations. In addition a PCA of the

Table 5.4.1

Site	#5vs#7 Slope	#4vs#7 Slope	#5vs#7 I	#4vs#7 I	#5vs#7 PCC	#4vs#7 PCC	#5vs#7 SD	#4vs#7 SD
Total	0.84	0.91	5.78	10.28	0.87	0.74	3.88	5.35
1	0.95	1.46	2.15	- 1.59	0.99	0.89	1.42	4.13
2	1.04	1.83	- 0.76	-14.47	1.00	0.68	0.88	7.64
3	0.83	0.73	5.95	15.27	0.99	0.99	0.63	0.67
4	1.06	0.96	- 2.12	10.14	0.99	0.99	0.63	0.76
5	0.86	0.88	3.16	10.34	0.96	0.91	1.05	1.58
9	0.97	1.00	- 1.68	3.74	0.70	0.58	5.75	6.55
10	0.46	0.49	22.50	24.96	0.53	0.57	5.02	4.77
11	0.40	0.39	20.91	22.78	0.90	0.82	1.90	2.44
12	0.74	0.87	9.53	14.34	0.79	0.71	2.39	2.76
13	0.48	0.80	17.36	13.37	0.54	0.74	3.79	3.00
14	0.12	0.48	33.48	26.16	0.21	0.40	3.33	3.13
15	0.98	1.12	1.39	5.87	0.90	0.88	2.23	2.39

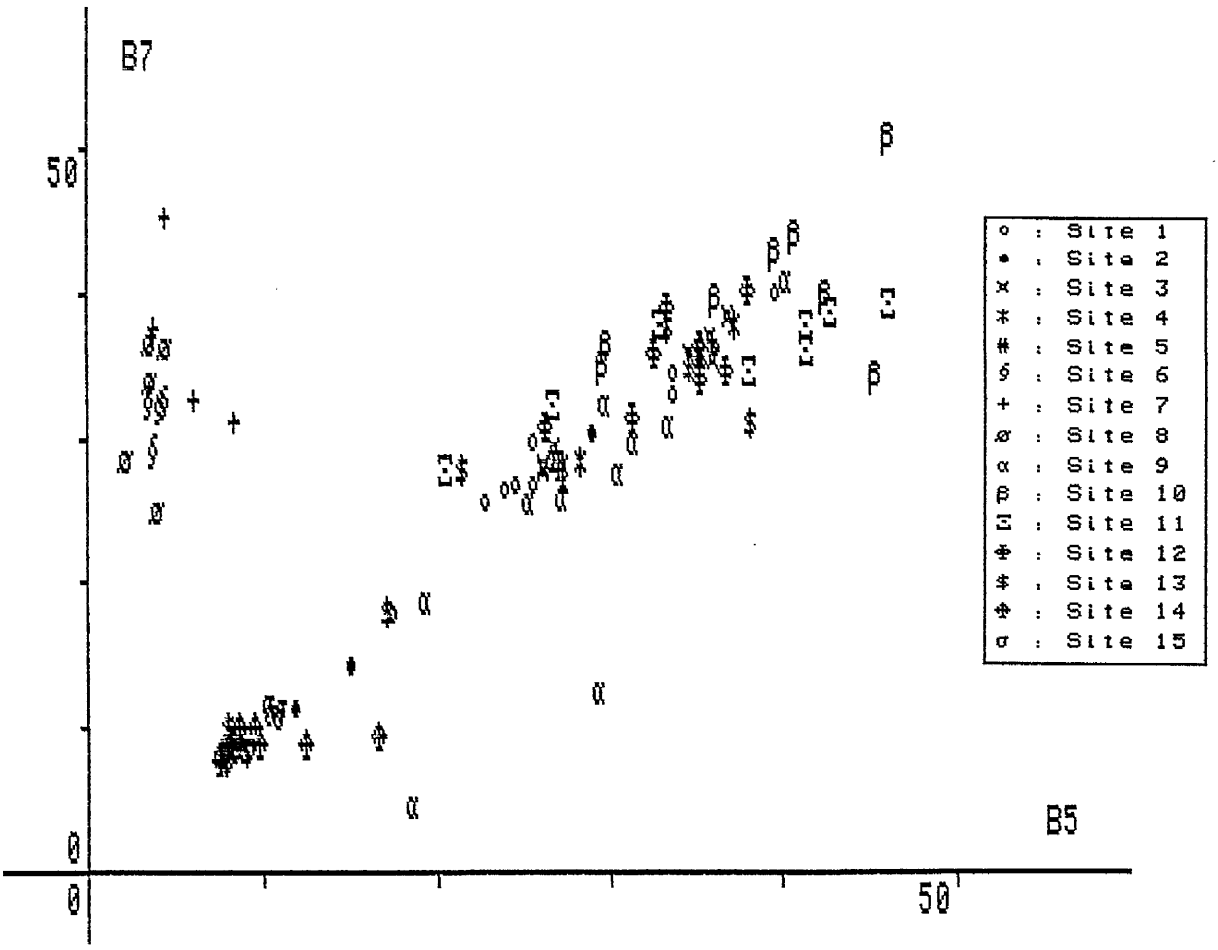

Figure 5.4.2

Annotated scatter plots of data from all fifteen field sites.

soil lines should reveal to us more about their nature and distribution.

Referring back to Figure 5.4.2, the vegetation reading furthest away from the soil line was recorded over a crop of irrigated barley at Burg el Arab, with an LAI, estimated from a vertical photograph taken at the time of recording, of about 90 percent. The values recorded were:

Bidirectional reflectance	Band 7 = 45.20
	Band 5 = 5.14
	Band 4 = 7.08

Table 5.4.2 below gives the values of PVI for each individual soil type and the mean soil lines for both of the band combinations. The PVI values were calculated assuming that the reflectance values given above represent 100 percent vegetation cover.

The values of PVI were calculated by subtracting the intercept of each soil line from the band 7 value of the maximum vegetation pixel. This subtraction translates the soil lines such that the intercept is at the origin. The soil lines were then rotated in a clockwise direction by an angle of ARCTAN (Slope). After this rotation, the soil lines become horizontal and coincident with the x axis. The point of maximum vegetation was also translated and rotated with each soil line so that the y value of this maximum vegetation point now becomes a measure of PVI.

TABLE 5.4.2

	PVI #7 vs #5		PVI #7 vs #4	
Site	FS units	Normalized	FS units	Normalized
Control	26.87	100%	21.33	100%
1	27.64	103%	20.56	96%
2	28.10	105%	22.40	105%
3	26.91	100%	19.96	94%
4	28.75	106%	20.42	96%
5	28.11	104%	21.49	101%
9	30.02	112%	24.40	114%
11	20.68	77%	18.34	86%
12	25.60	95%	18.68	88%
15	27.74	103%	20.88	98%
Mean	27.06	101%	20.79	98%
SD	2.68		1.85	

By following this procedure and by using the mean soil line data from Table 5.4.1 as a base or control soil line, we find that the point of maximum vegetation is 26.87 feature-space units away from the mean band 7 vs band 5 soil line, and 21.33 feature-space units away from the mean band 7 vs band 4 soil line. Table 5.4.2 shows the values of PVI in feature-space units, calculated for each of the discrete soil lines. The normalized values were calculated as percentages in relation to the control value. By way of an example the mean value is being taken as representing one hundred percent vegetation cover.

How does the value of PVI vary, however, for each of the individual soil lines? It can be seen from Table 5.4.2 that for the band 7 vs band 5 combination LAI varies between a minimum of 77 percent and a maximum of 112 percent, a total variation of 35 percent. Likewise, for the band 7 vs band 4 combination LAI varies between a minimum of 86 percent and a maximum of 114 percent, a total variation of 29 percent. The value of LAI is of course the same in each case, ie 100 percent. We are seeing a change in the value of PVI that we are measuring. This difference is not a change in leaf area index but is a change in the position of the soil line. The point of maximum vegetation is remaining constant while the soil line floats in feature-space.

It should be noted that the variance in PVI values is greater for band 7 vs band 5 than for band 7 vs band 4. This result is somewhat surprising when one considers that the variance in the slope of the individual soil lines is 0.042 for band 7 vs band 5 and 0.174 for band 7 vs band 4. In other words, one

would expect a wider variation in LAI values for the band 7 vs band 4 combination because of the wider variation in the slopes and position of the individual soil lines. Examination of Figure 5.4.3b, however, reveals that the soil lines in this plot tend to converge perpendicularly opposite to the point of maximum LAI, thereby minimising the variation in PVI between the soil lines. The variation, however, increases significantly away from this point.

The above analysis shows that by performing a PVI analysis whilst assuming that the soil line is a single entity, errors in estimating LAI can be of the order of plus and minus fifteen percent, when using combinations of bands 4, 5 and 7. We can assume that similar effects are taking place in Landsat MSS data and should therefore not expect to be able to measure LAI below this minimum threshold with any confidence. While PVI values may reflect a true representation of LAI at a given point on a scene, they may not do so over the whole scene, because of the spatial variability in soil types. Although the PVI was formulated to attempt to make the measurement of LAI independent of soils, it is apparent that this has only been partially successful. This inability of the PVI to make the measurement of LAI independent from soil type is particularly acute in attempting to utilize the method for rangeland monitoring in Egypt, when it is necessary to monitor changes in vegetation below twenty percent cover.

In the preceding analysis both band 7 vs band 5 and band 7 vs band 4 combinations have been studied. It is clear from Figure 5.4.3a that the band 7 vs band 5 combination provides the

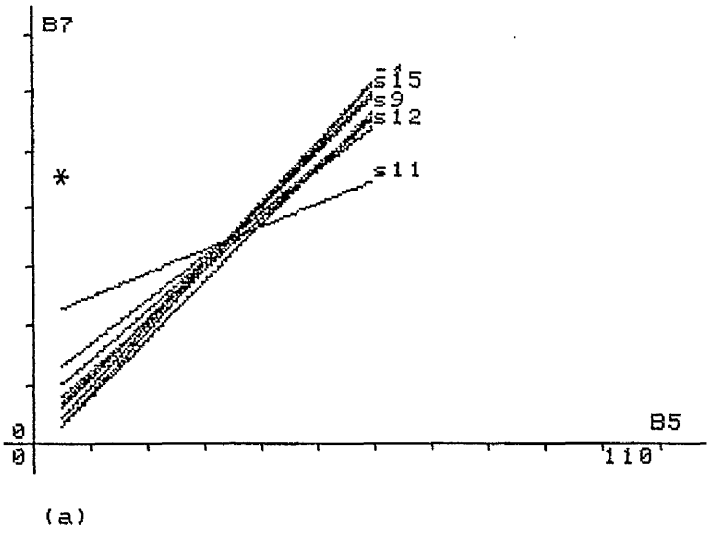

(a)

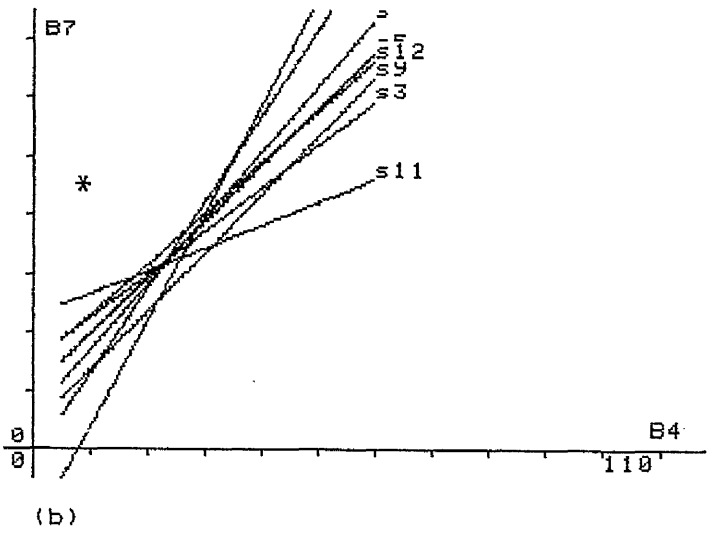

(b)

* : point of maximum vegetation

Figure 5.4.3

Scatter plots of the soil lines derived from regression data in Table 5.4.1. Also shown is the point of maximum vegetation.

tightest grouping of soil lines and therefore the best estimates when using the PVI, or any other ratio or difference vegetation index. The band 7 vs band 4 combination simply adds to the confusion between low levels of vegetation and bare soil. However, if we are to stratify our vegetation estimates and base the estimates on the location in feature-space of individual soil types, then the band 7 vs band 4 combination can help us to identify which soil types are worth separating.

5.5 PRINCIPAL COMPONENTS ANALYSIS OF FIELD DATA

The preceding sections have illustrated how the soils data are distributed. The analysis, however, has been limited to two dimensional projections of the data. A principal components analysis of the data should confirm the findings above and provide different views of the soil line's distribution. As PCA has been discussed at length elsewhere, this section shall present only the results obtained from a PCA on the field data. In order to perform the PCA a computer program was written in BASIC for the NewBrain micro computer. The procedure used for calculating the principal components follows that outlined in Mulder and Hempenius (1974), and the iterative method for solving the eigen values and vectors of a matrix being taken from Jeffery (1982).

The analysis was performed on the data for bare soils only in bands 4,5 and 7. The resulting eigen values and eigen vectors are presented below in Table 5.5.1.

TABLE 5.5.1

Lower Covariance Matrix:

18.3		
25.3	44.Ø	
23.3	42.8	47.Ø

Eigen Vector Matrix:

Ø.57	-1.26	-Ø.71
Ø.98	Ø.28	1.ØØ
1.ØØ	1.ØØ	-Ø.57

Normalized Eigen Values:

E1 = 93.72%

E2 = 5.Ø3 %

E3 = 1.24 %

As might be expected, from a PCA of Landsat data, the first component accounts for over ninety percent of the variance within the distribution. The results reflect the 'flattened cigar shape' of the soils plane described by Kauth and Thomas (1976). It can be seen from Figure 5.5.1 the way in which the data form a tight cluster in the PC2 vs PC3 plot; this plot represents a slice at right angles through the soils line (or plane). Similarly, the plots of PC3 vs PC1 and of PC2 vs PC1 represent slices longitudenaly through the soils line, through both the thinnest and thickest axes respectively. It is worth noting the the distribution of the PC2 vs PC3 slice through the soils line. This slice exhibits the planar nature of the soil 'plane' in three dimensions. The three dimensional nature of the soil plane is emphasised by Christ and Cicone (1984) for

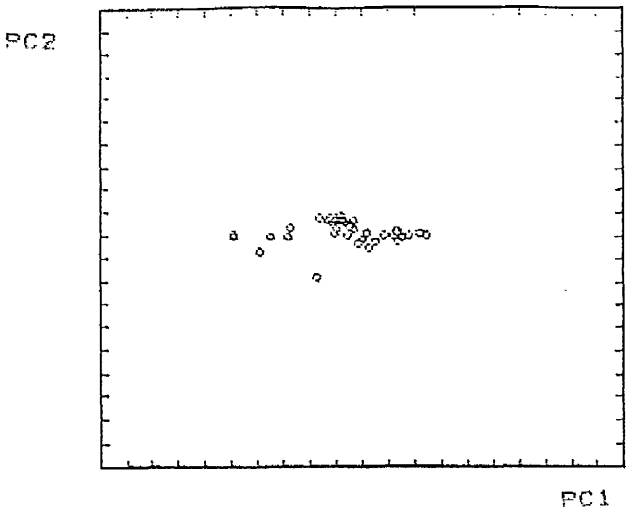

(a) PC2 vs PC1

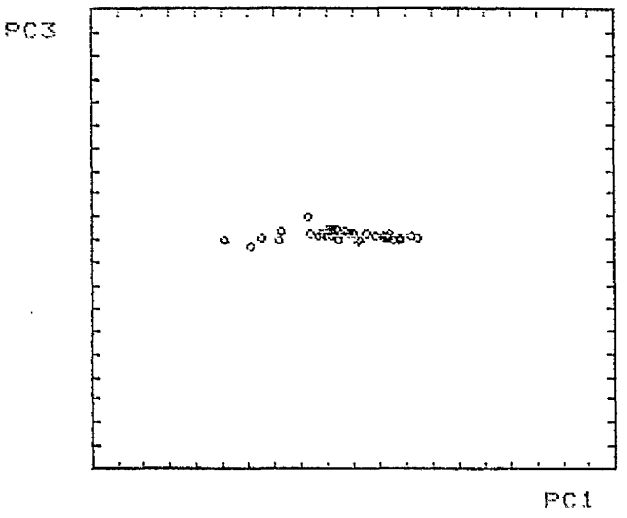

(b) PC3 vs PC1

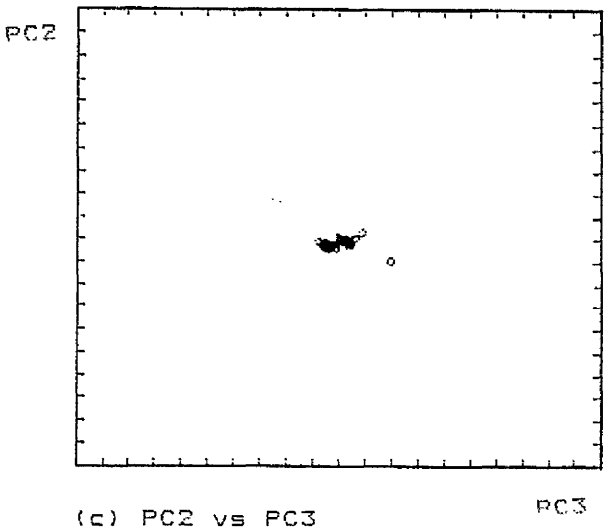

(c) PC2 vs PC3

Figure 5.5.1

Origin centred principal components plots of radiometric field data.

simulated Thematic Mapper data.

5.6 CONCLUSIONS

We have seen from the above analysis and discussion that the soil lines of individual soils are more tightly correlated in bands 5 and 7 than in bands 4 and 7. This observation is graphically illustrated by the PC2 vs PC3 plot in Figure 5.5.1, and also by the normalized eigen values of 5.03% and 1.24% for PC2 and PC3 respectively. In practical terms, however, what implications, if any, does this observation raise? First, the soils of northern Egypt, despite being very similar in colour (all but one of the soils tested had the same Munsell soil colour code) do indeed exhibit multiple soil lines, as described by Huete et al (1983). Secondly, if vegetation mapping of the region is to be performed by using ratios, difference ratios or the PVI; then an appropriate methodology should be followed. When mapping low levels of green vegetation cover, ie below twenty five percent cover, a stratified approach should be adopted, using three dimensional data stratified in terms of soil type, so as to estimate a GVI value for a specific soil type.

The second point above itself raises a number of questions. When applied to Landsat MSS data is such a methodology possible and how should it be applied? The problems of matching soils maps to Landsat data and of assessing soil lines for the different soil types are not trivial. These questions pose very real problems in practical terms and are addressed more fully

in the following chapter.

CHAPTER 6

FURTHER DIGITAL PROCESSING

6.1 THE EFFECT OF FIELD WORK UPON SUBSEQUENT DIGITAL PROCESSING

The effect of fieldwork experience on subsequent digital processing of the satellite data have been twofold. First, the experience of being in the field and of observing conditions on the ground alters the perception of the analyst who was not familiar with the environment in question. This alteration in perception can be profound and at least one example, regarding the erratic distribution of rainfall along the northern coast, is cited below. In particular, visual interpretation of the imagery is far more rewarding and effective when the environment has been experienced at first hand. Secondly, the results of the radiometric field data have implications in terms of sampling and stratifying the study area.

Whilst attempting to classify Transect 3 (see Plate 5.6.2) in the initial stages of the study, it was found that fields of dry-land barley cultivation, which were visible on the satellite imagery and which also appeared on the REMDENE land-use maps, could not be digitally classified or distinguished from their surroundings. The highly variable nature of the rainfall in this region, both in terms of frequency and location was not fully appreciated at the time. It was not at all clear why dry-land barley could be identified with ease in Transect 1 and not at all in Transect 3, where it was also known to occur. The fact that the locations of the fields were visible at all in Transect 3 was a result of them having been ploughed and prepared by the local Bedouin farmers. The lack of rainfall at El Omayed would have prevented the crops emerging, whilst an abundance of rain in and around Burg

el Arab enabled the development of a viable crop, which is quite easily visible on the imagery. This lack of appreciation of the localised nature of desert rainfall is also noted by Evanari et al (1971). The same situation is evident on the 1973 imagery in which large numbers of prepared fields are visible, but in which no crops are growing. The areas which were prepared are visible due to the rough surface structure of the ploughed fields, with a high degree of shadow being cast, in contrast to the relatively smooth shadow free surroundings.

The field trip also highlighted the dynamic nature of land-use which, compounded with the variable rainfall caused the initial confusion in the location of features. It became clear that the Bedouin farmers cultivate dry land crops on the superior soils of the coastal tract. The fields used for dry-land farming have, with the exception of the inner karms, no formal definition, although in some cases the boundaries of different soil types forms the boundary. A field which is cultivated in one year may be left fallow or only partially cultivated in another; and then again the crop may fail through lack of available moisture. These factors of climatic and dynamic land-use make comparisons between years very difficult. The Bedouin deals with the risk and uncertainty of dry-land cultivation by preparing as large an area as possible for cultivation. This acts as insurance against total failure and also strengthens the farmers claim to the land by occupation.

The dynamic nature of farming and land-use in the irrigated areas also makes comparisons between different imaging dates difficult. It should be quite feasible to differentiate between

different irrigated crops given suitable training areas as input to digital classifiers, such as a maximum likelihood or minimum distance classifier. However, as no suitable ancillary data were available , neither ground observations nor aerial photography, for the 1977/78 growing season, this has not been attempted.

Whilst the seasonal variability between the 1978 Landsat imagery and the 1979 aerial photography meant that it was not possible to make comparisons between the two, it is the multi-temporal nature of remotely sensed surveys that offers the greatest potential utility to planning and management in northern Egypt. It has in the past too frequently been the case that multi-temporal digital imagery was used in non-standard ways. By 'non-standard' I mean that imagery recorded on different dates were used to make direct comparisons. Not only will different sun-sensor-target geometries exist between the data sets but differences may also exist between the calibration coefficients of the MSS sensors.

There is a need to standardize satellite data in order to make it useful in a multi-temporal analysis environment. In addition, where ratios are performed, as in vegetation indices, there is a need to standardize individual images. The need for standardization has been recognised by some authors (Robinove 1982, Singh and Harrison 1985), but has been conspicuous in it's absence in much of the literature. In particular Singh and Harrison (1985) have argued that standardization may be preferable when conducting principal components transforms, which obviously has implications for the results presented in Chapter 4.

6.2 CONVERSION OF LANDSAT MSS DATA INTO PHYSICAL VALUES

Robinove (1982) describes a methodology for converting the arbitrary digital values recorded by the Landsat MSS into physical values of either radiance (mW cm^{-2}) or reflectance (%). This is a desireable procedure to follow when comparisons are to be made of Landsat scenes recorded on different dates and/or if band ratios are to be performed. In addition it may be desirable to account for the variation in the angle of the sun. The multi-spectral scanners of the Landsat series of satellites have all had different calibration coefficients relating received radiance to the digital values recorded on the C Ts. These calibration coefficients have varied between the satellites, both at launch time and at different times during the satellite's operational lives. The conversion of the data into physical values would therefore seem to be a prudent undertaking, particularly where the use of the data is marginal, such as in mapping rangeland in northern Egypt.

Robinove defines the relationship between radiance and the digital numbers as being:

$$\text{Radiance} = \frac{Dn}{Dmax}(Lmax - Lmin) + Lmin \qquad (1)$$

where:

Dn = the digital value of a pixel from the CCT

Dmax = the maximum digital number recorded on the CCT

Lmax = radiance measured at detector saturation in mW $cm^{-2}\,Sr^{-1}$

Lmin = lowest radiance measured by detector in mW $cm^{-2}\,Sr^{-1}$

The Landsat Data Users Notes (1979) lists the linear relationship (calibration) of the MSS sensors for the first three Landsat satellites. Table 6.2.1 shows the calibrations for Landsat 2b, which covers the scenes of Egypt recorded in 1978. The numbers show the relationship between the observed scene radiance and the detector saturation in the normally used low gain mode.

Table 6.2.1

Landsat 2b, 16.7.75 onwards.

Band	Lmin	Lmax
4	Ø.ØB	2.63
5	Ø.Ø6	1.76
6	Ø.Ø6	1.52
7	Ø.11	3.91

(Source: Landsat Data Users Notes, US Geological Survey, 1979, pp.AE-16)

Maintaining the assumption that the earth's surface acts like a Lambertian reflector, the author then relates the digital numbers to reflectance by:

$$\text{Reflectance} = \frac{PI}{E \sin(a)} * \text{Radiance} \qquad (2)$$

where:

E = irradiance in mW / cm-2
at the top of the atmosphere

Band 4 = 17.70 mW / cm-2

Band 5 = 15.15 mW / cm-2

Band 6 = 12.37 mW / cm-2

Band 7 = 24.91 mW / cm-2

a = solar elevation measured from the horizon.

(Source: Robinove 1982 pp.782)

In the view of Otterman (1983) the assumption of a surface acting as a Lambertian reflector is valid for bare soil in arid environments. He regards this as being possibly the only natural land surface for which this assumption holds true.

Robinove points out that the digital values in a single Landsat scene are consistant on a relative basis and therefore should pose no problems when performing classifcations. However, when ratioing bands incorrect values can occur because of the different calibrations relating DN to radiance in each wave band. Because of the implications of Robinove's observations for band ratios, such as the normalized difference vegetation index, an I2S function was written in FORTRAN 77 to correct the areas covered by Transects 1 and 3 for variations in both sensor calibrations and for sun angle. A copy of the program appears in Appendix A.

Robinove quotes the value for Dmax, in equation (1) as being 127

in bands 4, 5 and 6, and as 63 in band 7. However, it was found that these values only apply to Landsat data recorded at the EROS Data Centre in the United States. The radiometric calibration Look Up Tables found on the Fucino CCT headers, (which are used to correct for variations which occur between the individual MSS sensors and for the non-linear response of the sensors themselves), were found to stretch the digital numbers over the range Ø to 255 in all of the four wave bands. The value of Dmax was consequently set to 255 instead of 127 and 64 respectively. MacFarlane and Robinson (1984) also quote Dmax as being 255 for CCTs supplied by RAE Farnborough.

6.3 HAZE CORRECTION

Prior to the original DNs being converted into scaled values of reflectance, the data were haze corrected by subtracting from the images the minimum values found in each band. These values were determined from the entire image extract which covers Transects 1 and 3. The values used for the corrections were:

Band 4 : 14

Band 5 : 9

Band 6 : 3

Band 7 : Ø

These values are consistant with the expectation of increasing atmospheric scattering with increasing frequency, or decreasing wavelength, in the given wave bands. The minimum value of zero in band 7 did indeed appear to be a valid DN and expressed

variations in turbidity in the sea. The possibility of a minimum of zero being a data dropout and not an actual sensor reading was therefore discounted.

Robinove's conversion to physical values defines 'E' as being the irradiance at the top of the atmosphere and does not take into account any scattering or atmospheric effects which may be introduced by the path of the radiation through the atmosphere. This simple haze correction was therefore applied prior to the conversion to physical values of reflectance.

In addition to the haze correction it was hoped to deconvolve the imagery to counteract the effects of in-scan smoothing caused by the over sampling of the MSS in the direction of the scan. An operator to do this and to counter the effects of scatter from adjacent pixels above and below, is described by Mulder (1982). However, it was found that although the operator considerably enhanced and sharpened the image, the results of applying the operation on the two 512 * 512 extracts, for Transects 1 and 3, were inconsistent. Mulder's operator is designed such that no scaling or division of the image is necessary as a subsequent operation. The two 512 * 512 images, which had to be processed individually, showed marked differences in colour balance where there should have been none. The I2S function CONVOLVE which was used to perform the deconvolution was therefore suspected to be at fault, prior experience also indicated this. Consequently no deconvolution of the imagery was undertaken. Thus only the haze correction was performed prior to the conversion to reflectance.

6.4 THE EFFECTS OF CALIBRATION ON BAND RATIOS AND DIFFERENCES

Figure 6.4.1 shows the radiometric Look Up Tables used to convert the original Landsat digital values into reflectance. The calibration coefficients set out above were used along with a sun elevation of Ø.516 radians to convert to reflectance; using equations (1) and (2) in section 6.2. The values of reflectance were scaled so that 1ØØ per cent reflectance was represented by a value of 255 and Ø per cent reflectance was represented by a value of Ø. The conversion of DNs to values of reflectance can be considered as a 'DN in => Physical Value Out' transformation. Similarly the sensing of a pixel by the MSS is a 'Physical Value In => DN Out' transformation. The function relating these two states is defined by the sensor calibrations and the solar elevation; as shown in Figure 6.4.1. It is evident from the figure that in relative terms a DN to PV transformation compresses the range of band 5 values in relation to band seven and vice versa, although to a lesser extent. This relative compression of band five is evident in false colour imagery of the corrected scene and is expressed as a shift in colour balance towards the red (ie minus green). The shaded area between the band 5 and the band 7 transfer functions represents the increasing difference which occurs between the bands, ie (#7 - #5), with increasing intensity. The shaded area above and to the left of the 1:1 diagonal shows those values which will be increased by performing the transformation. Similarly, the shaded area below and to the right of the diagonal show those values which will be decreased by the transformation. From the figure we can note the following:

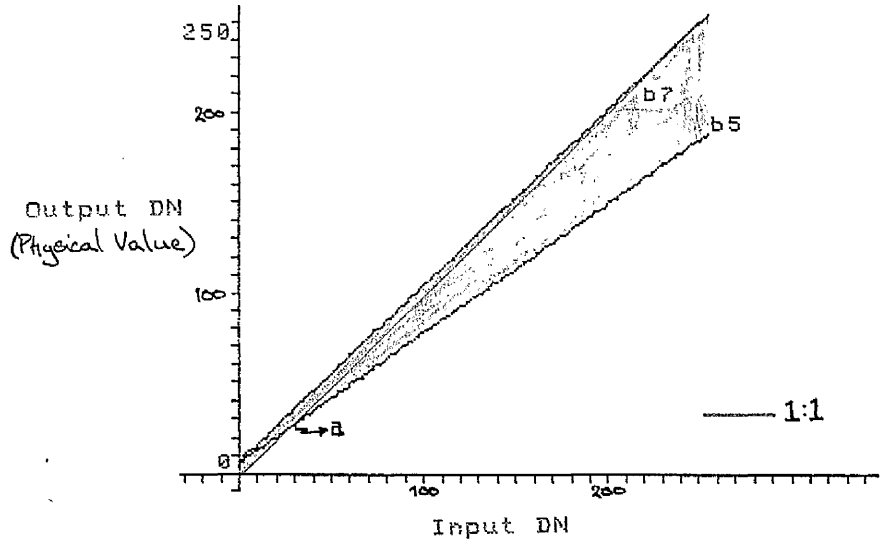

Figure 6.4.1

The radiometric Look Up Tables derived from equation (2) using calibration values for Landsat 2b.

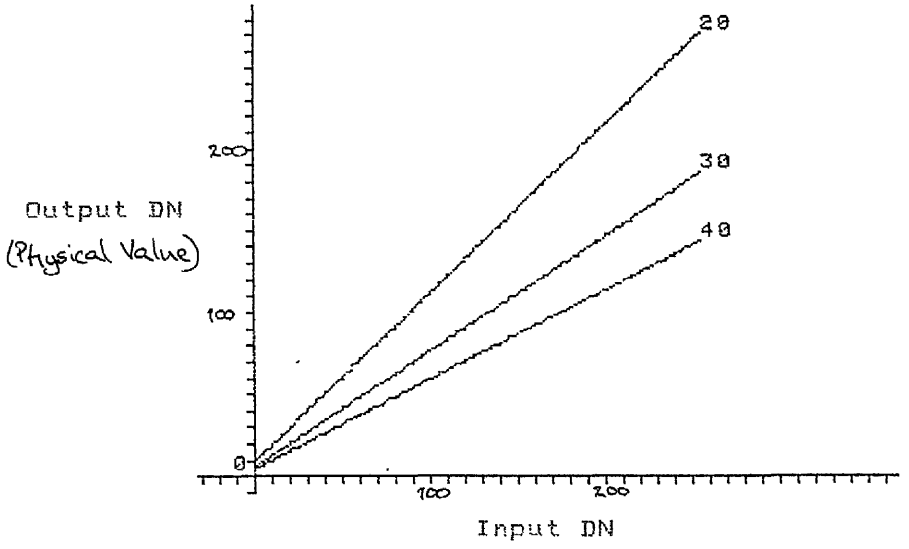

Figure 6.4.2

The effect on the band 7 Look Up Table of varying the angle of incidence. Values are given in degrees.

(1) The transformed values for band 5 and band 7 diverge.

(2) The transformed Band 7 values are always higher than the original values.

(3) The transformed Band 5 values are for the most part lower than the original values.

(4) Only at point 'a' is an input value the same as an output value.

It should be evident from the figure that the transformation modifies the DN feature-space in such a way that the band difference (#7 - #5) no longer subdivides the space into layers parallel to the 1:1 diagonal. The transformation has in fact performed a rotation and non-linear stretch of the data. This modification of feature-space by the transformation will be different for every different Landsat scene. Figure 6.4.2 shows the effect on the band 7 transfer function of varying the angle of incidence. It is clear that changes in the angle of incidence of ten degrees can lead to corresponding changes of tens of digital values in feature-space.

By way of an example the following table shows the effects of the transformation on the (#7 - #5) difference. The values are taken randomly from Transect 1.

Table 6.4.1

Raw Value			Corrected Value		
#7	#5	(#7-#5)	#7	#5	(#7-#5)
92	89	3	97	64	33
89	60	29	94	43	51
98	99	-1	102	71	31
99	106	-7	103	76	27
101	99	2	105	71	34
103	101	2	107	79	28

Negative values obtained for the (#7 - #5) difference are generally regarded as not being vegetation. It is quite apparent from the table that the corrected values, when differenced, provide a greater number of positive values. The -1 and the -7 difference values for the uncorrected data are both transformed into positive values when corrected. In addition the calibrated data differentiates between the last two values by transforming them into 34 and 28 respectively.

These results indicate, as do those of Robinove (1982), that the effect of conversion from MSS digital values to physical values of reflectance has a significant effect on vegetation indices. The need for calibration to standard units has thus been illustrated.

6.5 PRINCIPAL COMPONENTS ANALYSIS OF DN AND REFLECTANCE IMAGES

We have seen in section 6.4 how the difference (#7 - #5) and the NVI are affected by converting the Landsat DNs to reflectance. It was apparent that the results of the standard vegetation indices are all significantly affected by this procedure. However, are these changes reflected in the principal components of the images?

Singh and Harrison (1985) present results of the differences in principal component analysis carried out using both the covariance and the correlation matrices. They argue that by dividing the covariance matrix by the standard deviations, thereby reducing it to the correlation matrix, significantly different results are achieved. By using the correlation matrix in place of the covariance matrix, equal weight is given to each of the spectral bands. Singh and Harrison argue that this may be a more desirable way of calculating the PC transform as it provides a degree of standardization. By using the covariance matrix the PC transform is weighted by sensor system characteristics such as the dynamic range of the MSS bands and consequently the signal to noise ratio of those bands. Singh and Harrison suggest that the standardization might also be performed by conversion to reflectance, but they do not pursue this option. The results of a PCA on the standardized (reflectance) images are presented below.

The principal components for the study area were calculated using the 1Ø24 * 512 extract which covers both Transects 1 and 3. The statistics were derived from all four bands and

are presented in Tables 6.5.1 and 6.5.2 for both the raw and the transformed data.

The loadings for the principal component transfomation are shown in Figure 6.5.1. The shaded areas are loadings for the corrected data while the unshaded areas are the loadings for the raw CCT data. Both the raw and the corrected data conform to the classic principal component loadings as described by Donker and Mulder (1977) and by Singh and Harrison (1985). In this classic case the first principal component's loadings are all positive and indicate a summation of the bands (in this case they are negative but the effect is the same). The second component is an expression of the difference between the infrared and the visible bands, while the third and fourth components are expressions of the difference between the two visible and the two infrared bands respectively. We can see from Figure 6.5.1 that the data conform to this model. Singh and Harrison (1985) demonstrated that their standardization technique made the eigen vectors for PC1 more evenly weighted across all of the spectral bands. However, it is evident from Figure 6.5.1 that a standardization by conversion to physical values actually emphasises the importance of the bands with increasing band number. The conversion to reflectance has had a more marked effect on PC2 than on PC1 with the importance of band four being increased at the expense of band six.

Examination of the eigen values in Tables 6.5.1 and 6.5.2 reveals that the PC transformation from DNs to reflectance, reduces the variance of PC1 and increases the variance of PC3 and PC4, while PC2 remains the same. Indeed examination of the

TABLE 6.5.1

Raw Data

Lower triangle covariance matrix:

1	266.656			
2	632.331	1547.327		
3	666.263	1623.241	1748.496	
4	653.259	1600.401	1721.016	1700.929

Lower triangle correlation matrix:

1	1.000			
2	0.984	1.000		
3	0.975	0.986	1.000	
4	0.969	0.986	0.997	1.000

Eigen values:

	0.992	0.005	0.001	0.000

Eigen vector matrix:

1	-.221	-.541	-.577	-.569
2	-.369	-.722	0.381	0.443
3	0.800	-.399	0.346	-.282
4	0.417	-.159	-.633	0.631

Table 6.5.2

Corrected Data

Lower triangle covariance matrix:

1	233.883			
2	416.256	798.027		
3	457.356	878.695	985.071	
4	583.625	1113.836	1246.439	1600.700

Lower triangle correlation matrix:

1	1.000			
2	0.963	1.000		
3	0.952	0.991	1.000	
4	0.954	0.985	0.992	1.000

Eigen values:

	0.989	0.005	0.003	0.001

Eigen vector matrix:

1	-.246	-.469	-.523	-.667
2	0.767	0.423	-.131	-.471
3	0.531	-.539	-.411	0.506
4	-.259	0.563	-.734	0.275

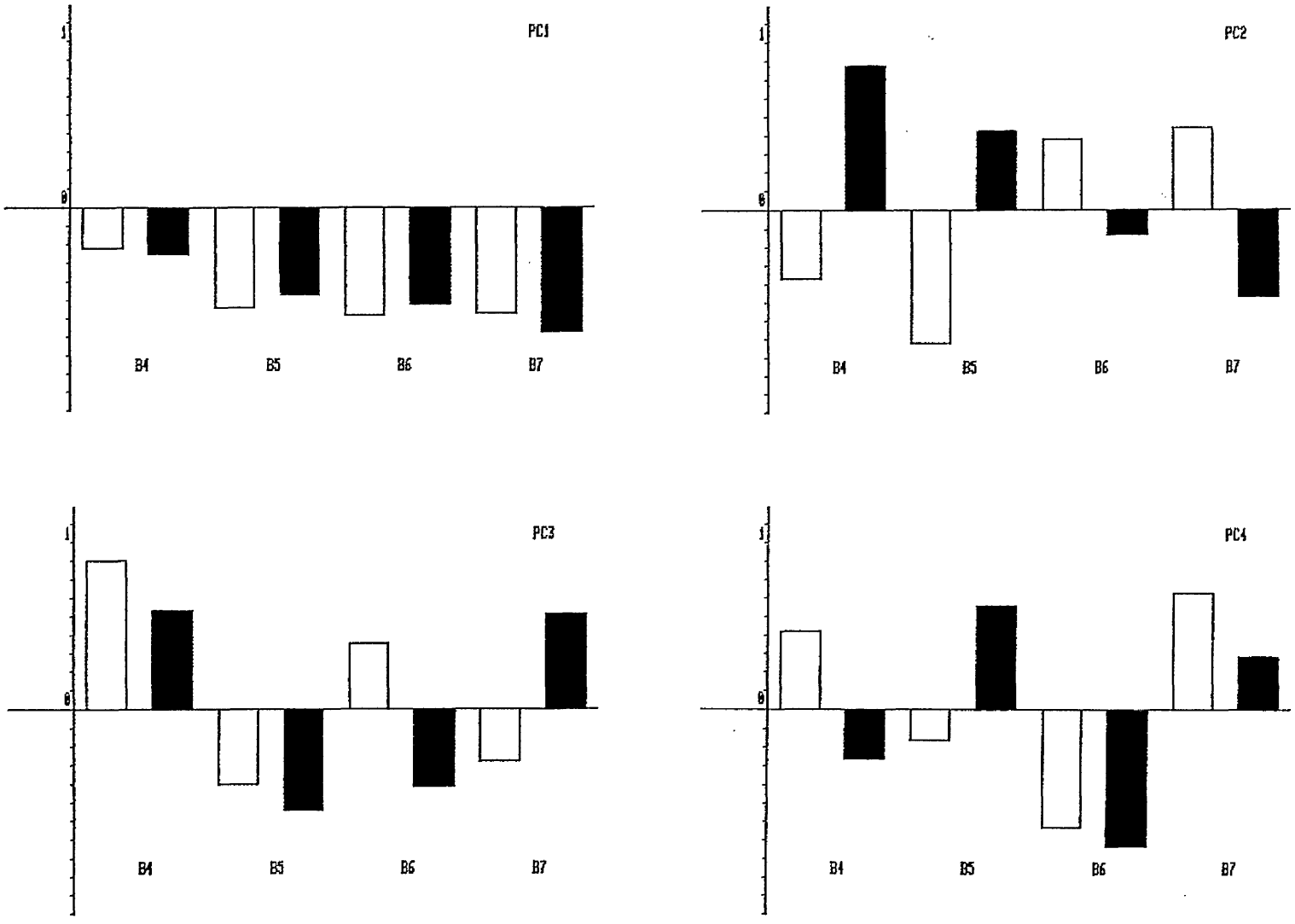

Figure 6.5.1 Principal Component Loadings (eigen vectors) for the raw and corrected data. The solid bars represent the corrected data.

PC images visually, confirms this shift in variances from PC1 to the lower order principal components. The high order principal components (PC1 and PC2) however, do remain very similar before and after the transformation, PC1 being reduced by Ø.ØØ3 or Ø.3 per cent. It should be realised that while changes of Ø.3 per cent may seem trivial they can indeed be significant. If one considers that not only is PC2's contribution to the total variance only Ø.5 per cent but also that it represents a high proportion of the vegetation in the scene, then the importance of these low eigen values becomes apparent. Their importance then, should be considered in relation to the data set as a whole. In this case vegetation covers only a small proportion of the total area and therefore only contributes a small amount to the total variance. The fact that vegetation covers only a small part of the scene, and therefore has a small eigen value associated with it, does not mean that the vegetation is unimportant. The fact of the matter is quite the opposite.

Singh and Harrison (1985) found that significant differences existed between the principal components derived from the covariance and correlation matrices, or nonstandardized and standardized data sets. By standardizing the Landsat data of northern Egypt, by converting to reflectance, it was found that although differences did exist between the data sets, that these differences were minimal for PC2, or the vegetation component. Principal components one, three and four were the components for which the eigen values differed. Although the question of standardized principal components is recognised as an important one, particularly in the context of multi-temporal studies, it's consequences are not pursued further here as PC2

essentially remained the same.

6.6 TWO DIMENSIONAL SOIL LINE ANALYSIS

The problems which arise by performing ratios, differences and principal components analysis on Landsat MSS data have been discussed above. These problems can be summarised as being the attributes of the non-alignment of the soil line(s) with either PC1 or a forty five degree diagonal in feature-space. We have examined PCA for both standard and non-standard data and have looked at the variation in soil line slopes for hand held radiometer data. In this section the soil line analysis described in the Chapter 5 is extended to standardised Landsat MSS data.

In order to investigate the soil lines using digital data an I2S function was written to calculate the slope, intercept and correlation coefficient of two dimensional scatterplots produced by the I2S function SCATTERGRAM. The least squares regression routine for this program was converted to FORTRAN 77 from a BASIC program published in Lee and Lee (1983). The source code of this new I2S function, called LEASTSQ, appears in Appendix A.

By first selecting representative areas of bare soil (or nearly bare soil), which were visited in the field, and by using the I2S function BLOTCH, scatterplots were produced of band 7 vs band 5 for the nine field sites listed in Table 6.6.1. The slopes, intercepts and correlation coefficients were then calculated using the function LEASTSQ.

The procedure taken involved the following five steps:

(1) For each of the soil types investigated one hundred representative pixels were chosen. This was done so as to try and sample a variety of soil pixels with different soil moisture states.

(2) Scatterplots for each of the soil sites were produced.

(3) The slope, intercept and correlation coefficient for each scatterplot were calculated using LEASTSQ.

(4) Stages (2) and (3) above were repeated using an aggregated soil line of all those sites with a correlation coefficient above Ø.9 (Ø.9 being regarded as a good fit).

(5) Bands 7 vs band 5 feature-space was rotated so that the aggregated soil line was horizontal.

The feature-space rotation was performed using a modified version of the I2S function MATRIX'TRANSFORM.

Table 6.6.1 shows the results of the soil line analysis for the corrected data.

TABLE 6.6.1

Corrected Data #7 vs #5

Site No	Slope	Intercept	CC	a(degrees)		
1	Ø.28	86.69	Ø.21	15.64		
2	Ø.Ø8	97.27	Ø.Ø8	4.57		
3/4	1.26	6.52	Ø.99	51.56	*	#
9	1.24	7.6Ø	Ø.98	51.12	*	#
1Ø	1.24	7.6Ø	Ø.98	51.12	*	
12	1.1Ø	21.83	Ø.88	47.73	*	
13	1.22	13.41	Ø.94	5Ø.66	*	#
14	1.Ø3	27.43	Ø.72	45.85	*	
15	Ø.95	31.95	Ø.82	43.53	*	
Mean of sites #	1.24	9.18		51.94		

Those sites marked with a '*' have a correlation coefficient greater than the Ø.Ø5 per cent one tailed significance value (Ø.3211 Source: Lee and Lee (1982)) for Pearson's correlation coefficient. Thus there was less than a Ø.Ø5 percent chance of these distributions being random. The sampling of the sites in inland areas where little or no variation in soil moisture occurs meant that for some of these sites it was not possible to obtain a representative soil line. These sites are conspicuous by their low correlation coefficients.

If we look at the values of slope for those soil lines with a correlation coefficient above Ø.9, we find that for the range between 1.22 and 1.26 or 5Ø.66 degrees to 51.56 degrees,

a variation of only Ø.9Ø degrees.

These results quite clearly show that, within the terms of reference of the experiment and with a correlation coefficient threshold of Ø.9, there are no significant differences in the slopes of the soil lines of the discrete soil types of the region. I would like to suggest, however, that the poor results obtained are more a function of an inadequate sample of points along the soil lines than anything else. The fact that there are only four out of nine sites which have a correlation coefficient above Ø.9 may confirm to this. If we lowered our correlation coefficient to Ø.8 we would find that six out of nine sites would be included and that the variation in slopes would be Ø.31, or 17.22 degrees. A variation in slope of 17.22 degrees would indeed be significant in terms of vegetation mapping, however a variation of Ø.94 is not. From an examination of the scatterplots of those sites with correlation coefficients below Ø.9, it was not felt that they were sufficiently representative of the soils to establish individual soil lines on them.

The sampling for the soil line analysis was carried out on the basis of field experience and a knowlege of areas with little or no vegetation and in some cases a range of soil moisture types. Random sampling, or even stratified random sampling was not possible. These two sampling methods would have required digital soils and vegetation maps along with properly geometrically corrected MSS data. The production of these three prerequisites can only be described politely as being non-trivial, particularly for this semi-desert area which contains

very few ground control points.

Rather than speculating further on the possible results obtained by improved sampling of the soil types, we shall proceed by using the results for those soil lines with a correlation coefficient above Ø.9 per cent.

The slopes and intercepts for those sites with correlation coefficients above our threshold of Ø.9, were averaged to provide values for an aggregated average soil line. The results of this averaging are given in Table 6.6.1. As described above, in a previous chapter, the non-alignment of the soil line with either the 1:1 diagonal (in band 7 vs band 5 feature-space) or PC1 leads to inaccuracies occurring in most forms of vegetation index, with the exception of the PVI. A rotation of band 7 vs band 5 feature-space so that the slope of the soil line becomes zero will enable a PVI to be performed with ease.

In order to perform the rotation of the feature-space it was necessary to modify the I2S function MATRIX'TRANSFORM so that the resulting images were only rotated and not scaled. Normally the transformed data are stretched to pad out the feature-space. Prior to performing the rotation the value of the intercept was subtracted from band 7 to ensure that the rotation would take place about the intercept of the soil line on the y axis. Having performed this translation of the intercept to the origin of the co-ordinate system negative rotations were made of 51.12 degrees and 41.99 degrees for the raw and the corrected data respectively. Thus the average soil lines were brought into alignment with the x axis of the

feature-space.

The results of the two dimensional vegetation analysis are shown in Plate 6.6.1. This particular image is at the correct aspect ratio but no further attempt has been made to geometrically correct the image.

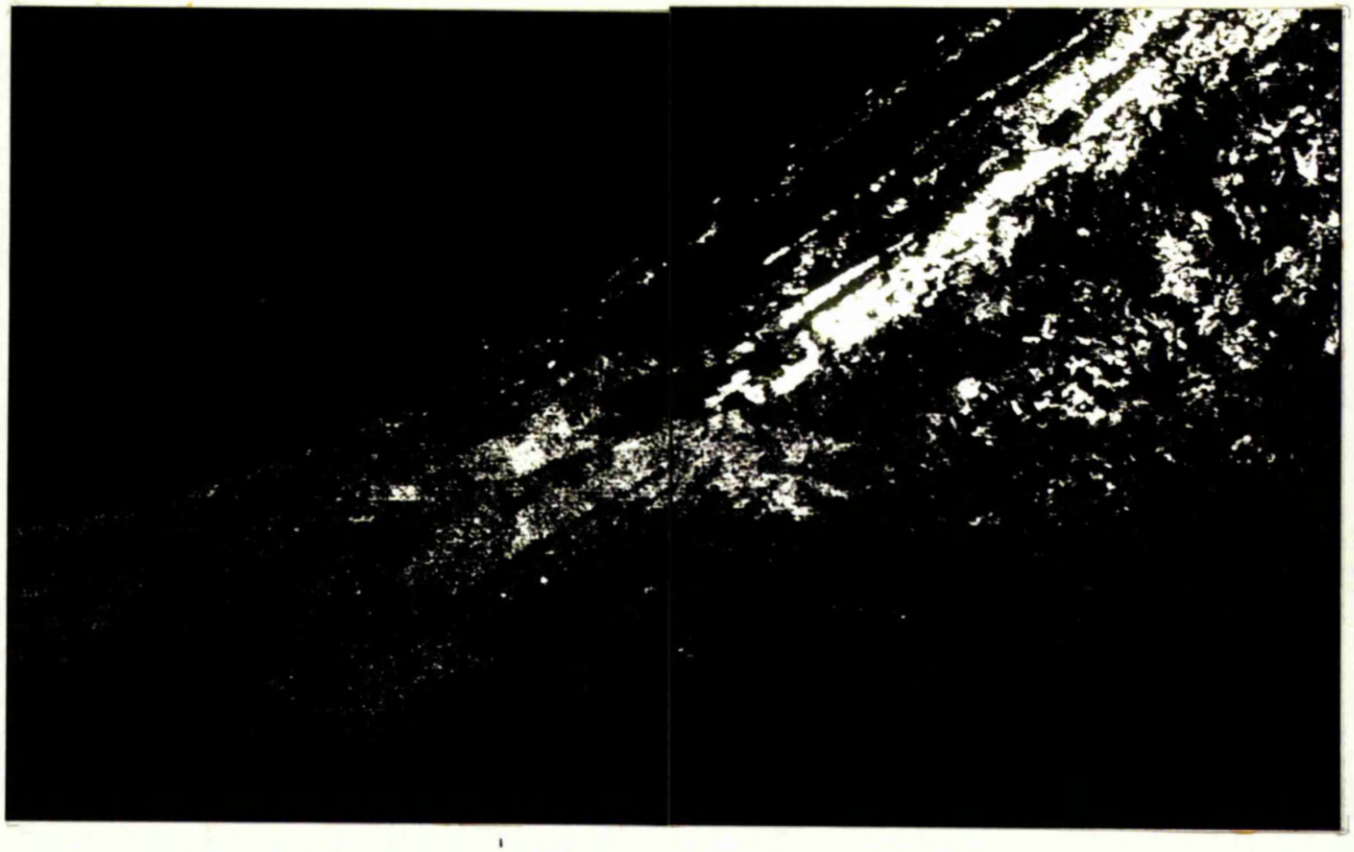

Plate 6.6.1

Transcts 1 and 3 Perpendicular Vegetation Index image.

CHAPTER 7

CONCLUSIONS AND RECOMMENDATIONS

7.1 SUMMARY

The near infrared and visible feature-space of digital Landsat satellite data of northern Egypt, has been examined and explored using principal components analysis. Decorrelating the data by using principal components analysis it was found that classifications of the major land cover types could be made by interpreting the PCA feature-space and manually defining boundaries within it. The decision boundaries could not optimally be defined because of software limitations. However, the results obtained from this classification were found to be superior in classifying rangeland vegetation to classifications made using a parallelpiped classifier.

Hand held radiometer data were recorded in the field on the major soil types which occur in the region. These data were used to construct soil lines for each of the different soils. An examination of the locations within Landsat feature-space of the soil lines showed that variations could result in differences in PVI values of plus or minus fifteen per cent, depending on which soil line was being used. This value of fifteen percent represents a minimum threshold below which it is not reasonable to estimate green vegetation cover.

This analysis was extended in Chapter 6 to the digital Landsat data. Prior to the analysis, the arbitrary Landsat digital values were standardized by conversion to physical values of reflectance. Principal components analysis of the reflectance image showed that the major axes of variance within the data are not significantly changed by the standardization procedure.

However the conversion to reflectance was found to have a significant influence upon band ratio values which are often used as an indication of vegetative activity.

By sampling band 7 and band 5 data from the major soil types, soil lines were constructed from the satellite data. Examination of the soil lines showed that for those soil lines which had a correlation coefficient above Ø.9, variations in the slope of the lines were in the order of 2.3 degrees. If the soil lines with correlation coefficients greater that Ø.8 are included then the variation in slope increases to 17.Ø degrees.

It has been found that although the spectral response of the major soil types of Burg El Arab and El Omayed do differ, these differences do not account for a significant variation in the measurement of vegetation using near infrared and visible waveband combinations.

It was not possible to register the satellite data sufficiently well with the soils maps, as very few control points could be found on the bland desert imagery.

7.2 CONCLUSIONS

Both hand held radiometer measurements made in the field and Landsat satellite data, have shown that the soils of the coastal tract exhibit soil lines with different slopes and intercepts. It has not, however, been possible to show here that the differences between the soil lines can be used to improve green vegetation estimates by stratifying an area into those soils

which exhibit discrete soil lines. Of the soils which were sampled in the study almost all have the same Munsell colour code and it can be infered that this similarity in the visible wavelengths, is the reason for the soil lines being tightly aligned around the mean. An extension of the study to areas which possess soils with more widely differing soil colours may indeed prove to be more fruitful. One example would be to extend the analysis to the Nile Delta with its dark organic soils.Ezra et al (1984) present results of a discrete soil line analysis, of an agricultural area in the United States, in which the variability of three soil lines are reduced from 14.5 percent to 3.8 percent of the PVI axis.

Although of limited success, the soil lines analysis has provided a 'real' or measured soil line about which rotations can be made, as opposed to the 'virtual' soil line which is assumed in vegetation indices such as the normalized difference (NDVI). By measuring the soil lines of the individual soils it has been possible to estimate the percentage PVI value below which soil data on one soil will be confused with vegetation data on another. From the hand held radiometer data this minimum threshold has been estimated as being fifteen per cent of the maximum PVI value possible.

In conclusion I would like to emphasise that the majority of problems which were encountered during the course of this study were all in relation to information acquisition and handling. The software and hardware that have been designed for the manipulation of remotely sensed data impose limitations in terms of their relationship to other forms of data. Although

these systems allow the data to be handled digitally, they introduce problems of transportability between machines and isolate the data from other forms of data which are not currently stored digitally. We therefore have a paradox in that computers allow us to use the data in new ways but at the same time it is the digital nature of the data which prevents us from using it in relation to other sources of information. The cost of good hardcopy which is visually and geometrically acceptable has been prohibitive and computer images are ephemeral.

7.3 MATCHING REMOTE SENSING TECHNIQUES TO REAL NEEDS

Three important developments have taken place in the nineteen eighties with respect to remote sensing monitoring of natural resources.

First, a new generation of high resolution sensors has become operational in the form of the Thematic Mapper, on board Landsats four and five, and more recently the push broom CCD sensor on board Spot. The Thematic Mapper provides data in seven spectral channels at a nominal spatial resolution of 30m. A seemingly vast improvement on the multi-spectral scanner's four bands at 80m spatial resolution. Spot on the other hand provides only three bands but at spatial resolutions of 20m and 10m. The 10m spatial resolution of Spot provides 64 times more spatial information than the 80m resolution of the Landsat MSS.

Secondly, computer technology is advancing at an ever increasing rate, providing increased processing power and speed. Powerful dedicated image processing systems are now widely available for processing digital satellite data.

Thirdly, it has become the policy of the American government that space be commercialised and that industry should bear the costs of data acquisition and distribution. The purpose of the privatisation was '...to maintain U.S. leadership in remote sensing from space and to foster the economic benefits of such data for the private and public good...' (Calio 1986). Thus EOSAT was formed on September 27 1985 to produce and market the products of the Landsat satellites and to build and operate a receiving station and a further two satellites. Their main competitor in this market will be the French company Spot Image who will also be providing data on a commercial basis.

These developments would seem to bode well for the future of the remote sensing industry. What are their implications, however, for the developing world in general and in particular for Egypt?

Intuitively one might think that the increased spectral and spatial resolution of the sensors would provide a better basis for classification and mapping. It has been shown, however, (Harrison 1985) that classification accuracy actually declines with increasing spatial resolution. With higher spatial resolution more heterogeneity occurs within predefined 'user' classes. This heterogeneity may or may not be desirable and may simply lead to within class variablility and increased

chance of misclassification. For example when digitally classifying woodland, (one class), high spatial resolution increases the occurrence of heterogeneous pixels, ie structure within the woodland (greater than one class). Thus we can see that the problem of classification is not just a question of spectral or spatial resolution but also involves the relationship between pixel size and feature or class size. We must therefore endeavour to match the data used for a specific problem not only with the perceived costs incurred, benefits derived and scale required, but also with class feature scale. We might envisage in a complex case (ie in Europe) a classification process that involves both spectral classification and contextural classification operating at a variety of scales depending upon feature or class type. At a more general level, rangeland mapping in Egypt for example, the increased spectral and spatial resolution of TM data are largely redundant.

Furthermore, the increased pressures on computing resources are not trivial. One Landsat MSS scene occupies one CCT or about thirty five megabytes. Alternatively one TM scene occupies seven CCTs or about two hundred and forty five mega bytes, and covers a slightly smaller area. Current generations of image processors generally have frame stores 512*512 pixels square. The distance on the ground represented by 512 pixels for a variety of different sensors is shown in Table 7.1.1. It is clear from the table that the Spot and TM sensors offer too restrictive an area for broad scale mapping when displaying images at this size. This may not be a serious problem but serves to show the limited display technology that we

currently live with and how restrictive it becomes when used with higher resolution imagery.

TABLE 7.3.1

Spot	5.1 km
TM	15.4 km
MSS	41.Ø km
AVHRR	563.2 km

The linear distance on the ground represented by 512 pixels for a range of different sensors.

For the past decade the cost of digital satellite data has been very inexpensive. Not only has the initial cost of a CCT been low but there have been no restrictions on the subsequent copying and exchange of the data. Data have therefore been freely exchanged and published. The advent of commercial remote sensing products has been heralded by a huge increase in the cost of all types of data, both photographic and digital. Research into remote sensing techniques which once relied upon a cheap source and free exchange of data may now diminish. Tragically the cost of the data to less developed nations, where the data's marginal utility is probably the greatest, may make it's use prohibitive. The data from Spot and Landsat will now, more than ever, become the domain of those who can afford it.

The use of technology should be appropriate to our objectives. This does not mean, however, that the use of remote sensing in

developing nations should be unnecessarily 'down market'. Despite the high cost of earth resources satellite data, sources of inexpensive data still exist in the form of the meteorological satellites, specifically TIROS-N and Meteosat. The popularity of the Landsat series of satellites has in the past obscured the potential utility of the meteorological satellite data for land inventory mapping. Happily this state of affairs is changing and many people are now seeing the potential of these systems with their high radiometric and temporal resolution. Technology can be used intelligently and today's 'state of the art' is tomorrow's intermediate technology.

Although advances in computer technology have meant that more data can be processed at higher rates, Philipson (1986) emphasises that computer developments have had little influence upon approaches to problem solving using remotely sensed data, and that the advances in computing technology have been offset by the increased costs of data. Philipson points out that the cost of a set of Thematic Mapper CCTs is now greater than the cost of a micro computer on which they can be processed. It would follow then that if advances in computer technology are to have an impact on the way that we use remotely sensed data then the changes will have to be from the bottom up rather than from the top down. In other words, if we are to use remotely sensed data to our advantage we can use the advances in computer technology to enable us to process more of the data by providing us with smaller cheaper systems. We will thus be able not only to start processing the vast archives of data which have never been looked at, but also to start tapping a source

of free data (AVHRR and Meteosat) by collecting and processing it where it matters most, ie in situ.

The NOAA Global Vegetation Index is a remarkable product but it has yet to make any real impact upon food and environmental problems on the ground. The FAO is currently installing an information system which makes use of this product, however it does not and cannot use AVHRR data at the full resolution of 1.1 km. It is proposed here that this mapping can and should be done at this resolution on a national level in addition to the efforts of mapping and monitoring made by NOAA on a global scale.

Watson (1981) has illustrated the importance of sampling in remotely sensed surveys and has also addressed the problems of data presentation (Watson (1981), Watson and Nimmo (1985)). The problems of data handling and presentations are very real ones and are only compounded by increased spectral, spatial and temporal resolutions. Watson and Nimmo (1985) state that 'our capability to collect and analyse natural resource information now exceeds by orders of magnitude our capability to use it'. Far more data are transmitted than can be received and archived, let alone used. It should now be the role of technology to make more effective use of what we already have rather than drown us in a deluge of data. The effective acquisition and presentation of environmental data for natural resource management is particularly important in the developing world where the marginal utility of the data is far higher in human terms than in the west.

7.4 REQUIREMENTS FOR OPERATIONAL MONITORING

Although computing technology has been advancing at great speed, commercially available machines for image processing have not really kept pace with the increasing volumes of data. There has been a lag between the introduction of new sensors and image processors which can make effective use of the data. This lag will continue to exist although time is now ripe for the processing technology to catch up with the data, even though it may be only for a short time.

A dedicated image processing system such as an I2S or GEMS can cost in excess of $100 000 if a host mini computer and software are included. In addition to this initial outlay running costs are high in terms of data acquisition, maintenance and personnel. What is required is an inexpensive data capture and processing system which is matched to the needs in hand. Current micro computer technology meets these requirements and a powerful system could be configured at minimal cost. Such systems would not be limited to use in Egypt but could provide medium resolution data for meteorological and vegetation mapping over much of Africa. Such a system should be specific to a task and should not be general purpose in terms of software as are the I2S and GEMS machines.

An ideal system should be capable of receiving, processing and storing AVHRR and Meteosat data at full resolution. Not only should it be able to perform these tasks but it should also be able to access other sources of data within the framework of a geographic information system. The system should

be suitably robust and reliable for use in hot, dusty and humid environments and should be easy to use and have specific uses.

The distinction between mapping and monitoring should be emphasised. Mapping is a process whereby specific ground features are sampled and mapped at an appropriate scale. A mapping exercise in northern Egypt might make use of what aerial photography is available in conjunction with satellite data, Spot or TM, and the wealth of data and maps which have been prepared by the SAMDENE and REMDENE projects. A mapping exercise would be conducted maybe once a decade and would require a large input of human and financial resources for the production of maps at 1:50 000. A monitoring exercise, however, would assume that the mapping had already been performed and would make use of larger scale imagery such as AVHRR or Meteosat. Monitoring should and can be performed on a continual basis and in the case of vegetation could be performed once a fortnight or once a month from composite imagery constructed along similar lines to the NOAA vegetation index, as well as incorporating methods outlined in the previous chapters. Such monitoring should be done at a scale of 1:100 000 and should be in the form of a calibrated vegetation index. As the index would be derived from meteorological satellite data it makes sense also to provide a rainfall estimation procedure in the same package, various methods for rainfall estimation are available, Barrett et al (1986). Once produced it is the opinion of the author that these products should become part of an electronic REMDENE database along the lines described by Watson and Nimmo (1985).

7.5 AN INTEGRATED INFORMATION SYSTEM

Watson and Nimmo (1985) have described an information system designed to contain the contents of a survey of livestock resources in Somalia. The system which they describe comprises of a relational database containing diverse sources of information relating to the survey. Watson and Nimmo state that when the data have been entered into the system then 'the 3,200 kg of paper and photographs will have been converted into a flexible, dynamic and inter-acting information system' (Watson and Nimmo 1985 pp 5). The concept and implimentation of a relational database is not new but Watson and Nimmo describe an 'intelligent interface' based upon an Expert System which they claim can provide, amongst other things:

- impartial and apolitical evaluation of proposed management activities;

and

- more accessible and easily understood information for planners and strategists.

Watson and Nimmo's arguments are persuasive and can be applied not only to the case of Somalia but also to that of Egypt and the REMDENE study. Intelligent information systems are of course applicable in a general sense and it is not implied that their use is appropriate only to developing nations. Such an information system would be dynamic rather than static, as are conventional reports. Data can be continually updated, corrected and archived. Specifically remotely sensed data, such as a local 1.1 kilometre NOAA GVI type product could form a

basis for vegetation monitoring and would be available for cross referencing with socio economic data such as :

- number of livestock;
- tonnes of imported fodder;
- tonnes of meat production;
- product prices and demand;
- location of settlements;
- population density;
- etc;

in addition to the environmental data necessary for effective mapping:

- climatalogical data;
- terrain data;
- soil maps;
- geological maps;
- vegetation maps;
- etc.

Such information is essential to regional management and it is only with powerful digital systems such as these that remotely sensed data can be effectively incorporated into the resource management process.

The term GIS (Geographic Information System) is currently in vogue in relation to remote sensing. It's popularity in the remote sensing community is probably due to the fact that remotely sensed data have all too frequently been used and

applied in isolation to other forms and types of data. This has been caused by both conceptual and technical bottle necks with respect to satellite imagery. The type of 'intelligent' system described by Watson and Nimmo, incorporating a stronger GIS element, offers the appropriate tools for effective regional planning and management, especially where remotely sensed data are concerned.

The types of information systems briefly described above clearly show the way forward in terms of information handling. In the case of Egypt, however, it is important to realise that if remote sensing is to have any real impact then a local receiving station should be set up to map vegetation and rainfall. In my opinion the REMDENE and SAMDENE studies should become electronic databases in a similar way to the Somalian rangeland study of Watson and Nimmo (1985).

Specifically concerning vegetation, maps should be produced on a fortnightly or monthly basis at the full 1.1 kilometre resolution of the NOAA AVHRR. Vegetation indices should be produced using data which has been calibrated by conversion to physical values and using a real soil line, ie one (or many) which have been measured, rather than a virtual soil line such as the diagonal through feature-space that the normalised difference vegetation index uses.

Only when such products are available on an operational basis will remote sensing provide a truly useful input to REMDENE.

7.6 A LOW COST MONITORING SYSTEM

This section outlines the hardware requirements for a low cost operational monitoring system.

THE RECEIVING STATION

Hobby electronics have advanced to the stage where receivers and decoders for NOAA/AVHRR and Meteosat data are available for less than two hundred pounds and systems are installed in schools and colleges throughout the UK for the purpose of teaching electronics, computing and meteorology. More robust systems are available for less than six thousand pounds and are used in various industries for weather 'now casting', where weather conditions in the very near future are of importance. These systems equipped with analogue to digital converters are amply suited to data collection for environmental mapping purposes.

THE PROCESSOR

Ideally a multitasking processor(s) and operating system would be desirable. Coupled with a floating point processor a multitasking system would be able to manage the acquisition and processing of data simultaneouly. A system based upon the Inmos Transputer would be able to accomplish these multiple processes with ease and would be upwardly expandable. A dedicated processor(s) would be available for each job at hand, ie image calibration, geometric correction, vegetation processing, interactive analysis etc. Until such Transputer

systems become common other relatively low cost super-micros capable of performing the tasks are available.

THE FRAME STORE

Various frame store devices are available for the storage of digital imagery, one of the most notable of these being the PLUTO colour graphics board. While some micro computers offer their own colour graphic systems, such as the IBM professional colour graphics system, these are not considered to be suitable for the requirements. The PLUTO offers hardware zoom and pan facilities and is upgradable, ie the system can be entered at a variety of different levels depending upon requirements and costs. A fully expanded PLUTO system configuration would be a more than adequate basis for the imaging system. It comprises of a 512*512 square frame store with a depth of 24 bits. This configuration can be utilised in a variety of different ways. It can be used to display three bands of multi-spectral data, such as Spot, or it could be used to store and display two AVHRR bands for vegetation mapping. It would also provide a suitable configuration for various rainfall monitoring procedures (Barrett et al (1985)).

STORAGE MEDIA

The cost of high capacity Winchester discs for micro computers have fallen drastically over the past few years. It is proposed that a high speed 40 megabyte hard disc be used as a scratch pad and system disc. This type of disc is reliable and is hermetically sealed excluding any particles of dust or grit. In

addition to the hard disc another type of storage media is required for archival use. Traditionally this would be a tape streamer or floppy disc. Both of these media are non-permanent and are sensitive to environmental adversity (dust, humidity and static electricity). Write once laser discs are now available and offer superb qualities for data archiving. They can store 550 mega bytes of data per disc, are very fast to access, provide a permanent record and are very inexpensive. For image achiving they are ideally suited. If, for example a 1024*1024 two band AVHRR image was acquired once a day and a vegetation index product was produced and archived along with the original bands then a total of six months data could be stored on one twelve centimetre compact disc. Such images would cover over one thousand kilometres square and would form a valuable historical archive.

BIBLIOGRAPHY

Ajai, Kamat, Chaturvedi, Singh, Sinha (1983), 'Spectral assessment of leaf area index, chlorophyll content, and biomass of chickpea', Photogrammetric Engineering and Remote Sensing Vol 49, pp 1721-1727.

Allan JA, Richards TS (1983), 'Use of satellite imagery in archaeological surveys', Journal of Libyan Studies, 14, pp 4-8.

Allan JA, Richards TS (1983), Radiometric field data of norther Egypt. Unpublished.

Angell IO (1981), 'A practical introduction to computer graphics', J Wiley & Sons, Halsted Press.

Arnon I (1972), 'Crop production in dry regions (volume I)', Leonard Hill, London, pp 95.

Ayyad MA, El-Kadi HF (1982), 'Effect of protection and controlled grazing on the vegetation of a Mediterranean desert ecosystem in northern Egypt', Vegetatio, 49, pp 129-139.

Ayyad MA (1978), 'A preliminary assessment of the effect of protection on the vegetation of the Mediterranean desert ecosystem', Taeckholmia, 9, pp 85-101.

Barker GWW, Jones GDB (1982), 'UNESCO Libyan valleys survey 1979-81', The Society for Libyan Studies.

Barrett EC, Beaumont MJ, Harrison AR, Richards TS (1985), 'BIAS-I2S Users Guide', AgRISTARS Stage 5, Remote Sensing Unit, Bristol University.

Beer JS, Sijmons K, Weinreich H (1978), 'Intensity and colour coding of relief and ground cover on PC transformed Landsat data', ITC Journal 1978-2, pp 347-352.

Brichambaut G, Perrin DE, Wallen CC (1963), 'A study of agroclimatology in semi-arid and arid zones of the near east', Technical Bullitin of the World Meteorological Organization 56, pp 64.

Calio (1985), 'Landsat commercialization', Landsat Data Users Notes, No 34, November 1985.

Card DH (1982), 'Using known map category marginal frequencies to improve estimates of thematic map accuracy', Photogrammetric Engineering and Remote Sensing, Vol 48, pp 431-440.

Congalton RG, Oderwald RG (1983), 'Assessing Landsat classification accuracy using discrete multivariate analysis statistical techniques', Photogrammetric Engineering and Remote Sensing, Vol 49, pp 1671-1678.

Crist EP, Cicone RC (1984), 'Application of the tasselled cap concept to simulated thematic mapper data', Photogrammetric Engineering and Remote Sensing, Vol 50, pp 343-352.

Crist EP, Kauth RJ (1986), 'The tasseled cap de-mystified', Photogrammetric Engineering and Remote Sensing, Vol 52, pp 81-86.

Curran PJ (1981), 'Multispectral remote sensing for estimating biomass and productivity', Plants and the Daylight Spectrum, Edited by H Smith, pp 65-99, Academic Press.

Curran PJ (1983), 'Estimating green leaf area index from multispectral aerial photography', Photogrammetric Engineering and Remote Sensing, Vol 49, pp 1709-1720.

Dalsted KJ, Worcester BK, DeVries ME (1978), 'Influence of soils on Landsat spectral signatures of corn', J.Article No SDSU-RSI-J-78-14.

Daultrey S (1976), 'Principal components analysis', Concepts and Techniques in Modern Geography, Geo Abstracts.

Davis JC (1973), 'Statistics and data analysis in Geology', John Whiley and Sons.

Dixon C, Leach B (1977), 'Sampling methods for geographical research', Concepts and Techniques in Modern Geography, 17, Geo Abstracts.

Duggin MJ (1974), 'On the natural limitations of target differentiation by means of spectral discrimination techniques', Proceedings of the 9th Symposium on Remote Sensing of Environment pp 499-516.

Duggin MJ (1983), 'Factors controllong the relationship of remotely sensed radiance to ground cover', Proceedings of the Remote Sensing Society Annual Conference, 1983.

Duggin MJ (1980), 'The field measurement of reflectance factors', Photogrammetric Engineering and Remote Sensing, Vol 46, pp 643-647.

Duggin MJ, Philipson (1981), 'Ground level reflectance measurement techniques: an evaluation with emphasis on the importance of spectral calibration', 15th International Symposium on Remote Sensing of Environment, Ann Arbor.

Duggin MJ (1982), 'Simulation studies and the need for field reflectance studies', AIAA/SPIE Technical Meeting, San Diego.

Evanari M, Shanan L, Tadmor N (1971), 'The Negev : The Challenge of a Desert', Harvard University Press.

Ezra CE, Tinney LR, Jackson RD (1984), 'Effect of soil background on vegetation discrimination using Landsat data', Remote Sensing of Environment, Vol 16, pp233-242.

FAO (1970), 'Preinvestment survey of the northwestern coastal region - physical conditions and water resources', ESE:SF/UAR 49 Technical Report 2.

Farnsworth RK, Barrett ECB, Dhanju MS (1984), 'Application of remote sensing to hydrology including ground water', UNESCO IHP-II Project A.1.5.

Forshaw , Haskell A, Miller PF, Stanley DJ, Townshend JRG (1983), 'Spatial resolution of remotely sensed imagery - a review paper', International Journal of Remote Sensing, Vol 4, pp 497-520.

Gordon F (1983), 'The time-space relationships amoung data points from multispectral spatial scanners', International Journal of Remote Sensing, Vol 4, pp 555-570.

Graetz RD, Gentle MR (1982), 'The relationship between reflectance in the Landsat wavebands and composition of an Australian semi-arid shrub rangeland', Photogrammetric Engineering and Remote Sensing, Vol 48, pp 1721-1730.

Griffiths G, Collins W (1982), 'Mapping semi-arid vegetation in northern Kenya from Landsat digital data', Proceedings of the Remote Sensing Society Conference 1982.

Hardy JR (1982), 'Integrating ground data in remote sensing', Course notes - Remote Sensing for Lands Use Inventories, JRC, ISPRA.

Haydn R, Dalke GW, Henkel J, Bare JE (1982), 'Application of the IHS colour transform to the processing of multisensor data and image enhancement', International Symposium on Remote Sensing of Arid and Semi-Arid Lands, Cairo, Egypt, pp 599-616.

Heilman JL, Boyd WE (1986), 'Soil background effects on the spectral response of a three-component rangeland scene', Remote Sensing of Environment, 19, pp 127-137.

Hellden U (1984), 'Remote sensing for drought impact assessment - a study of land transformation in Kordofan, Sudan', Advances in Space Research : Remote Sensing from Satellites, Ed Carter WD, Engman ET, Pergamon Press.

Hielkema JU (1981), 'Desert locust habitat monitoring with satellite remote sensing', ITC Journal, 1981-4, pp 387-417.

Holben B, Fraser RS (1984), 'Red and near-infrared sensor responce to off-nadir viewing', International Journal of Remote Sensing, Vol 5, pp 145-160.

Holben BN, Justice CO (1980), 'The topographic effect on spectral responce from nadir-pointing sensors', Photogrammetric Engineering and Remote Sensing,46, 9, pp 1191-1200.

Howard JA, Schade J (1982), 'Towards a standardized hierarchical classification of vegetation for remote sensing', FAO RSC Series 11, Bulletin.

Huete AR, Post DF, Jackson RD (1984), 'Soil spectral effects on 4-space vegetation discrimination', University of Arizona Remote Sensing Newsletter, 83-1

Huete AR, Post DF, Jackson RD (1983), 'Soil spectral effects on 4-space vegetation discrimination', Remote Sensing of Environment, 15: pp 155-165.

Huete AR Jackson RD, Post DF (1985), 'Spectral response of a plant canopy with different soil backgrounds', Remote Sensing of Environment, 17: pp 37-53.

Hutchinson CF (1982), 'Remote sensing of arid and semi-arid rangeland', International Geoscience and Remote Sensing Symposium, Munich, 1982.

Ingebritsen SE, Lyon RJP (1985), 'Principal components analysis of multitemporal image pairs', International Journal of Remote Sensing, Vol 6, pp 687-696.

Jackson RD, Slater PN, Pinter PJ (1983), 'Adjusting the tasselled-cap brightness and greenness factors for atmospheric path radiance and adsorption on a pixel by pixel basis', International Journal of Remote Sensing, Vol 4, pp 313-323.

Jeffrey A (1982), 'Mathematics for Engineers and Scientists', Van Nostran Reinhold, Second Edition.

Justics CO, Wharton SW, Holben BN (1981), 'Application of digital terrain data to quantify and reduce the topographic effect on Landsat data', International Journal of Remote Sensing, Vol 2, pp213-230.

Kamal S (1983), PhD Theses material. Unpublished.

Kaufman L (1974), 'Sight and mind : an introduction to visual perception', NYOUP.

Kauth RJ, Thomas GS (1976), 'The tasselled cap - a graphical description of the spectral-temporal development of agricultural crops as seen by Landsat', Proceedings of the Symposium of Machine Processing of Remote Sensing Data, 6/29-72,LARS,Purdue,IEEE, pp 4B41-4B51.

Kauth RJ, Lambek PF, Richardson W, Thomas GS, Pentland AP, (1979), 'Feature extraction applied to agricultural crops as seen by Landsat', The LACIE Symposium, NASA (JSC-16015), pp 705-716.

Kay MG, Stephens W, Carr MKV (1985), 'The prospects for small scale irrigation in sub-Saharan Africa', Outlook on Agriculture, Vol 14, pp 115-121.

Keates JS (1982), 'Understanding Maps, Longman.

Khalid I (1980), 'Egypt, economic management in a period of transition', A World Bank Country Economic Report.

Kimes DS, (1984), 'Directional reflectance factor distributions of a cotton row crop', International Journal of Remote Sensing, Vol 5, pp 263-277.

Lacaze B (1982), 'Remote sensing from space applied to the evaluation and surveying of pastoral resources in arid areas', Remote Sensing for Land Use Inventories, CEC, ISPRA.

Lee JD, Lee TD (1982), 'Statistics and computer methods in BASIC', Van Nostrand Reinhold.

MacFarlane N, Robinson IS (1984), 'Atmospheric correction of Landsat MSS data for a multidate suspended sediment algorithm', International Journal of Remote Sensing, Vol5, pp 561-576.

Marble DF, Calkins HW, Peuquet DJ (1984), 'Basic readings in Geographic Information Systems', SPAD Systems Ltd

Marr D (1982), 'Vision : a computational investigation into the luman representation and processin of visual information', W H Freeman & Co.

Mather PM (1976), 'Computational methods of multivariate analysis in physical geography', John Wiley an Sons

Misra PN, Wheeler SG (1978), 'Crop classification with Landsat multispectral data', Pattern recognition, Vol 10, pp 1-13.

Mitchell CW (1975), 'The applications of Landsat 1 imagery to the Sudan savanna project', Journal of the British Interplanetary Society, Vol 28, pp 659-672.

Mitchell CW (1973), 'Terrain evaluation', Longman.

Moik JG (1980), 'Digital Processing of Remotely Sensed Images', Scientific and Technical Branch, NASA.

Mulder NJ, Hempenius SA (1974), 'Data compression and data reduction techniques for the visual interpretation of multispectral images', ITC Journal, 1974-3, pp 414-423.

Mulder NJ (1980), 'A view on digital image processing', 14th Congress of the International Society of Photogrammetry, Hamburg.

Mulder NJ (1981), 'Spectral correlation filters and natural colour coding', ITC Journal, 1981-3, pp 237-251.

Mulder NJ (1982), 'Methodology of colour coding MSS and other data', Symposium of International Society of Photogrammetry Commission III Helsinki, Finland.

Mulder NJ (1982), 'Generalized operators for geometric correction, resampling and deconvolution', Symposium of the International Society of Photogrammetry, Commission III, Helsinki, Finland.

Mulder NJ, Hempenius SA (1974), 'Data compression and data reduction techniques for the visual interpretation of multispectral images', ITC Journal, 1974-3, pp 414-423.

Newcomb WW, Schutt JB, Pinter PJ, Jackson RD (1984), 'Directional reflectance factor distributions of a cotton row crop', International Journal of Remote Sensing, Vol5, pp 263-278.

Newman WM, Sproull RF (1979), 'Principles of interactive computer graphics', Second Edition, McGraw-Hill.

Olsson K (1984), 'Estimating canopy cover in drylands with Landsat MSS data, 'Advances in Space Resources, Vol 4, pp 161-164.

Olsson L, Stern M (1981), 'Large area data sampling - for remote sensing applications and statistical analysis of environment', Lund University, Sweden.

Otterman J (1981), 'Satellite and field studies of man's impact on the surface on arid regions', Tellus 33, pp 68-77.

Otterman J (1983), 'Effects of an optically thin Rayleigh atmosphere on the absorption of solar radiation by a Lambert surface', Tellus 35B, 5.

Otterman J (1985), 'Bidirectional and hemispheric reflectivities of a bright soil plane and a sparse dark canopy', International Journal of Remote Sensing, Vol 6, pp 897-902.

Otterman J, Ungar S, Ohring G, Malingreau JP, Goward SN (1985), 'Multi-parameter characterization of the surface by multi-temporal satellite observations', Proceedings of the International Conferance of the Remote Sensing Society / CERMA, pp 473-474.

Otterman J, Weiss G (1984), 'Reflection from a field a randomly located vertical protrusions', Applied Optics, Vol 23, pp 1931.

Otterman J (1984), 'Atmospheric effects on radiometry from zenith of a plane with dark vertical protrusions', International Journal of Remote Sensing, Vol 5, pp 909-923.

Otterman J, Robinove CJ (1982), 'Landsat monitoring of desert vegetation growth, 1972-1979, using a plant-shadowing model', Paper 10.2.4. of Symposium SLTPFS & GO, COSPAR.

Otterman J, Dishon M, Rehavi S. (1983), 'Point spread functions in imaging a Lambert surface through a thin scattering layer', International Journal of Remote Sensing, Volumn 4, pp 583-599.

Otterman J, Chou M D, Arking A (1984), 'Effects of nontropical forest cover on climate', Journal of Climate and Applied Meteorology, Vol 23, pp 762-767.

Pech RP, Graetz RD, Davis AW (1986), 'Reflectance modelling and the derivation of vegetation indices for an Australian semi-arid shrubland', International Journal of Remote Sensing, Vol 7, pp389-403.

Philipson W R (1986), 'Problem-solving with remote sensing: an update',Photogrammetric Engineering and Remote Sensing, Vol 52, pp 109-110.

Rasmussen R O. (1983), 'Evaluation of grazing capacity in south-western Greenland by means of Landsat data', Proceedings of Annual Conference of The Remote Sensing Society 1983, pp 80-92.

Reeves RG, (1975), 'Manual of remote sensing', American Society of Photogrammetry, Falls Church, Virginia, First Edition.

Ricardson A J, Wiegand C L, (1977), 'Distinguishing vegetation from soil background information', Photogrammetric Engineering and Remote Sensing, Vol 43, pp 1541-1552.

Roberts P A. (1981), 'The use of terrain height information with satellite imagery', Proceedings of the Annual Conference of The Remote Sensing Society 1981, pp 317-328.

Robinove C J. (1982), 'Space platform albedo measurements as indicators of change in arid lands', [USGS] Paper 10.2.4. of Symposium on the Study of Land Transformation Processes from Space and Ground Observation. COSPAR 1982.

Robinove C J. (1982), 'Computation with physical values from Landsat digital data', Photogrammetric Engineering and Remote Sensing, Vol 48, pp 781-784.

Rosenfield GH, Fitzpatric-Lins K, Ling HS (1982), 'Sampling for thematic map accuracy testing', Photogrammetric Engineering and Remote Sensing, Vol XLVIII, pp 131-138.

Rosenfield GH (1982), 'Sample design for estimating change in land use and land cover', Photogrammetric Engineering and Remote Sensing, Vol 48, pp 793-801.

Rosenfield A, Kak A (1976), 'Digital picture processing', Academic Press.

Sabins FF Jr (1978), 'Remote sensing principles and interpretation', WH Freeman & Co, San Francisco.

Schowengert RA (1983), 'Techniques for image processing and classification in remote sensing', Academic Press.

Schowengert R, Park SK, Gray R (1984), 'Topics in the two-dimensional sampling and reconstruction of images', International Journal of Remote Sensing, Vol 5, pp 333-348.

Shata A (1971), 'The geomorphology, pedology and hydrogeology of Mediterranean coastal desert of UAR. Symposium on the Geology of Libya, April 1969, pp 431-446, Faculty of Science, University of Libya.

Singh A, Harrison A (1985), 'Standardized principal components', International Journal of Remote Sensing, Vol 6, pp 883-896.

Slater PN (1980), 'Remote sensing - optics and optical systems', Addison-Wesly Publishing Company.

Smith JA, Tzue LL, Ranson KJ (1980), 'The Lambertian assumption and Landsat data', Photogrammetric Engineering and Remote Sensing, Vol 46, pp 1183-1189.

Steven MD (1983), 'The physical and physiological interpretation of infrared/red spectral ratios over crops', Proceedings of a one day Meeting of the Royal Chemical Society and the Remote Sensing Society, Imperial College, London, 2.2.83

Suits G (1972), 'The calculation of the directional reflectance of a vegetation canopy', Remote Sensing of Environment, Vol 2, pp 117-125.

Suits GH (1972), 'The cause of azimuthal variations in directional reflectance of vegetative canopies', Remote Sensing of Environment, Vol 2, pp 175-182.

Swain PH (1973), 'Pattern recognition: a basis for remote sensing data analysis', LARS Information Note 111572, Purdue University.

Tackholm V (1974), 'Student's flora of Egypt', Cairo University.

Taylor BF, Dini PW, Kidson JW (1985), 'Determination of seasonal and interannual variation in New Zealand pasture growth from NOAA-7 data', Remote Sensing of Environment 18: pp 177-192.

Tom VT, Carlotto MJ, Scholten DK (1984), 'Spatial resolution improvement of TM thermal band data' SPIE vol.504 Applications of Digital Image Processing VII, pp 384-390.

Townshend JRG, Tucker CJ (1981), 'Utility of AVHRR of NOAA 6 and 7 for vegetation mapping', Proceedings of the International Conference of the Remote Sensing Society, 1981, pp 97-109.

Townshend JRG (1981), 'Terrain analysis and remote sensing', George Allen & Unwin.

Tucker CJ, Gatlin A, Schneider SR (1984), 'Monitoring vegetation in the Nile Delta with NOAA-6 and NOAA-7 AVHRR', Photogrammetric Engineering and Remote Sensing, Vol 50, pp 53-61.

Tucker CJ, Miller LD (1977), 'Soil spectral contributions to grass canopy spectral reflectance', Photogrammetric Engineering and Remote Sensing, Vol 43, pp 721-726.

Tucker CJ, Townshend JRG, Goff TE (1985), 'African land-cover classification using satellite data', Science, Vol 227, No 4685, pp 369-375.

Jackson RD, Pinter PJ, Reginato RJ, Idso SB (1980), 'Hand-held radiometry', US Department of Agriculture Science and Education Administration, ARM-W-19/Oct 1990.

Tucker CJ, Townshend JRG, Goff TE (1985), 'African land-cover classification using satellite data', Science, Vol 227, No 4685, pp 369-375.

Tueller PT (1982), 'Remote sensing for range management', Chapter 12, Remote Sensing for Resource Management, Ed Johannsen CJ, Sanders JL.

US Geological Survey/NOAA (198?), 'Landsat 2 data users handbook.', US Geological Survey/NOAA.

US Geological Survey/NOAA (1984), 'Landsat 4 data users handbook.', US Geological Survey/NOAA.

Vita-Finzi C (1969), 'The Mediterranean valleys - geological changes in historical times', Cambridge University Press.

Wardley NW (1984), 'Vegetation index variability as a function of viewing geometry', International Journal of Remote Sensing, Vol 5, pp 861-870.

Watson RM, (1981), 'Down market remote sensing', Proceedings of the International Conference of the Remote Sensing Society, 1981, pp 5-35.

Watson RM, Hemming CF (1985), 'Can remote sensing save the nomad', Proceedings of the Internation Conference of the Remote Sensing Society, 1983, pp 123-133.

Watson RM, Nimmo JM (1985), 'Information to management:- are chips the missing link?', Proceedings of the International Conference of the Remote Sensing Society, 1985, Supplementrary Papers, pp 1-10.

Westin FC, Lemme GD (1978), 'Landsat spectral signatures: studies with soil associations and vegetation', Photogrammetric Engineering and Remote Sensing, Vol 44, pp 315-325.

Wheeler SG, Misra PN (1980), 'Crop classification with Landsat multispectral scanner data II', Pattern Recognition, Vol 12, pp 219-228.

APPENDIX A

FORTRAN 77 PROGRAMS

```
      PROGRAM LEAST
C
C     Program to find the slope and intercept of a SCATTERPLOT image.
C
      INTEGER FCB(4000)
      REAL RFCB(1)
      EQUIVALENCE (FCB, RFCB)
C
      INTEGER NIDS, NODS, IBUF, RBUF, BUFSIZ
C
C     Fetch function control block
C
      CALL FCBSET (FCB)
      FCB(3) = 4000
      CALL STRTUP (FCB)
C
C     Get offsets of important arrays and constants
C     within FCB
C
      CALL SYSCON (FCB, NIDS, NODS, IBUF, RBUF, BUFSIZ)
C
C     Call driver
C
      CALL LEASD (FCB, FCB(NIDS), FCB(NODS),
     1           FCB(IBUF), RFCB(RBUF), FCB(BUFSIZ))
C
C     Return function control block
C
      CALL SHUTDN (FCB)
C
C     That's all
C
      END
```

```
      SUBROUTINE LEASD(FCB, NIDS, NODS, BUFFER, REALBF, BUFSIZ)
C
C     This is the driver subroutine for the LEASTSQ function.
C     The function will find the slope and intercept of a distribution
C     in a SCATTERPLOT image.
C     AUTHOR: Tim Richards 25.9.85
C
      INTEGER FCB(1), BUFFER(1)
      REAL    REALBF(1)
      INTEGER NIDS, NODS, BUFSIZ
C
C     Locals
C
      INTEGER ILINE, PARMS(60), CHANLS(1), LEVELS, NS, NL, NBANDS
      INTEGER DMASK, CHCODE, IBIT, CODE
      INTEGER INTERC, ISX, ISY, IPLANE
      INTEGER*4 ISX2, ISY2, IXVAL, IYVAL, ISXY
      INTEGER*4 ITOTX, ITOTY, INUMB, IX, IY, IBUFF, IXB, IYB
      REAL    RSX2, RSY2, RSQU, RSQRT, RCORRL, RINTER, RSLOPE
      REAL    RED, GREEN, BLUE
C
C     Check NIDS & NODS
C
      IF (NIDS .NE. 1) CALL DOOM(FCB, 1100)
      IF (NODS .NE. 0) CALL DOOM(FCB, 1100)
C
      CALL MOVCH (16HPLANE           , BUFFER, 0, 0, 16)
      CALL PARMI (FCB, PARMS, IPLANE, BUFFER, 0, 1, 1, 1)
      IPLANE = 0
C
      CALL MOVCH (16HRED             , BUFFER, 0, 0, 16)
      CALL PARMR (FCB, PARMS, RED, BUFFER, 1, 1, 1, 2)
      RED = 1.0
C
      CALL MOVCH (16HGREEN           , BUFFER, 0, 0, 16)
      CALL PARMR (FCB, PARMS, GREEN, BUFFER, 1, 1, 1, 3)
      GREEN = 0.0
C
      CALL MOVCH (16HBLUE            , BUFFER, 0, 0, 16)
      CALL PARMR (FCB, PARMS, BLUE, BUFFER, 1, 1, 1, 4)
      BLUE = 0.0
C
      CALL DEFINE (FCB, PARMS, 4, 0)
      IPLANE = DMASK(IPLANE)
C
C     Open input SCATTERPLOT image
C
      CALL DOPI(FCB, BUFFER, NIDS, NS, NL, NBANDS, CHANLS, LEVELS)
C
      IF (NS .NE. 512 .AND. NL .NE. 512) CALL DOOM(FCB, 1100)
C
      CALL DADRS (CHCODE, CHANLS, CODE, 1)
C
C     Loop through image & find the sums of x & y
C
         ITOTX = 0
         ITOTY = 0
         INUMB = 0
C
      DO 100 IY = 128, 383
```

```
C
        CALL IMAGE (FCB, BUFFER, 128, IY, 256, CHCODE, -1, 0,
     1             0, 4, 0, 0, 1, 0, 3)
C
          DO 200 IX = 1, 256
            IF (BUFFER(IX) .NE. 0) THEN
C
              IXVAL = IX
              IYVAL = JIABS(IY-384)
C
               IBUFF = BUFFER(IX) + 1
C
              ITOTX = ITOTX + (IXVAL * IBUFF)
              ITOTY = ITOTY + (IYVAL * IBUFF)
              INUMB = INUMB + IBUFF
C
            END IF
200       CONTINUE
100     CONTINUE
C
C       Find the means
C
        IXB = ITOTX / INUMB
        IYB = ITOTY / INUMB
C
C       Calculate the sum of squares
C
        ISX = 0
        ISY = 0
        ISXY = 0
        ISX2 = 0
        ISY2 = 0
C
        DO 400 IY = 128, 383
          CALL IMAGE (FCB, BUFFER, 128, IY, 256, CHCODE, -1, 0,
        1             0, 4, 0, 0, 1, 0, 3)
C
          DO 300 IX = 1, 256
            IF (BUFFER(IX) .NE. 0) THEN
              IBUFF = BUFFER(IX)
              IXVAL = IX
              IYVAL = JIABS(IY-384)
               ISX = IXVAL - IXB
               ISY = IYVAL - IYB
              ISXY = ISXY + ((ISX * ISY) * IBUFF)
              ISX2 = ISX2 + ((ISX * ISX) * IBUFF)
              ISY2 = ISY2 + ((ISY * ISY) * IBUFF)
            END IF
300       CONTINUE
400     CONTINUE
C
C       Calculate results
C
        RSX2   = FLOATJ(ISX2)
        RSY2   = FLOATJ(ISY2)
        RSXY   = FLOATJ(ISXY)
        RTOTY  = FLOATJ(ITOTY)
        RTOTX  = FLOATJ(ITOTX)
        RNUMB  = FLOATJ(INUMB)
C
```

```
      RSLOPE = RSXY / RSX2
      RINTER = (RSX2*RTOTY-RTOTX*RSXY) / (RNUMB * RSX2)

      RSQU   = RSX2 * RSY2
      RSQRT  = SQRT(RSQU)
      RCORRL = FLOATJ(ISXY)
      RCORRL = RCORRL / RSQRT
C
C     Write out results
C
      WRITE (5, 520) '-----------------------------------------------'
      WRITE (5, 600) 'Slope                       = ', RSLOPE
      WRITE (5, 600) 'Intercept                   = ', RINTER
      WRITE (5, 600) 'Correlation Coefficient = ', RCORRL
      WRITE (5, 520) '-----------------------------------------------'
500   FORMAT (1X, A, I)
600   FORMAT (1X, A, F10.2)
520   FORMAT (1X, A)
C
C     Draw slope/intercept function
C
      INTERC = ININT(RINTER)
      ISLOPE = ININT(RSLOPE)
C
      RY2 = RSLOPE * 255. + RINTER
      IY2 = ININT(RY2)
      IY2 = (255 - IY2) + 128
      IX2 = 255 + 128
      IX1 = 128
      IY1 = ININT(RINTER)
C
      IF (IY1 .LT. 0) THEN
         RA = RINTER / RSLOPE
         IX1 = ININT(RA)
         IX1 = IX1 + 128
         IY1 = 383
      END IF
C
C
      CALL STCOL (FCB, BUFFER, IPLANE, RED, GREEN, BLUE, 1)
      CALL XCOLR (FCB, BUFFER, IPLANE, 1)
      IVALUE = 255
C
      CALL DVECT (FCB, BUFFER, IVALUE, IX1, IY1, IX2, IY2,
     1            1, -32768, IPLANE)
C
C     Close files and exit
C
      CALL ICLOS(FCB, 1)
C
2000  RETURN
      END
```

```
      PROGRAM LNDCAL
C     **************
C
C     program to Calibrate Landsat (1 - 3) images
C
      INTEGER FCB (4000)
      REAL    RFCB (1)
      EQUIVALENCE (FCB, RFCB)
C
      integer NIDS, NODS, IBUF, RBUF, BUFSIZ
C
C     FETCH FunCtion Control BloCk
C
      CALL FCBSET (FCB)
      FCB (3) = 4000
C
      CALL STRTUP (FCB)
C
C     get offsets of important arrays and Constants
C     within FCB
C
      CALL SYSCON (FCB, NIDS, NODS, IBUF, RBUF, BUFSIZ)
C
C     CALL driver
C
      CALL LCAL (FCB, FCB(NIDS), FCB(NODS),
     1           FCB(IBUF), RFCB(RBUF), FCB(BUFSIZ))
C
C     return FunCtion Control BloCk
C
      CALL SHUTDN (FCB)
C
C
C
      end
```

```
      SUBROUTINE LCAL (FCB, NIDS, NODS, BUFFER, REALBF, BUFSIZ)
C
C     Will convert a four band  Landsat (1 - 3) image from digital
C     numbers into radiance in mW cm-2 str-1
C
      INTEGER FCB(1), BUFFER(1)
      INTEGER NIDS, NODS, BUFSIZ
      REAL    REALBF(1)
C
C     Locals:
C
      INTEGER LSAT, NS, NL, NB, FTYPE, ITYPE, DTYPE, DEBUG
      INTEGER PARMS(60), ICENT
      REAL    ALPHA
C
C     check for 1 input & 1 output
C
      IF (NIDS .NE. 1) CALL DOOM (FCB, 1100)
      IF (NODS .NE. 1) CALL DOOM (FCB, 1100)
C
C     Open input & output images
C
      CALL IMOPI (FCB, BUFFER, 1, DTYPE, FTYPE, ITYPE, NS, NL, NB)
C
      CALL IMOPO (FCB, BUFFER, 2, 1, FTYPE, 0, NS, NL, NB)
C
C     find which Landsat the image was recorded on
C
C     print out Landsat options
C
      CALL MOVCH (15HA  :  Landsat 1, BUFFER, 0, 0, 15)
      CALL PRINTR (FCB, 1, BUFFER, 15, 32)
C
      CALL MOVCH (36HB  :  Landsat 2a   22.6.75 - 16.7.75,
     1            BUFFER, 0, 0, 36)
      CALL PRINTR (FCB, 1, BUFFER, 36, 32)
C
      CALL MOVCH (36HC  :  Landsat 2b    after  - 16.7.75,
     1            BUFFER, 0, 0, 36)
      CALL PRINTR (FCB, 1, BUFFER, 36, 32)
C
      CALL MOVCH (36HD  :  Landsat 3a    5.3.78 -  1.6.78,
     1            BUFFER, 0, 0, 36)
      CALL PRINTR (FCB, 1, BUFFER, 36, 32)
C
      CALL MOVCH (36HE  :  Landsat 3b    after  -  1.6.78,
     1            BUFFER, 0, 0, 36)
      CALL PRINTR (FCB, 1, BUFFER, 36, 32)
C
C     Set up parameters
C
      CALL MOVCH (16HLSAT             , BUFFER, 0, 0, 16)
      CALL PARMI (FCB, PARMS, LSAT, BUFFER, 266, 1, 0, 1)
C
C     Find which data centre the image is from
C
      CALL MOVCH (16HFUCINO           , BUFFER, 0, 0, 16)
      CALL PARMI (FCB, PARMS, ICENT, BUFFER, 0, 1, 1, 2)
      ICENT = 1
C
```

```
C       find sunangle in radians
C
        CALL MOVCH (16HALPHA           , BUFFER, 0, 0, 16)
        CALL PARMR (FCB, PARMS, ALPHA, BUFFER, 9, 1, 0, 3)
C
        CALL MOVCH (16HDEBUG           , BUFFER, 0, 0, 16)
        CALL PARMI (FCB, PARMS, DBUG, BUFFER, 67, 1, 0, 4)
C
        CALL ZBUFF (BUFFER, 10)
        CALL PRINTR (FCB, 1, BUFFER, 10, 32)
C
        CALL DEFINE (FCB, PARMS, 4, 0)
C
        CALL CALCL (FCB, BUFFER, BUFSIZ, ICENT, LSAT, ALPHA,
        1                NS, NL, NB)
C
        CALL ICLOS(FCB, 1)
        CALL ICLOS(FCB, 2)
C
        RETURN
        END
```

```
      SUBROUTINE CALCL (FCB, BUFFER, BUFSIZ, ICENT, LSAT, ALPHA,
     1                  NS, NL, NB)
C
C     subroutine to calibrate Landsat images
C
      INTEGER FCB(1), BUFFER(1), DSRN, BUFSIZ
C
      INTEGER ICENT, NS, NL, NB, LSAT
      INTEGER DMAX, DMAX7
C
      REAL    E(4:7), LMAX(4:7), LMIN(4:7)
      REAL    REALBF(1), ALPHA, LUT(0:255, 4:7), IRRAD (4:7)
      REAL    CALIB(4:7), PI, IVAL
C
C     Subroutine to convert Landsat DN's into radiance in mw cm-2 str-1
C
C     Reflectance = pi / E sin(ALPHA) * (DN / Dmax (LMAX(-LMIN() + LMIN()
C       ALPHA     = the sun angle above the horizon in degrees
C      E4 - E7    = irradiance at the top of the atmosphere in mW cm-2 str-1
C     LMIN & LMAX = MSS sensor calibrations for specific time periods
C
C     Cf   Robinove CJ (1982)
C     Photogrammetric Engineering and Remote Sensing Vol 48 No 5 May 1982
C
C
      PI = 3.1415927
C
      IF (ICENT .EQ. 1) THEN
        DMAX = 255
        DMAX7 = 255
      END IF
C
      IF (ICENT .EQ. 0) THEN
        DMAX = 127
        DMAX7 = 63
      END IF
C
      E(4) = 17.70
      E(5) = 15.15
      E(6) = 12.37
      E(7) = 24.91
C
      IF (LSAT .EQ. 65 .OR. LSAT .EQ. 97) THEN
        LMIN(4) = 0.0
        LMIN(5) = 0.0
        LMIN(6) = 0.0
        LMIN(7) = 0.0
C
        LMAX(4) = 2.48
        LMAX(5) = 2.00
        LMAX(6) = 1.76
        LMAX(7) = 4.00
C
      ELSE IF (LSAT .EQ. 66 .OR. LSAT .EQ. 98) THEN
        LMIN(4) = 0.10
        LMIN(5) = 0.07
        LMIN(6) = 0.07
        LMIN(7) = 0.14
C
        LMAX(4) = 2.10
```

```
          LMAX(5) = 1.56
          LMAX(6) = 1.40
          LMAX(7) = 4.15
C
        ELSE IF (LSAT .EQ. 67 .OR. LSAT .EQ. 99) THEN
          LMIN(4) = 0.08
          LMIN(5) = 0.06
          LMIN(6) = 0.06
          LMIN(7) = 0.11
C
          LMAX(4) = 2.63
          LMAX(5) = 1.76
          LMAX(6) = 1.52
          LMAX(7) = 3.91
C
        ELSE IF (LSAT .EQ. 68 .OR. LSAT. EQ. 100) THEN
          LMIN(4) = 0.04
          LMIN(5) = 0.03
          LMIN(6) = 0.03
          LMIN(7) = 0.03
C
          LMAX(4) = 2.20
          LMAX(5) = 1.75
          LMAX(6) = 1.45
          LMAX(7) = 4.41
C
        ELSE IF (LSAT .EQ. 69 .OR. LSAT. EQ. 101) THEN
          LMIN(4) = 0.04
          LMIN(5) = 0.03
          LMIN(6) = 0.03
          LMIN(7) = 0.03
C
          LMAX(4) = 2.59
          LMAX(5) = 1.79
          LMAX(6) = 1.49
          LMAX(7) = 3.83
        END IF
C
C       Set up constants
C
          DO 10 IB = 4, 7
            IRRAD(IB) = PI / (E(IB) * SIN(ALPHA))
10        CONTINUE
C
C       Load LUT'S FOR EROS IMAGES
C
        IF (ICENT .EQ. 0) THEN
        DO 20 IB = 4, 6
          DO 30 IS = 1, 256
            RIS = FLOATI(IS-1)
            LUT(IS-1, IB) = (RIS/127.) * (LMAX(IB)-LMIN(IB)) + LMIN(IB)
            LUT(IS-1, IB) = (LUT(IS-1, IB) * IRRAD(IB)) * 255
30        CONTINUE
20      CONTINUE
        DO 140 IS = 1, 256
            RIS = FLOATI(IS-1)
            LUT(IS-1, IB) = (RIS/63.) * (LMAX(IB)-LMIN(IB)) + LMIN(IB)
            LUT(IS-1, 7) = (LUT(IS-1,7)*IRRAD(7))*255
140     CONTINUE
        GOTO 120
```

```
      END IF
C
C     LOAD LUT'S FOR FUCINO TAPES
C
C
      DO 120 IB = 4, 7
        DO 130 IS = 1, 256
          RIS = FLOATI(IS-1)
          LUT(IS-1, IB) = (RIS/255.) * (LMAX(IB)-LMIN(IB)) + LMIN(IB)
          LUT(IS-1, IB) = (LUT(IS-1, IB) * IRRAD(IB)) * 255
      WRITE (5, 500) IS-1, LUT(IS-1, IB)
500   FORMAT (1X, I, F10.3)
130     CONTINUE
120   CONTINUE
C
C     Now process the image !
C
      DO 40 IB = 4, 7
        DO 50 IL = 1, NL
          CALL IMRD (FCB, 1, 2, BUFFER, 0, 1, NS, IL,
     1               1, IB-3, 1)
          DO 60 IS = 1, NS
            BUFFER(IS) = ININT (LUT(BUFFER(IS), IB))
60        CONTINUE
         CALL IMWRT(FCB, 2, 2, BUFFER, 0, 1, NS, IL,
     1               1, IB-3, 1)
50      CONTINUE
40    CONTINUE
C
      RETURN
      END
```